

MODEL OF GLIOBLASTOMA RECURRENCE

A PRE-CLINICAL MODEL OF GLIOBLASTOMA RECURRENCE TO IDENTIFY
PERSONALIZED THERAPEUTIC TARGETS

By MALEEHA AHMAD QAZI, (H)B.Sc.

A Thesis Submitted to the School of Graduate Studies in Partial Fulfillment of the
Requirements for the Degree Doctor of Philosophy

McMaster University © Copyright by Maleeha Ahmad Qazi, March 2019

DOCTOR OF PHILOSOPHY (2019)
Biochemistry and Biomedical Sciences
McMaster University
Hamilton, ON, Canada

TITLE: A pre-clinical model of glioblastoma recurrence to identify personalized
therapeutic targets

AUTHOR: Maleeha Ahmad Qazi, (H)B.Sc. (McMaster)
SUPERVISOR: Dr. Sheila Kumari Singh
NUMBER OF PAGES: xiii, 233

ABSTRACT

Glioblastoma (GBM) is the most common and lethal primary tumour affecting the central nervous system in adults. Despite aggressive, multi-modal treatment consisting of surgical resectioning of the tumour followed by radiotherapy and chemotherapy, GBM remains incurable. Almost all patients experience relapse 7-9 months post-diagnosis and median survival has not extended beyond 15 months over the past decade. Extensive research in the molecular and cellular biology of GBM has revealed extensive inter- and intra-tumoural heterogeneity caused by dysregulation at genomic, epigenomic, transcriptomic and proteomic levels. Although this has led to the identification of molecular targets for therapeutic development, large body of GBM research has focused on the study of primary GBM, with little exploration of the biological landscape of recurrent GBM. Recent genomic studies suggest that recurrent GBM evolves significantly during the course of therapy and represents a distinct biological entity and therefore therapies developed based on primary GBM biology will not present efficacy against recurrent GBM. Thus, I postulate that models that capture the evolution of GBM biology in response to standard-of-care (SoC) chemoradiotherapy will allow for the identification of therapeutic targets specific to recurrent GBM and can be used for personalized medicine.

Here I show the development of an *in vitro* and *in vivo* model of GBM recurrence that can be used as a surrogate to identify personalized therapeutic targets for recurrent GBM. We use established cancer stem cell models combined with patient-derived glioblastoma stem cells (GSC) to profile and characterize the evolution of GBM through *in vitro* and *in vivo*

adapted SoC. Through our *in vitro* model, I identified that combined chemoradiotherapy leads to increased sphere formation capacity of GBM and the global gene expression profiling of treatment-refractory GBM populations identified a poor-prognostic subtype of GBM. Next, I used patient-derived recurrent GBM to identify tyrosine kinases EphA2 and EphA3 as therapeutic targets in recurrent GBM and developed a bispecific antibody to co-target these receptors for therapeutic benefit. Lastly, I show the establishment of a novel patient-derived xenograft SoC model to profile the clonal evolution of GSCs through therapy. I show that this model can be coupled with multiple technologies, such as single cell RNA-sequencing and cellular DNA barcoding, to characterize the minimal residual cellular populations driving recurrence and identify personalized therapeutic targets for the treatment of GBM recurrence.

Altogether my thesis highlights the importance of developing clinically relevant models of GBM recurrence and using poly-targeting approaches for the treatment of recurrent GBM.

ACKNOWLEDGEMENTS

“O my Lord, increase me in knowledge.” (Holy Quran, Chapter 20, verse 115)

First and foremost, I want to thank Almighty Allah for giving me the strength, the knowledge and the ability to complete this work.

I thank my supervisor, Dr. Sheila Singh, for her unwavering support and mentorship, right from when I joined the lab as a 21-year-old to now 7 years later. You gave me the freedom to undertake the most exciting research and provided me with all the opportunities I needed to grow as a scientist. I also thank my graduate supervisory committee members (Dr. Bhatia, Dr. Fleming and Dr. Moffat) for their continued support and encouragement. To all members of the Singh lab – thank you! You have made every single day in the lab completely worthwhile.

Most importantly, I want to thank my family. To my parents, Hakeem and Saira, who left their lives behind in hopes of giving us a brighter future. Your love and dedication to your children is unparalleled and I hope that I have made you both very proud. To my sisters, Monahil and Mishaal, for being the coolest sisters one could ask for and for making life so much fun.

To my husband, Ali, who has been my strongest pillar of support. Thank you for joining me in the lab whenever I asked, for helping me with all my manuscript preparations, and for being the most caring, supportive and loving husband. I also thank my parents-in-law, Malik and Ayesha, for always taking care of me like their own.

I dedicate this thesis in memory of my cousin, Mariyam Sufi, whose hard-fought battle with cancer motivates me to make cancer a disease of the past.

Table of Contents

ABSTRACT	iii
ACKNOWLEDGEMENTS	v
List of Figures and Tables	viii
List of Abbreviations and Symbols	x
Declaration of Academic Achievement	xii
CHAPTER 1: Introduction	1
1.0 Preamble	1
1.1 Glioblastoma	2
1.1.1 Clinical characteristics	2
1.1.2 Current standard of care and disease prognosis	3
1.1.3 MGMT promoter methylation – a prognostic factor	4
1.2 Molecular classification of GBM	5
1.2.1 Mutational profile of GBM	5
1.2.2 Transcriptomic subgrouping of GBM	8
1.2.3 Development of targeted therapies	11
1.3 Intratumoral heterogeneity in GBM	12
1.3.1 Spatiotemporal heterogeneity in GBM	12
1.3.2 Intratumoral heterogeneity at a single cell level	14
1.4 Evolution of treatment-refractory, recurrent GBM	16
1.4.1 Transcriptomic subgrouping of recurrent GBM	16
1.4.2 Therapy may drive GBM recurrence	17
1.4.3 Spatio-temporal patterns of GBM recurrence.....	18
1.5 Cancer stem cell hypothesis: identification of glioblastoma stem cells	21
1.5.1 Identification of cancer stem cells in GBM	21
1.5.2 Markers of glioblastoma stem cells	23
1.5.2 Role of GSCs in mediating therapy resistance	26
1.6 Shifting the focus to the study of recurrent GBM biology	28
1.7 Summary of Intent	30
CHAPTER 2: A novel stem cell culture model of glioblastoma recurrence	37
Preamble	37
Abstract	39
Introduction	40
Materials and Methods	42
Results	44
Discussion	50
References	53
CHAPTER 3: Cotargeting ephrin receptor tyrosine kinases A2 and A3 in cancer stem cells reduces growth of recurrent glioblastoma	74
Preamble	74

Abstract.....	77
Introduction.....	78
Materials and Methods.....	80
Results	88
Discussion	98
References.....	104
CHAPTER 4: Intratumoral heterogeneity: Pathways to treatment resistance and relapse in human glioblastoma	133
Preamble	133
Abstract.....	135
Introduction.....	136
Intratumoral heterogeneity in GBM.....	137
Intratumoral heterogeneity in recurrent GBM	139
Brain tumor initiating cells may drive GBM recurrence.....	142
Models to study intratumoral heterogeneity in GBM recurrence.....	144
Therapeutic Implications of Intratumoral Heterogeneity	149
Conclusion	151
References.....	153
CHAPTER 5: A pre-clinical <i>in vivo</i> model of glioblastoma recurrence	170
Preamble	170
Development of a therapy-adapted patient-derived xenograft model of GBM recurrence.....	172
Single cell RNA-sequencing to profile minimal residual disease.....	173
Cellular DNA barcoding in GBM to identify clonal evolution through therapy	175
Materials and Methods.....	178
References.....	181
CHAPTER 6: Discussion and future directions.....	193
6.1 Modelling GBM recurrence.....	193
6.1.1 In vitro model of GBM recurrence	193
6.1.2 In vivo model of GBM recurrence.....	194
6.2 Targeting the minimal residual disease: a novel therapeutic window to prevent GBM recurrence	196
6.3 Improving EphA2/EphA3 targeting – developing immunotherapeutic modalities	198
6.4 Immune microenvironment of recurrent GBM.....	201
6.5 Concluding Remarks	203
References.....	205
Appendix - Article Re-use Permissions.....	227

List of Figures and Tables

CHAPTER 1 FIGURES.....	34
Figure 1: BTSC model of GBM recurrence - chemoradiotherapy of primary glioblastoma (GBM) selects for treatment refractory BTSC populations that seed tumor relapse.	34
Figure 2: Mouse model of GBM recurrence to profile multi stages of disease progression.	35
CHAPTER 2 FIGURES AND TABLES.....	59
Figure 1: Inter-tumoral heterogeneity exists in <i>BMI1</i> and <i>SOX2</i> expression as well CD15 and CD133 cell surface expression in P-GBMs.	60
Figure 2: <i>In vitro</i> chemoradiotherapy increases the expression of BMI1 and SOX2 in P-GBMs.....	62
Figure 3: <i>In vitro</i> chemoradiotherapy enriches for CD15+/CD133- cell population in P-GBM and increases secondary sphere formation capacity, a profile similar to that of R-GBMs.....	64
Figure 4: Transcriptional analysis of <i>in vitro</i> treated P-GBM cultures identifies pathways associated with resistance and hyper-aggressive subtypes of brain tumors.	66
Figure 5: <i>In vitro</i> chemoradiotherapy of P-GBM models the biology of R-GBM.	67
Supplementary Table S1: Primer sequences used for RT-PCR experiments.	68
Supplementary Table S2: MGMT promoter methylation specific primer sequences.	68
Supplementary Table S3: Molecular subtype of samples used.	68
Supplementary Table S4: Significant network analysis pathways for common control/Tx2 variable genes.....	69
Supplementary Figure S1: MGMT promoter methylation status of GBM samples.	70
Supplementary Figure S2: <i>In vitro</i> radiotherapy changes the expression of <i>BMI1</i> and <i>SOX2</i> in P- GBMs.....	71
Supplementary Figure S3: <i>In vitro</i> chemoradiotherapy refractory BT458 cells are resistant to TMZ and radiation and have increased secondary sphere formation capacity but decreased proliferation capacity.	72
Supplementary Figure S4: Modules for network analysis of common Control/ Tx2 variable genes.....	73
CHAPTER 3 FIGURES AND TABLES.....	110
Figure 1: EphA2 and EphA3 have higher expression in recurrent GBM and co-express with glioblastoma stem cell (GSC) markers.	111
Figure 2: High EphA2 and EphA3 co-expression correlates with poor brain tumor patient survival.....	113
Figure 3: Co-expression of EphA2 and EphA3 marks a highly clonogenic and tumorigenic cell population in recurrent GBM.....	115
Figure 4: EphA2 and EphA3 knockdown in rGBM inhibits clonogenicity, decreases GSC and mesenchymal marker expression and prolongs survival.....	117
Figure 5: Treatment of rGBM with EphA2/A3 BsAb decreases EphA2 and EphA3 expression and decreases activation of Akt and Erk1/2.....	119
Figure 6: Treatment of rGBM with EphA2/A3 BsAb inhibits <i>in vitro</i> clonogenicity, increases differentiation and reduces tumor burden.	121

Table S1: Patient Demographics.....	122
Figure S1: Protein expression of EphA2, EphA3, CD133, CD15, Bmi1, Sox2, FoxG1 and ITGA6 in GBM.....	123
Figure S2: Characterization of EphA2+/EphA3+ sorted cell population overtime for changes in EphA2 and EphA3 surface expression.	124
Figure S3: Knockdown of EphA2 and EphA3 alters cell cycle and increases apoptosis in recurrent GBM.....	126
Figure S4: High affinity EphA2/A3 BsAb is internalized, leading to decreased expression of EphA2 and EphA3.....	128
Figure S5: Recurrent GBMs express low levels of ephrin A1/A5 ligands, and treatment with EphA2/A3 BsAb leads to EphA2 phosphorylation but does not alter other EphR expression.	130
Figure S6: EphA2/A3 BsAb also targets EphA2+/EphA3- and EphA2-/EphA3+ cell populations, does not affect cell cycle or apoptosis, and leads to increased expression of GFAP and MAP2.....	132
CHAPTER 4 FIGURES AND TABLES.....	163
Figure 1: Subclonal populations in primary glioblastoma escape therapy and give rise to treatment-refractory, heterogeneous recurrent glioblastoma.	164
Figure 2: Development of recurrent glioblastoma models for the identification of novel targets to prevent disease relapse.....	166
Table 1: Characterization of intra-tumoral heterogeneity in GBM in the past decade. ...	167
CHAPTER 5 FIGURES AND TABLES.....	182
Figure 1: Mouse-adapted chemoradiotherapy protocol for human glioblastoma.....	182
Figure 2: Chemoradiotherapy leads to tumor regression, which eventually relapses locally or distally.	183
Figure 3: Modified chemoradiotherapy protocol for modelling MBT06 GBM recurrence.	184
Figure 4: Treatment increases survival but also enriches for glioblastoma stem cell population in MBT06.....	185
Figure 5: single cell RNA sequencing of MBT06 at MRD shows treatment-dependent changes in gene expression.....	187
Figure 6: scRNAseq shows control and treated samples can be divided in 8 clusters with differential gene expression profile.	189
Figure 7: Optimization of cellular DNA barcoding and barcode amplification in primary human GBM cells.	191
Table 1: Primer sequences for BCLA barcode amplification.....	192

List of Abbreviations and Symbols

62-RS	62-gene resistance signature
APC	Allophycocyanin dye
AF488	Alexa-fluor 488 dye
Astro	Astrocytomas
BBB	Blood-brain barrier
BMI1	B-lymphoma Mo-MLV region 1 homolog
BsAb	Bispecific Antibody
BTIC	Brain tumour initiating cell
BTSC	Brain tumour stem cell
CA9	Carbonic anhydrase 9
CCL2	C-C motif chemokine Ligand 2
CCNB1	Cyclin B1
CCNB2	Cyclin B2
CDC20	Cell division cycle 20
Cla or CLA	Classical
CNA	Copy number alterations
CNS	Central nervous system
CytoF	Cytometry Time Of Flight
DMSO	Dimethyl sulfoxide
EGFR	Epidermal growth factor receptor
EphR	Ephrin receptor
ERK	Extracellular signal-regulated kinase
FGFR	Fibroblast growth factor receptor
FISH	Fluorescence in situ hybridization
FoxG1	Forkhead Box G1
FoxM1	Forkhead Box M1
GAPDH	Glyceraldehyde-3-phosphate dehydrogenase
GBM	Glioblastoma multiforme
GFAP	Glial fibrillary acidic protein
GIC	Glioblastoma initiating cell
GSC	Glioblastoma stem cell
H&E	Hematoxylin and Eosin
HIF1A	Hypoxia inducible factor 1 subunit alpha
IDH1	Isocitrate dehydrogenase 1
IDO1	Indoleamine 2,3-dioxygenase 1
IF	Immunofluorescence
ITGA6	Integrin subunit alpha 6
ITH	Intratumoral heterogeneity
KD	Knockdown
L1CAM	L1 cell adhesion molecule
LDA	Limiting dilution assay
LMO2	LIM domain only 2
MAP2	Microtubule associated protein 2

Mes or MES	Mesenchymal
MET	Mesenchymal-epithelial transition factor
MGMT	O-6-Methylguanine-DNA methyltransferase
NF1	Neurofibromin 1
NMF	Non-negative matrix factorization
NOD-SCID	Nonobese diabetic-severe combined immune-deficiency
NSG	NOD-SCID gamma
OG	Oligodendroglioma
Olig2	Oligodendrocyte transcription factor 1
P-GBM or pGBM	primary GBM
PI3K	Phosphatidyl inositol 3 kinase
PN	Proneural
PTEN	Phosphatase and tensin homolog
R-GBM or rGBM	Recurrent GBM
REMBRANDT	REpository for Molecular BRAin Neoplasia DaTa
RT-PCR	Real-time polymerase chain reaction
RTK	Receptor tyrosine kinase
SoC	Standard of care
SOX2	Sex determining region Y-Box 2
TACC3	Transforming acidic coiled-coil containing protein 3
TCGA	The cancer genome atlas
TMZ	Temozolomide
Tx	Treatment
VEGF-A	Vascular endothelila growth factor A
VEGFR	Vascular endothelial growth factor receptor
PDGFR	Platelet derived growth factor receptor
VHD	Variable heavy domain
WHO	World Health Organization

Declaration of Academic Achievement

I contributed to the design and execution of the work presented in this thesis. I performed the data analysis, interpretation and writing of all the sections. Dr. Sheila Singh supervised all research projects and aided in data interpretation. Contributions of co-authors to each publication are noted in preface for Chapters 2-5. This thesis is presented in the format of a “sandwich” thesis as outlined in the “guide for preparation of Master’s and Doctoral Theses” (v2016).

Chapter 1 gives an overview of the field of glioblastoma research and contains excerpts from following published works:

Qazi MA, Vora P, Venugopal C, Sidhu S, Moffat J, Swanton C, Singh SK. Intratumoral Heterogeneity: Pathways to Treatment Resistance and Relapse in Human Glioblastoma. *Annals of Oncology*, 28(7):1448-1456, 2017. DOI: 10.1093/annonc/mdx169.

Bakhshinyan D*, **Qazi MA***, Garg N, Venugopal C, McFarlane N, Singh SK. (2015). Isolation and Identification of Neural Cancer Stem/Progenitor Cells. In: Principles of Stem Cell Biology and Cancer: Future Applications and Therapeutics. John Wiley & Sons, Ltd., UK. (*co-authors).

Chapter 2 is an original published article describing the development of an *in vitro* model of GBM recurrence:

Qazi MA, Vora P, Venugopal C, McFarlane N, Subapanditha MK, Murty NK, Hassell JA, Hallett RM, Singh SK. A novel stem cell culture model of glioblastoma recurrence. *Journal of Neuro-Oncology*, 126(1):57-67, 2016.

Chapter 3 is an original published article describing the identification and co-targeting of EphA2 and EphA3 in recurrent GBM:

Qazi MA, Vora P, Venugopal C, Adams J, Singh M, Hu A, Gorelik M, Subapanditha MK, Savage N, Yang J, Chokshi C, London M, Gont A, Bobrowski D, Grinshtein N, Brown KR, Murty NK, Nilverbrant J, Kaplan D, Moffat J, Sidhu S, Singh SK. Cotargeting ephrin receptor tyrosine kinases A2 and A3 in cancer stem cells reduces growth of recurrent glioblastoma. *Cancer Research*, 78(17):5023-5037, 2018.

Chapter 4 is an original published review article exploring themes of intratumoral heterogeneity in primary and recurrent GBM, role of cancer stem cells in GBM recurrence, and the clinical implications of intratumoral heterogeneity:

Qazi MA, Vora P, Venugopal C, Sidhu S, Moffat J, Swanton C, Singh SK. Intratumoral Heterogeneity: Pathways to Treatment Resistance and Relapse in Human Glioblastoma. *Annals of Oncology*, 28(7):1448-1456, 2017.

Chapter 5 presents unpublished data on the development of *in vivo* model of GBM recurrence and the characterization of the minimal residual disease in GBM.

Chapter 6 discusses the implications of the research presented in this thesis and explores future research directions to improve our understanding of recurrent GBM biology, identify novel targets and develop better therapies for the treatment of recurrent GBM.

CHAPTER 1: Introduction

1.0 Preamble

This chapter presents a general introduction to the present field of glioblastoma (GBM) research, highlighting current treatment options for patients, the clonal evolution of primary GBM to recurrent GBM through therapy, our present understanding of the cancer stem cell hypothesis and models as applied to the study of GBM, and the need to develop models to profile and characterize recurrent GBM biology. Lastly, I present the hypothesis and overall aims of this thesis.

This chapter contains excerpts from the following published review and book chapter:

1. **Qazi MA**, Vora P, Venugopal C, Sidhu S, Moffat J, Swanton C, Singh SK. Intratumoral Heterogeneity: Pathways to Treatment Resistance and Relapse in Human Glioblastoma. *Annals of Oncology*, 28(7):1448-1456, 2017. DOI: 10.1093/annonc/mdx169.
2. Bakhshinyan D*, **Qazi MA***, Garg N, Venugopal C, McFarlane N, Singh SK. (2015). Isolation and Identification of Neural Cancer Stem/Progenitor Cells. In: Principles of Stem Cell Biology and Cancer: Future Applications and Therapeutics. John Wiley & Sons, Ltd., UK. (*co-authors).

1.1 Glioblastoma

1.1.1 Clinical characteristics

Glioblastoma (GBM) is the most common and malignant tumour affecting the adult nervous system (WHO Grade IV)(Louis et al., 2016). Between 2009-2013, 5,830 Canadians were diagnosed with GBM, at an incidence rate of 4.06 per 100,000 persons per year, making GBM the most commonly diagnosed tumor of the neuroepithelial origin (59.2% [CI 58.2%-60.2%] of all neuroepithelial tumors)(Walker, Davis, CBTR founding affiliates, 2019). Histopathologically, GBM shows astrocytic features and is characterized by multifocal palisading necrosis and microvascular proliferation(Aldape, Zadeh, Mansouri, Reifenberger, & Deimling, 2015). The cells are marked by nuclear atypia and mitotic figures with high Ki67 proliferation index, indicative of the high malignancy associated with GBM. Although morphologically similar, GBM can be divided into two categories: primary GBM and secondary GBM. Vast majority of the cases (~90%) consists of rapidly growing de novo primary GBM with no previous evidence of a less malignant neoplastic growth. Primary GBM is generally diagnosed in older patient population (>45 years) and represents poorer overall survival(Ohgaki & Kleihues, 2013). Secondary GBM, on the other hand, represents the progression of the disease from a lower grade astrocytoma (grade II or III) and manifests in younger patients (<45 years). Further molecular characterization of these two GBM types has led researchers to identify distinct underlying biological mechanisms that differentiates between primary and secondary GBM and may drive the differences that are observed in clinical outcomes of patient. In this introduction,

I will focus the rest of our discussion on exploring the biology and treatment paradigms pertaining specifically to primary GBM.

1.1.2 Current standard of care and disease prognosis

For newly diagnosed primary GBM, a multi-modal approach is undertaken to offer treatments to the patient. The current standard-of-care consists of surgical resectioning, followed by radiation and chemotherapy:

1. Surgical resectioning: Surgery remains one of the most important steps in the management of malignant brain tumors. Although the invasive phenotype of GBM makes it difficult to define the tumour margins, the extent of tumour resection is an important predictor of patient outcome. Gross total resection of the tumor mass has been shown to improve survival of patients(De Vleeschouwer et al., 2017; Sanai, Polley, McDermott, Parsa, & Berger, 2011), with the goal of maximally safe resection that maybe influenced by tumour location. The use of fluorescent agents, such as 5-aminolevulinic (5-ALA) has led to improvement in ability to perform gross total resection and also leads to improvements in progression free survival for patients(Stummer et al., 2006).
2. Radiotherapy: For the longest time, radiotherapy was the only additional treatment administered to patients diagnosed with GBM. Current standard of care for radiotherapy consists of fractionated focal irradiation of 2 Gy given daily for 5 days over a 6-week period, resulting in a total dose of 60 Gy(Stupp, Mason, & Van Den Bent, 2005).

3. Chemotherapy: Chemotherapy became a part of standard-of-care for GBM only in 2005 when Stupp et al. showed that concomitant and adjuvant treatment with temozolomide (TMZ), a DNA methylating agent, to radiotherapy led to increase in median overall survival from 12.1 to 14.6 months(Stupp et al., 2005). The current treatment consists of 75mg/m² of oral TMZ daily throughout radiotherapy. This is followed by 150-200mg/m² of oral TMZ administered daily for 5 days every 28 days for up to 6 cycles.

Despite aggressive, multi-modal treatment administered to GBM patients as described above, almost all patients with GBM relapse 7-9 months post-diagnosis. The 2-year survival rate for GBM stands at an abysmal 16.9% with only 5.5% of patients surviving at 5-years and 2.9% at 10-years(Ostrom et al., 2016).

1.1.3 MGMT promoter methylation – a prognostic factor

The mechanism of action of TMZ is driven by its ability to alkylate/methylate at O6 guanines in the DNA (J. Zhang, Stevens, & Bradshaw, 2012). This carcinogenic and toxic lesion causes mispairing of the methylated guanine with thymine, which activates DNA mismatch repair (MMR) during DNA replication. MMR recognizes the mismatch but is only able to repair the thymine and therefore excises thymine in the daughter strand, while the methylated guanine, which was the original lesion remains intact in the template strand. This causes MMR to go into futile repair cycling, inducing successive strand breaks to fix the mismatch, eventually resulting in G2/M arrest and triggering apoptosis (Wick et al.,

2014). However, the presence of O6-methylguanine methyltransferase (MGMT) enzyme allows the cell to fix the mismatch whereby MGMT is able to remove the methyl adduct and restore guanine binding with cytosine (J. Zhang et al., 2012). This allows for cell to survive. In the case of GBM, where TMZ as a chemotherapeutic is used to induce cytotoxicity, the presence of MGMT reduces cellular response to TMZ. One of the ways the expression of MGMT is regulated is through the methylation of the MGMT gene promoter, causing transcriptional repression. The promoter methylation status of MGMT is a prognostic factor in the efficacy of TMZ and leads to favorable clinical outcomes (Hegi et al., 2005). The median survival of patients with methylated MGMT promoter improves to 21.7 months as compared to 12.7 months for patients with unmethylated MGMT promoter when treated with TMZ and radiation. The 2-year survivorship is also extended to 46% for patients with methylated MGMT promoter compared to only 13.8% in the unmethylated group. However, due to lack of other therapeutic options for patients with unmethylated MGMT promoter, MGMT is not currently used as a clinical criterion for administering TMZ; rather all GBM patients receive concomitant and adjuvant TMZ.

1.2 Molecular classification of GBM

1.2.1 Mutational profile of GBM

Given the high malignancy of GBM, it was essential to dissect the tumour biology and improve our understanding of the mutational landscape that allows GBM to become such an aggressive disease. Studies on copy number alterations (CNA) started to identify regions of amplifications and deletions that potentially play a role in GBM tumorigenesis (Beroukhi et al., 2007; Bredel et al., 2005; Kotliarov et al., 2006).

Collectively over 300 glioma samples were included in these studies, and a pattern of amplifications/deletions started to emerge. Amplifications were mostly noted in regions with oncogenes such as epidermal growth factor receptor (EGFR), mesenchymal-epithelial transition factor (MET), platelet derived growth factor receptor (PDGFR), and Myc, and in p53 signalling (MDM2 and MDM4) to name a few. Meanwhile, deletions were observed in regions with tumour suppressors such as phosphatase and tensin homolog (PTEN) and retinoblastoma protein (RB1).

In 2008, studies from The Cancer Genome Atlas (TCGA) and Parsons et al. further clarified the mutational landscape of GBM (McLendon et al., 2008; Parsons et al., 2008). With over 200 GBM samples characterized through DNA copy number, gene expression, and DNA methylation profiling, TCGA was able to identify three critical signalling networks that harbours the most frequent mutations: Receptor tyrosine kinase (RTK) signalling, p53 signalling, and RB signalling. In fact, 74% of all GBM sample harboured a dysregulation in all three pathways, which suggested an integral role of these pathways in GBM tumorigenesis.

In over 88% of the samples, RTK signalling was altered either in the form of an amplification, a mutation or a deletion. EGFR amplifications or mutations accounted for the most common activating aberration at 45%, followed by mutations in Phosphatidylinositol 3 Kinase (PI3K, mutations in 15%), and PDGFRA (amplification in 13%). The most common inactivating aberration was found in PTEN, with 36% of GBM samples

harbouring a mutation or homozygous deletion, followed by neurofibromin 1 (NF1; mutation or homozygous deletion in 18%). All together, these aberrations contributed to proliferative capacity of GBM, leading to increased tumorigenicity of GBM cells.

p53 signalling was the next highest altered signalling pathway (in 87% of samples). Amplification in MDM2 was the most common activating aberration (14%) that led to altered p53 signalling followed by MDM4 amplifications in 7% of the samples. Both these genes play a role in inhibiting TP53 activity and contribute to cell survival. Homozygous deletions or mutations in CDKN2A (49%) and TP53 (35%) were the most common inactivating aberration. Together, these aberrations prevented p53 mediated cell-death or senescence, allowing for GBM cell survival.

Lastly, RB signalling was altered in 78% of GBM samples, with CDK4 amplification constituting the highest frequency of activating aberration (18%). Inactivating homozygous deletions and mutations in P16/INK4A (52%) and homozygous deletions in CDKN2B (47%) were the most common. These aberrations lead to a loss of cell cycle checkpoints, allowing GBM cells to divide and proliferate. At the same time, the Vogelstein group performed a more in-depth analysis of CNA in 22 glioma samples and identified a recurrent R132H mutation in isocitrate dehydrogenase 1 (IDH1), which was not identified in the TCGA database(Parsons et al., 2008). Further studies have characterized IDH1 mutation has a hallmark of secondary GBM while only 3-7% of primary GBM harbour this mutation(Dunn et al., 2012). Together, these pathways formed the basis of exploring GBM

biology further and serve as the core signalling networks that GBM relies on for tumour growth.

1.2.2 Transcriptomic subgrouping of GBM

Although the mutational landscape of GBM highlights multiple avenues of targeting, the clinical outcomes related to these mutations remained elusive. Hence, more robust correlations between dysregulated signalling networks and patient outcomes had to be determined to identify targets that would lead to potential therapeutic benefit. Gene expression profiling in the mid 2000s started to elucidate the gene signatures associated with clinical outcomes and patient survival (Freije et al., 2004; Mischel et al., 2003; Nutt et al., 2003). These studies showed that histopathological GBM actually represented multiple molecular subtypes with extensive inter-tumoural heterogeneity. Two seminal studies by TCGA and the Aldape group set the foundation for molecular classification of GBM subgroups (H. S. Phillips et al., 2006; Verhaak et al., 2010). Phillips et al. classified tumour gene expression based on prognostic groups and survival differences. They identified three main subtypes of high grade gliomas: Proneural, Proliferative and Mesenchymal, names based on the dominant feature of the gene list that characterized each subtype. The proneural subgroup presented the most favourable survival outcome, was associated with younger patient population, had similarities to normal neurogenesis, and was distinguished by activated Notch signaling. The proliferative and mesenchymal subtypes represented poorer survival outcomes, was associated with older patient population, and was distinguished by activated Akt signalling. While both subtypes also harboured PTEN loss and in some case cases EGFR amplification, the mesenchymal subtype was also associated

with angiogenesis. Although comprehensive gene expression linked with the proliferative subtype was elusive, the proneural and mesenchymal subtype represented robust subtypes and were always mutually exclusive, suggesting that these two subtypes may arise from different cells of origin.

In contrast, based on gene expression profile of almost 200 GBM samples, Verhaak et al. identified four transcriptomic subtypes of GBM: proneural, neural, classical and mesenchymal, which was then validated in a separate 260 GBM dataset. The classical subgroup is marked by amplifications or mutations in the EGFR; the neural subgroup is characterized by expression of neuronal genes; the pro-neural subgroup expresses neural stem cell genes such as Sox2 (sex determining region Y-box2) and Olig2 (oligodendrocyte transcription factor 2) and is driven by PDGFRA signaling; and the mesenchymal subtype is distinctly identified by expression of mesenchymal markers (such as CHI3L1 and MET) and mutations in NF1. Despite clearly distinct transcriptional profiles of the four subgroups of GBM, the clinical prognosis of each subgroup remained the same with only a slight survival advantage of aggressive chemoradiotherapy for the classical subgroup. Secondary GBMs largely fell into the pro-neural subgroup and were characterized by mutations in IDH1 and 2 as well as upregulated PDGFRA signaling. Although the methodologies and samples differ between the two studies, the identification of the proneural and mesenchymal subtype were the most concordant of all the gene expression subtypes. Both studies identified DLL3 and OLIG2 as important markers of the proneural subtype and CHI3L1 (or YKL40) as a marker of the mesenchymal subgroup. Further proteomic studies

by Brennan et al. corroborated these findings by identifying three signalling subgroups driven by EGFR-related signalling, PDGF-related signalling, or signalling alterations due to NF1 mutations, which could represent the classical, pro-neural and mesenchymal transcriptomic subtypes, respectively.

With the advancement in RNA-sequencing technologies, it also became possible to map the gene-fusion landscape of GBM. A study by Shah et al. first identified that 30-50% of GBM patient samples harbour a gene fusion event(Shah et al., 2013). They determined hotspots for gene fusions in GBM, with fusions frequently occurring on chromosomes 7p and 12q as well as on chromosomes 1, 4, 6, and 19. However, a majority of the gene fusions were limited to a single patient sample and very few recurred in multiple patient samples. Further exploration of gene fusions led to the identification of low-frequency but recurrent gene-fusions such as FGFR1-TACC3 (~1% of GBM samples) and FGFR3-TACC3 (~3-8% of GBM samples), which were associated with the activation of the ERK signalling network(Frattini et al., 2018; D. Singh et al., 2012). EGFR-SEPT14 gene fusion was identified in ~4% of the GBM samples and EGFR-PSPH in ~2% of the samples, which tend to activate STAT signalling(Frattini et al., 2013; Shah et al., 2013). Fusions of the neurotrophic tyrosine kinase receptor (NTRK) gene have been identified in ~1.5% of GBM samples {Kim:da}, while PTPRZ1-MET gene fusion, which leads to unfavourable prognosis, has been seen in 3% of GBM samples (H.-M. Chen et al., 2015).

Altogether, gene expression profiling combined with genomic mutational analysis set the stage for the development of targeted therapies which aimed to bring much needed hope for improving therapeutic options for patients diagnosed with GBM.

1.2.3 Development of targeted therapies

Given that angiogenesis plays an important role in GBM growth and microvasculature is a histopathological marker of GBM, some of the earliest targeted therapies were directed towards curbing the vascularization of the tumour. Vascular endothelial growth factor A (VEGF-A), an important mitogen for vascularization and angiogenesis, was constituted a good target for inhibiting the growth of blood vessels, and therefore Bevacizumab, a humanized monoclonal antibody against VEGF-A, was given accelerated FDA approval for testing in recurrent GBM. Although treatment with Bevacizumab seemed to led to improved progression free survival of recurrent GBM, systematic Cochrane review failed to find enough evidence for its use in primary or recurrent GBM (Ameratunga et al., 2018).

Since almost half of all primary GBM samples carry aberrations in EGFR (amplification, mutations), EGFR directed therapy were considered of significant importance for improving patient outcomes. EGFR kinase inhibitors such as erlotinib and gefitinib have been extensively tested in pre-clinical *in vitro* and animal models as well as in clinical trials for both primary and recurrent GBM(Chakravarti et al., 2013; Peereboom et al., 2010; Raizer et al., 2010; Uhm et al., 2011). Additionally, almost 20% of GBM also harbor deletions in exon 2-7 of EGFR, resulting in EGFRvIII, which alters the extracellular domain of EGFR and leaves the receptor constitutively active(Brennan et al., 2013). Since

conventional EGFR inhibitors fail to target EGFRvIII, a EGFRvIII peptide vaccine, Rindopepimut was developed for targeting and showed efficacy in pre-clinical and early phase trials. The targeting of both EGFR and EGFRvIII was achieved by the development of ABT-414, an anti-EGFR antibody drug conjugate. ABT-414 demonstrated cytotoxicity against patient-derived xenograft models of GBM (A. C. Phillips et al., 2016) and improves progression free survival rates in patients (Reardon et al., 2017; van den Bent et al., 2017). Although EGFR targeting showed great promise in pre-clinical studies, they failed to improve clinical outcomes of patients with GBM.

Similar efforts have been undertaken to target other molecular alterations in GBM. PDGFRA inhibition (e.g. dasatinib), FGFR gene fusion targeting by FGFR inhibitors, and MET inhibition (e.g. crizotinib) have all been tested in pre-clinical and early clinical trials. Although great effort was undertaken to dissect the genetic and transcriptomic alterations in GBM, unfortunately directed targeting has not been as fruitful as was expected. The disappointing results in clinical trials despite good pre-clinical efficacy suggests that GBM is more complex than presented through early genomic and transcriptomic studies and further in-depth understanding of the tumor biology is required to identify stronger therapeutic targets.

1.3 Intratumoral heterogeneity in GBM

1.3.1 Spatiotemporal heterogeneity in GBM

Although improper patient selection without molecular enrichment for the clinical trials and lack of strong pre-clinical validation in disease-relevant models could have led to poor

outcomes for the targeted therapies discussed earlier, even when these criteria were met, many therapies failed to show efficacy. This suggested relevance of certain targets to GBM biology may not be as universal as presumed and perhaps GBM presents heterogeneity at an intratumoral level that prevents targeted therapies to improve disease outcomes.

Considering the role of RTKs in GBM tumorigenesis, Stommel et al. used an RTK antibody array combined with single cell immunofluorescence (IF) to investigate RTK activation pattern in glioma cells lines and primary GBM tissue. They identified co-activation of multiple RTKs, including EGFR, PDGFRA and MET in single GBM tissue samples(Stommel et al., 2007). Single cell IF showed similar pattern of co-expression of multiple activated RTKs. In fact, the authors showed that co-targeting of multiple RTK was required to abrogate downstream PI3K signaling, illustrating the redundancy in the RTK signaling networks. Further studies using fluorescence in situ hybridization (FISH) analysis on GBM tissue specimens showed heterogeneous amplifications of EGFR, PDGFRA and MET(Snuderl et al., 2011; Szerlip, Pedraza, & Chakravarty, 2012). In fact, these studies demonstrated that different regions of the same tissue have differential RTK amplifications and that co-amplifications of EGFR, PDGFRA and/or MET were not mutually exclusive in single cells.

Spatiotemporal heterogeneity in GBM was further supported by surgical multisampling of single GBM and characterization using copy number and gene expression arrays(Sottoriva et al., 2013). This study found that different regions of a brain tumour harboured different

aberrations and alterations in gene copy numbers. Additionally, different fragments of a GBM tumour presented distinct transcriptional profile and could be classified in different GBM subtypes. Furthermore, phylogenetic reconstruction of each fragment led the researchers to identify that CNAs in EGFR and CDKN2A/B are early events in the tumorigenic process while mutations in PDGFRA and PTEN appear later in the cancer progression. Altogether, these studies identified the presence of extensive intratumoral heterogeneity in GBM, which could explain the lack of response to single agent targeted therapies.

1.3.2 Intratumoral heterogeneity at a single cell level

With further technological advances, it became possible to investigate intratumoral heterogeneity (ITH) using the sequencing platforms at a single cell level. Two studies have looked at the genomic and transcriptomic profiles of individual GBM cells to identify the extent of ITH (Francis et al., 2014; Patel et al., 2014). In EGFR-amplified GBMs only, the researchers identified the presence of multiple EGFR mutations coexisting in the same GBM tumour. In addition, EGFR variants, though present in bulk analysis, exist in mutually exclusive cellular subpopulations, giving the tumour unprecedented heterogeneity and diversification in its EGFR expression and mutational profile (Francis et al., 2014). With the ITH in EGFR expression in mind, researchers have tested whether gefitinib targeted a specific subpopulation of EGFR expressing cells. Parker et al. found that gefitinib specifically targets a high-burst cellular subpopulation in EGFR-amplified tumours only, which could explain the lack of gefitinib efficacy in targeting GBM due to the presence of multiple subpopulations that have differential response to therapy (J. J. Parker et al., 2018).

At a single cell level resolution, the study by Patel et al. showed that using single cell RNA-sequencing, a single tumor consisted of a heterogeneous mixture of cells representing all of the different GBM subgroups(Patel et al., 2014). When examining the pro-neural subgroup, which had the best survival of all GBM subgroups, the authors showed that patients with pro-neural tumors that also displayed markers of other subgroups had poorer survival, especially if the relative representation of the alternative subgroups was high in the tumor(Patel et al., 2014), emphasizing the role ITH may play in therapy resistance. Another study by Reinartz et al. show that single cell derived GBM subclones have distinct genetic identity and maintain differential drug resistance profile(Reinartz et al., 2016). Similarly, there is heterogeneity in the methylation of the MGMT promoter that could explain why certain MGMT promoter methylated patients do not respond to TMZ treatment while some unmethylated patients do (N. R. Parker et al., 2016). Multiple spatial samplings of the GBM tissue specimen have shown variations in MGMT methylation status in up to 14% of the samples and this was independent of the transcriptional subgrouping each sample belonged to. In addition, the researchers also showed ITH in the MMR and BER pathway genes that can also promote therapy-resistance independent of the MGMT promoter methylation status. Additionally, a study by Meyer et al. demonstrated that clonal populations derived from single cells have variable response to TMZ as well other drugs, linking genomic heterogeneity to functional heterogeneity(Meyer et al., 2015). These single-cell derived clonal populations also presented with differential EGFR expression and MGMT promoter methylation status. On a larger scale, heterogeneous patterns of overall

DNA methylation profile have been seen in GBM samples (Klughammer et al., 2018). These studies together present that GBM harbors extensive ITH at genomic, epigenomic, and transcriptomic levels and could potentially be a source of resistance to current standard-of-care treatment, leading to disease relapse.

1.4 Evolution of treatment-refractory, recurrent GBM

1.4.1 Transcriptomic subgrouping of recurrent GBM

Considering the extent of ITH in primary GBM, it is important to consider whether the subtyping of GBM is maintained post-chemoradiotherapy or a certain subtype dominates the recurrent GBM biology. Early works by Phillips et al. suggested that recurrent GBM preferentially moved towards a mesenchymal gene expression profile, which was concordant with the aggressive nature of recurrent GBM (H. S. Phillips et al., 2006). Longitudinal studies to identify whether subtype switching occurs in GBM has led to mixed results. Using single sample GSEA, Wang et al. (2016) showed that 2/3 of primary GBM cases switch their subtype at recurrence (Jiguang Wang et al., 2016). However, similar undertaking by the Verhaak group showed subtype switching upon recurrence in only 45% of the IDH-WT GBM samples (Qianghu Wang et al., 2017). Despite the differences in the percentage of primary GBM that switch subtype at recurrence, both studies agreed that mesenchymal subtype was the most stable and predicted the poorest survival at recurrence. In addition, the significant loss of the classical subtype at recurrence could be explained by the loss of EGFR or EGFRvIII expression over therapy, which results in gene expression for another subtype to dominate the tumour profile.

Interestingly, the mesenchymal subtype presented low tumour purity with high expression of tumour associated macrophages/microglia(Qianghu Wang et al., 2017). In particular, tumours of mesenchymal subtypes had significantly higher expression of anti-inflammatory and tumour-promoting M2 macrophage phenotype. This was also supported by a decrease in activated natural killer cell gene signature, together suggesting that the mesenchymal subtype may intrinsically support a tumour-promoting immune microenvironment, that could be a potential therapeutic target. In addition, DNA methylation profiles could also be used to predict GBM subtypes and identify subtype switching in GBM samples over the course of disease progression (Klughammer et al., 2018). Although, subtype switching gives insights into some mechanisms of disease relapse, this still has to be studied with caution as tumour sampling bias still clouds our knowledge of the extend of the subtype ITH present in the tissue sample and whether the tumour region sequenced actually represents the subtype of the entire tumour or not.

1.4.2 Therapy may drive GBM recurrence

In order to understand GBM recurrence, we need to identify whether therapy plays a role in promoting GBM recurrence and further resistance to therapy. Given that patients with GBM receive radiotherapy and methylating/alkylating chemotherapy, both these treatments induce DNA damage as their mechanism of action and can in fact lead to an accumulation of more mutations that can give certain cellular subpopulations survival advantage. Studies so far have identified that TMZ leads to the accumulation of a hypermutated phenotype in GBM at recurrence(Hunter et al., 2006; Jiguang Wang et al., 2016; Qianghu Wang et al., 2017). A large number of mutations were accumulated in genes

involved in the MMR pathway, which has also been observed in the malignant progression of low-grade gliomas treated with TMZ(van Thuijl et al., 2015). The main gene harbouring the mutation in MMR pathway is the MSH6 gene, a critical component for identifying base-base mismatches, with the mutation generally resulting in a loss of function(Jiguang Wang et al., 2016). Other genes that harboured mutations at recurrence included LTBP4, PRDM2, and IGF1R. Upon further investigation, the authors discovered that the mutations in LTBP4 gene led to increased expression of the gene, which was correlated with significantly poorer survival in recurrent GBM. LTBP4 is part of the TGF- β pathway and activation of this gene exclusively in recurrent GBM could suggest that TGF- β may act as a therapeutic target in recurrent GBM. In addition, Verhaak et al. also showed that the hypermutated phenotype also correlated with higher CD8⁺ T cell expression in the tumours(Qianghu Wang et al., 2017). This could result from the generation of neoantigens due to the TMZ-associated hypermutation resulting in the activation of the immune system and could potentially make the tumour more responsive to checkpoint blockade therapies. In summary, chemotherapy using TMZ is associated with higher mutational burden in recurrent GBM, which could have long-lasting effects on tumour biology by making the tumour more resistant to future therapeutic interventions(Muscat et al., 2018).

1.4.3 Spatio-temporal patterns of GBM recurrence

In a study of 23 paired primary-recurrent GBM samples, Kim et al. performed whole exome sequencing to identify clonal composition patterns in GBM(H. Kim et al., 2015a). They found that in p53 mutated GBM, there was an increase in subclonal mutation frequency as compared to p53 wild-type GBM. Further analysis through whole genome sequencing of

10 paired primary-recurrent GBM samples showed two patterns of recurrence: ancestral origin and clonal evolution. In the ancestral pattern of recurrence, primary and recurrent GBM tumours share some cluster of clonal mutations while significant clusters of clonal mutations are not present in the recurrence, leading to less overlap between the mutations in primary and recurrent GBM. This would suggest an ancestral origin of the recurrent tumour, which also gave rise to the primary tumour but was much earlier in tumour progression and therefore did not have other clonal mutations that were present in the primary tumour. In the clonal evolution recurrence pattern, there is a higher degree of overlap of clonal mutations in primary and recurrent GBM samples. This suggests that over the course of therapy, the tumour is reduced to a residual disease and from this population the recurrent tumour emerges, and therefore it harbors the clonal mutations of the primary tumour plus additional private mutations as the tumour progresses. The authors also mention the presence of recurrence patterns that incorporate both these models, which again points to the extensive ITH present in the region where spatially distinct regions of the tumour may be driven by an ancestral origin or a clonal evolution of the primary tumour. A case study by Swanton and colleagues (Favero et al., 2015) again showed that the clonal mutation (IDH R132H) in a primary GBM was lost in the recurrence, which itself was dominated by a subclone consisting of whole genome doubling and a double-minute chromosome, that carried amplified regions of PDGFRA, KIT and CDK4.

While treatment can lead to differential recurrence patterns in GBM, another important observation regarding the location of recurrent GBM has emerged and how that can explain

the resulting tumour biology. While majority of GBM relapse locally, some tumour relapse distally. Kim et al. wanted to explore whether the recurrence patterns also had specific evolutionary patterns. Using 34 paired primary-recurrent GBM samples, the authors subjected the specimens to whole-exome sequencing and identified two groups of recurrence: high mutation retention (~80%) and low mutation retention (~30%)(J. Kim et al., 2015b). When compared to clinical parameters for correlations with these groups, the authors identified that the low mutation retention group belonged to GBMs that recurred distally and high retention mutation retention was found in local recurrences. This suggests that distal recurrence originated from an ancestral cell population in the primary tumour, followed a divergent evolutionary trajectory and therefore retained lower mutations as those found in its counterpart primary tumour. On the other hand, local recurrence, which represents the majority of the tumour, follow a clonal evolution trajectory by branching off later in the primary tumour progression and therefore retaining more mutations of the primary tumour. This study suggests that exploring treatment options for recurrent GBM based on the primary GBM profile may turn futile considering extensive evolution of the tumour after therapy, especially for tumour that recur distally. A similar study looked at the difference in mutations between focal GBM tumour and multi-focal GBM tumours(J.-K. Lee et al., 2017). As expected, multi-focal GBM tumour presented much more heterogeneous and divergent mutational profile as compared to focal tumour, that shared large number of clonal and subclonal events. Despite emerging patterns of GBM recurrence, given the extensive patient-to-patient variation and ITH, the pattern of clonal evolution will likely vary from patient to patient, and only large population-based studies

of the clonal maps of hundreds of sequenced GBMs will eventually discern reproducible cohorts of patients that recur in a similar manner. In any case, intratumoral heterogeneity in clonal cell populations may represent the root of therapy failure, the driver of development of treatment resistance, and ultimately results in recurrence of the malignancy. However, given the large number of mutational signatures identified in recurrent GBM, how do we evaluate which of the mutations or signalling network represents functionally valid target for therapeutic development?

1.5 Cancer stem cell hypothesis: identification of glioblastoma stem cells

1.5.1 Identification of cancer stem cells in GBM

According to cancer stem cell hypothesis, within a heterogeneous cancer, a small population of cells, the cancer stem cells (CSC), exhibits stem cell properties of self-renewal, proliferation and multilineage differentiation(Dalerba, Cho, & Clarke, 2007). At the cellular level, functional GBM heterogeneity can then be explained by the existence of these CSCs, variably labeled in the literature as BTSCs (brain tumor stem cells) or GSCs (glioblastoma stem cells)(Clarke & Fuller, 2006; Dalerba et al., 2007; S. K. Singh, 2003; S. K. Singh et al., 2004). GSCs may arise from the dysregulation of genes that govern self-renewal, the cardinal property of stemness that allows a stem cell, at each cell division, to generate an identical functional copy of itself and a cell of the same or different phenotype(Reynolds & Weiss, 1992). In brain tumours, BTSC were identified and purified as a subpopulation of human GBM that exhibited stem cell properties both *in vitro*(Galli et al., 2004; Hemmati et al., 2003; S. K. Singh et al., 2003) and *in vivo*(S. K. Singh et al., 2004). The assays were adopted from the study of normal neural stem cell (NSC), where

neural stem cell displayed their self-renewal capacity through the formation of neurospheres, a cluster of cells believed to originate from the clonal expansion of a single NSC in serum-free conditions supplemented with EGF and FGF(Reynolds & Weiss, 1992). When brain tumours were grown in similar cell conditions, they also gave rise to neurospheres, indicating the presence of CSCs in GBM and other brain tumours. For further experimentation to prove the tumour-initiating property of BTSCs, researchers adopted *in vivo* models from hematopoietic cancer stem cell xenografts that allows human cells to be engrafted in immune-compromised mice and showed that BTSC allows for tumour formation(Bonnet & Dick, 1997; S. K. Singh et al., 2004). The GSC model of GBM is thought to recapitulate the functional heterogeneity that exists within a tumor, as a GSC has been shown to give rise to all the cellular subpopulations within a tumor(Hemmati et al., 2003; S. K. Singh et al., 2004), including endothelial cells(Chroschinski, Sampey, Maherali, Reproducibility Project: Cancer Biology, 2015; Ricci-Vitiani et al., 2010; Soda et al., 2011; Rong Wang et al., 2010b) but not immune cell infiltrates, which may arise from bone-marrow derived macrophages or brain-resident microglia(Quail et al., 2016). Although GSCs can originate from mutations in any of the cellular compartments in the neural lineages, a recent study suggests that the cell-of-origin of GBM is a postulated astrocyte-like NSC that resides in the SVZ region of the brain(J. H. Lee et al., 2018). By isolating normal SVZ tissue that was away from the tumour and comparing it to mutations in the tumour as well as normal cortical tissue or blood for reference genome, the researchers were able to identify low-levels of driver mutations in the cells from the SVZ. This suggests that GBM arises from mutations in the NSCs that allows for the hijacking of

stem cell properties and gives rise to the malignant disease phenotype of GBM.

1.5.2 Markers of glioblastoma stem cells

Over the years, multiple GSC markers have been identified that represent potential targets for therapeutic development. Prospective sorting of GBM cells using CD133, a marker previously described for NSCs(Uchida et al., 2000), led to the identification of first GSC marker as CD133+ preferentially gave rise to neurospheres in cultures and had significantly higher tumour initiating capacity in *in vivo* limiting dilution assays as compared to CD133- GBM cells(S. K. Singh et al., 2003; 2004). CD133 expression is also linked to Wnt signalling, further suggesting that the CD133+ GSC may represent the dysregulated counterparts to normal NSC(Mak et al., 2012; Venugopal et al., 2015) and could be at the apex of tumour cell hierarchy. CD133 expression is also linked with patient survival as GBM patients with higher CD133 expression have poorer overall survival(Pallini et al., 2008; Venugopal et al., 2015).

Although CD133 marks a more tumorigenic population in GBM, it does not mark the entire BTSC population in GBM as subsequent studies have shown that in some GBM samples, CD133- cells are also able to initiate tumors in xenograft models(R. Chen et al., 2010; Hau et al., 2007). This led to the identification of additional markers of BTSCs in GBM. CD15/SSEA-1, a carbohydrate adhesion molecule which is synthesized by FUT4, was shown to also for enrich GSC population from GBM and could act as GSC marker in cases where CD133 is unable to define a GSC population due to very low or no expression(Son, Woolard, Nam, Lee, & Fine, 2009). Studies from the Rich lab have also identified

additional GSC markers that are also co-expressed with CD133, such as L1CAM and integrin $\alpha 6$ (Bao et al., 2008; Lathia et al., 2010). L1CAM, a neural cell adhesion molecule, regulates neural cell growth, survival, migration, and axonal outgrowth and neurite extension during central nervous system development. Its overexpression in GBM as well as coexpression with CD133 suggests that L1CAM could further enrich for the GSC compartment in CD133+ cells. Similarly, integrin $\alpha 6$, a component of the $\alpha 6\beta 1$ laminin receptor, plays an important role in niche-NSC interactions in the subventricular zone (SVZ) and enrich for NSC activity (Campos et al., 2004; Lathia et al., 2007; Leone et al., 2005). Further studies have found that integrins, through their interaction with glycoproteins on the surface of GBM cells, promote a mesenchymal phenotype in GBM, implicating GSC markers in the maintenance of aggressive GBMs (Barnes et al., 2018). Together these studies suggest that further exploration of the GSC marker landscape will allow for further enrichment and purification of the CSC population in GBM and other brain tumours.

Along with cell surface markers, multiple transcription factors have also been identified as putative GSC markers and regulator of stemness. Bmi1, a member of the PRC complex, which represses gene expression, was first shown to prevent premature senescence in NSCs (Molofsky, He, Bydon, Morrison, & Pardal, 2005). It was then determined that Bmi1 also regulates glioma formation in mouse models (Bruggeman et al., 2007), is regulated by the sonic hedgehog pathway (X Wang et al., 2012), and maintain GBM tumorigenicity (Abdouh et al., 2009). In NSCs, Bmi1 cooperates with FoxG1 to maintain

NSC stemness, and this relationship was also confirmed in brain tumours whereby FoxG1 is downstream of Bmi1 and both regulate each other's gene expression through promoter binding(Manoranjan et al., 2013). A study by Suva et al. explored the transcriptional programs that dictate the GSC phenotype in GBM. They achieved this by comparing GSCs to their differentiated counterparts (terms differentiated glioblastoma cells or DGCs) and looked for markers that govern these two cell states(Suva et al., 2014). The authors identified 19 GSC specific transcription factors that were expressed at very low levels in DGCs. Of the 19 transcription factors, four core transcription factors could sufficiently induce a GSC phenotype in DGCs, namely POU3F2, SOX2, SALL2 and OLIG2, all part of the normal neurodevelopmental programs as well. Sox2 (SRY box 2) is critical for the maintenance of neural stem cells and its expression downregulated during progenitor final cell cycle during differentiation.

Multiple studies have also implicated the Eph tyrosine kinase receptors (EphR) and ephrin ligands in malignant progression of GBM tumours and are associated with poor prognosis(Day, Stringer, & Boyd, 2014). EphRs, which represent the largest family of tyrosine kinases in human, play integral roles in cellular sorting, axon guidance in the brain, at the neural synapses, and in angiogenesis(Klein & Kania, 2014; Merlos-Suárez & Battle, 2008; Pasquale, 2008). Various members of EphA/ephrin-A and EphB/ephrin-B have individually been shown to have functional roles in GBM cell migration, invasion and angiogenesis mediated through GSCs(Binda et al., 2012; Miao et al., 2009). Specifically, EphA2 and EphA3 have been explored as potential GSC markers(Binda et al., 2012; Day

et al., 2013; Miao et al., 2014; Wykosky, 2005). Co-expression of EphA2 along with CD15 was shown to mark a highly tumorigenic population in GBM and could be targeted with an EphrinA1-Fc, the natural ligand of EphA2(Binda et al., 2012). Similarly, EphA3 has also been shown to be a GSC marker and regulated the tumorigenic potential of GSCs through Akt pathway(Day et al., 2013). However, considering the redundancy in the function of EphR in normal and neoplastic environments, it is important that all EphR be more comprehensively profiled in the context of GBM tumorigenesis and disease progression. Hence, numerous markers of GSC have been implicated in GBM and they offer multiple avenues for functional therapeutic targeting in GBM.

1.5.2 Role of GSCs in mediating therapy resistance

The aberrant dysregulation of stem cell signaling and properties of GSCs as described earlier may allow the cancer to persist despite aggressive radiotherapy and chemotherapy (Figure 1). For example, CD133+ GSCs have higher activation of hypoxia signaling, c-Myc signaling as well Akt, suggesting that CD133+ could potentially survive in stressful environments and especially through therapy. In particular, given the hypoxic microenvironment in GBM, the activation of HIF2 α in CD133+ GBM could allow it to GSCs to survive in hypoxic cores of the GBM tumour and shift its metabolic signaling as well(Li et al., 2009). Right after the identification of CD133 as a GSC marker, CD133+ cells were also shown to be radiotherapy-resistant, with radiation leading to enrichment and survival of the CD133+ cells. CD133+ cells maintain their radio-resistant phenotype through the activation of DNA damage checkpoint pathway, allowing the cells to repair radiation induced DNA damage by arresting cell cycle(Bao et al., 2006). Notch signalling

in GSC has also been shown to be important regulators of GSC radio-resistance, with constitutive activation of Notch1 and Notch 2 protecting GSC against radiation-induced cell death while inhibition of the Notch pathway renders GSC radiation-sensitive (Jialiang Wang et al., 2010a). Additionally, hypoxia also regulates GSC survival through the recruitment of the Notch signaling in GBM(Man et al., 2018). Radiation resistance has also been shown to results from the presence of DNA replication stress particularly in CD133+ cells, which exhibit higher levels of stalled replication forks and therefore maintain radiation-resistance through constitutive activation of the DNA damage response pathways (Carruthers et al., 2018). EZH2, a member of the PRC2 complex, which has also been identified as a GSC specific marker, also maintains GSC radiation-resistance through the activation of the MELK/FOXM1 pathway (S.-H. Kim et al., 2015c). Furthermore, m6A demethylase ALKBH5 has been shown to sustain FoxM1 expression to sustain GSC tumorigenicity, linking RNA modification to gene expression changes, and in turn modulating resistance profile of the tumours(S. Zhang et al., 2017). Moreover, expression of EZH2 and Bmi1 represent two different subpopulations of GBM cells and a study by Jin et al. showed that co-targeting of both EZH2 and Bmi1 was necessary to reduce tumour burden(Jin et al., 2017).

GSC also maintain cellular mechanisms to protect against chemotherapy. Resistance to TMZ seen in CD133+ cells seems to be mediated through multiple mechanisms including higher expression of MGMT to maintain DNA repair mechanism and increased expression of anti-apoptotic genes and ABC transporters such as BCRP1 in CD133+ cell

population(Liu et al., 2006). In addition, loss of Sox2 leads to a loss of drug-resistance in CD133+ cells suggesting that resistance in CD133+ cells is mediated through the Sox2 signalling (Song et al., 2016).

Together, these studies demonstrate that GSCs not only maintain the functional hierarchy and ITH in GBM but also are resistant to current SoC chemotherapy and radiotherapy offered to patients. Further identification and characterization of the post-treatment GSC population in recurrent GBM would enable the researchers to identify targets that can have therapeutic benefits for an otherwise treatment-refractory recurrent GBM patient population.

1.6 Shifting the focus to the study of recurrent GBM biology

Since it is evident that recurrent GBM represents a biologically distinct entity in the progression of GBM, it is pertinent that further research focus on the study and characterization of the recurrent GBM biology. Longitudinal studies of GBM over therapy have largely focused on genomic landscape of the recurrent GBM, which limits researchers' ability to decipher between driver and passenger mutations and what are functionally relevant mutations that influence the disease progression(H. Kim et al., 2015a; J. Kim et al., 2015b). One of the potential targets identified include members of the MMR pathway and especially MSH6(Jiguang Wang et al., 2016). Given that TMZ induced DNA methylation activates MMR, it would be expected to find mutations in the MMR pathways as a resistance mechanism and target for recurrent GBM. Loss of function mutations in MSH6 were exclusively found in recurrent GBM, suggesting that further understanding of

the network governed by MSH6 and other MMR proteins could result in finding a therapeutic target to resensitize cells to chemotherapies, such as TMZ.

Activation mutations in LTBP4 have also been found in recurrent GBM only and plays a role in the TGF- β pathway. Further studies need to be undertaken to fully explore the signaling governed by LTBP4 and find opportunities for targeting. Another important aspect that has been highlighted by genomic studies is the importance of targeting truncal mutations rather than subclonal mutations to achieve therapeutic efficacy (J.-K. Lee et al., 2017). Lee et al. demonstrated that in patient derived glioblastoma cells, targeting of truncal mutations with chemical screens led to more efficacious response than targeting of private events in reducing tumour burden. Of course, the ability to target truncal events is limited by our ability to profile multiple samples from every patient. Nonetheless, looking for clonal changes in tumour evolution is an important avenue to pursue for treatment of recurrent GBM. Lastly, increasing evidence is suggesting the important role of the tumour microenvironment in disease recurrence and especially with many recurrent GBM preferentially being mesenchymal subtype, they have increased presence of tumour associated macrophages and higher levels of pro-tumorigenic M2 phenotype (Qianghu Wang et al., 2017). Targeting of the tumour niche through the regulation of the immune system offers another window to treating recurrence and needs to be explored further.

Although advances in genomic and transcriptomic profiling of GBM has led to the identification of potential targets for the treatment of recurrent GBM, current models do

not capture the entire spectrum of disease progression. In addition, given the extensive intratumoral heterogeneity, few studies have focused on co-targeting of multiple targets in recurrent GBM that could be representative of different subclonal populations found within a single recurrent GBM. Studies now need to focus on developing functionally and clinically relevant models of recurrent GBM that have the potential to be applied in a personalized medicine setting to treat each GBM as an individual and distinct tumour entity and model its unique disease progression through therapy to identify relevant therapeutic targets.

1.7 Summary of Intent

Glioblastoma (GBM) is the most common and aggressive primary brain tumour (World Health Organization grade IV), feared for its near uniformly fatal prognosis (Louis et al., 2016; Stupp et al., 2005). Despite multimodal therapy, consisting of surgical resectioning followed by chemotherapy and radiation therapy, patients on average experience tumour relapse at 7-9 months and median survival rarely extends beyond 15 months (Stupp et al., 2005; Walker et al., 2019). Though breakthrough with adjuvant chemotherapeutic temozolomide (TMZ) has extended survival by three months, GBM remains an incurable disease. The poor disease prognosis for GBM has been attributed to extensive cellular and genetic heterogeneity existing at both inter- and intra-tumoral level (McLendon et al., 2008; Patel et al., 2014; Verhaak et al., 2010). Recent studies have demonstrated the utility of stem cell models to interrogate intratumoral heterogeneity, using single-cell transcriptome analysis to identify important stem cell signatures driving tumor recurrence (Patel et al., 2014). Consequently, our brain tumor initiating cell (BTIC) model (S. K. Singh et al., 2003;

2004), combined with genomic deep-sequencing technologies may begin to resolve the extent of GBM intratumoral heterogeneity. Although data suggests that GBM BTICs are chemo- and radioresistant, no study has prospectively identified whether such BTICs are causal of tumor relapse, and whether the same BTIC populations that drive tumor initiation also drive recurrence (Bao et al., 2006; Liu et al., 2006). Additionally, research to identify therapeutic targets in recurrent GBM is very sparse. Given the unmet clinical need to develop new therapies for patients with recurrent GBM, **I hypothesize that a pre-clinical model of GBM recurrence that tests the combined role of chemoradiotherapy in disease recurrence will allow for the identification of functionally relevant, recurrent GBM-specific targets for therapeutic development.**

The aims of this thesis were to:

Aim 1: To develop an in vitro stem cell culture model of GBM recurrence.

Aim 2: To develop a therapy-adapted human-mouse xenograft model of GBM recurrence using patient derived GBM samples.

Aim 3: To identify genes and signaling pathways exclusively driving GBM recurrence and develop potential therapies against them.

The ability to develop a pre-clinical model of GBM recurrence that recapitulates the clinical progression of the disease as seen in patients could help identify targets before the patient experiences relapses and allow for personalized medicine approaches to be applied for the treatment of recurrent GBM (conceptually reviewed in **Chapter 4**).

To this extent, I first developed an *in vitro* stem cell culture model of recurrent GBM that

used physiologically and clinically relevant combined doses of radiotherapy and chemotherapy, TMZ (**Chapter 2**). As GBM stem cell cultures enable us to maintain the functional intratumoural heterogeneity present in the patient, profiling the changes in the GSC compartment over the course of treatment could lead to identification of functionally relevant signaling networks that allow for therapy resistance. I show that *in vitro* chemoradiotherapy of primary, treatment naïve GBM leads to increased sphere formation capacity of the cells and GSCs are marked by higher expression of Bmi1 and Sox2 and a switch to a CD133-/CD15+ GSC marker expression. Gene expression profiling of post-treated GSCs showed differential gene expression between radiation only treatment and combined chemoradiotherapy treatment, with enrichment of important GBM signaling networks.

I next developed an *in vivo* xenograft model of GBM recurrence to profile all steps of the disease progression as observed in the patient: from primary, treatment naïve GBM stage to post-treatment minimal residual disease (MRD) timepoint, to final recurrence of the tumour post-therapy (Figure 2). The model we developed is amenable to modification in the treatment protocol as per the therapy administered to the patient and can include testing of novel compounds for pre-clinical validation (**Chapter 5**). I show that cellular DNA barcoding and single cell RNA-sequencing can be easily incorporated in the model and will lead to greater understanding of the clonal evolution of the tumour and discovery of therapeutic targets.

Lastly, using an EphR profiler, single cell proteomics by CyTOF, and *in vitro* and *in vivo* stem cell assays, I identified that EphA2 and EphA3 together mark a highly tumorigenic GSC population in patient-derived recurrent GBM samples (**Chapter 3**). We then developed a bispecific antibody (BsAb) that co-targets both EphA2 and EphA3 and I identified the BsAb mediates its mechanism of action through receptor phosphorylation and internalization that leads to reduced activation of the Akt and Erk pathways, resulting in a loss of stemness, increase in cellular differentiation, and decrease in tumorigenic potential of recurrent GBM.

Collectively, in this thesis I have developed models of GBM recurrence that can be used as surrogates to profile and characterize mechanisms of therapy resistance in GBM and identify targets in a patient-specific manner. Given the extensive ITH in GBM, I also demonstrate the significance of using multi-targeting approaches to achieve therapeutic benefit in recurrent GBM.

CHAPTER 1 FIGURES

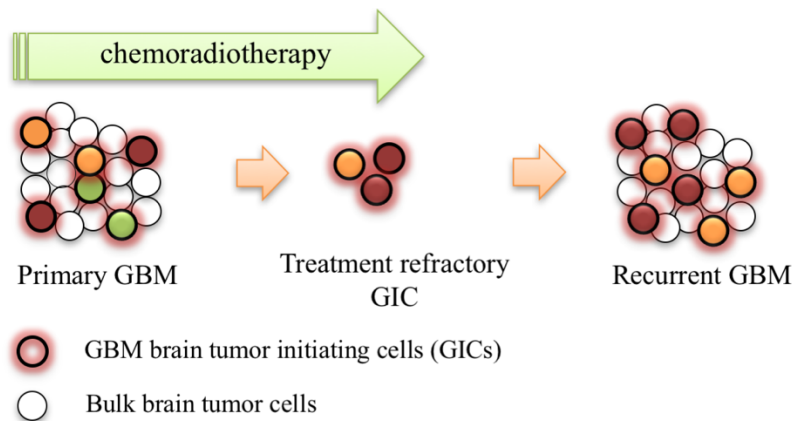


Figure 1: BTSC model of GBM recurrence - chemoradiotherapy of primary glioblastoma (GBM) selects for treatment refractory BTSC populations that seed tumor relapse.

Primary GBM is a heterogeneous population consisting of differentiated tumor cells and multiple BTSC populations (represented by multiple colors). Treatment of primary GBM with chemotherapeutic temozolomide (TMZ) and radiation leads to tumor cell death and reduction in tumor volume; however, small BTSC subpopulations that are resistant to chemoradiotherapy survive treatment and over time allow for tumor regrowth, leading patient to GBM recurrence.

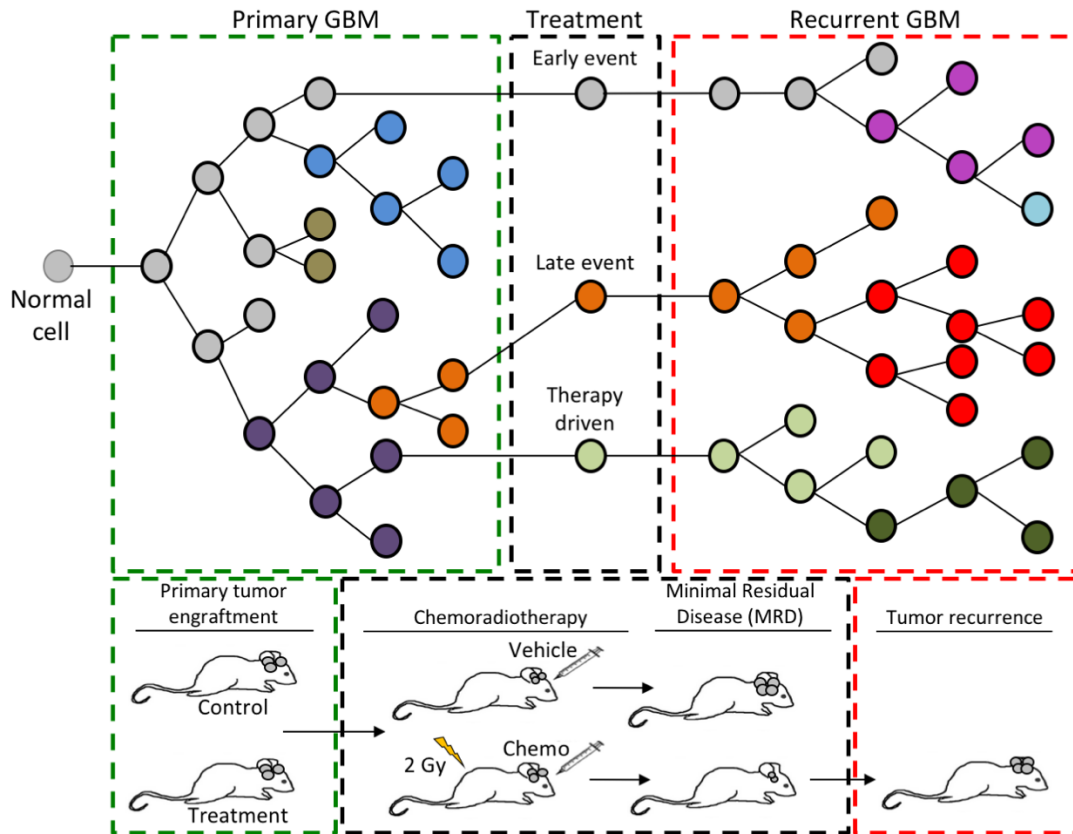


Figure 2: Mouse model of GBM recurrence to profile multi stages of disease progression.

After a normal cell acquires mutations (black outlined circles), it expands into multiple subclonal populations of glioblastoma with selectable traits against any stress (represented by different coloured circles), including therapy. The administration of therapy for primary glioblastoma, leads to the selection of subclonal cell populations (early event subclone or late event subclone) or gives rise to a therapy-driven resistant subclone. These treatment-refractory subclonal populations then seed tumor relapse and lead to the formation of a heterogenous recurrent glioblastoma that has a distinct clonal composition from primary

glioblastoma. Mice engrafted with primary GBM can be used to investigate each stage of the tumour progression through multiple platforms such as cellular DNA barcoding and single cell RNA sequencing (adapted from Qazi et al. 2017 *Annals of Oncology*).

CHAPTER 2: A novel stem cell culture model of glioblastoma recurrence

Preamble

This is a pre-copyedited, author-produced version of an article accepted for publication in *Journal of NeuroOncology* following peer review. The version of record **Qazi MA**, Vora P, Venugopal C, McFarlane N, Subapanditha MK, Murty NK, Hassell JA, Hallett RM, Singh SK. A novel stem cell culture model of glioblastoma recurrence. *Journal of Neuro-Oncology*, 126(1):57-67, 2016 is available online at:

<https://link.springer.com/article/10.1007%2Fs11060-015-1951-6>, DOI: 10.1007/s11060-015-1951-6.

MAQ designed the project, acquired and analyzed the data, interpreted the results, and wrote the manuscript. PV designed the project, interpreted the results, and wrote the manuscript. CV designed the project, interpreted the results, and revised the manuscript. NM acquired and analyzed flow cytometry data. MKS acquired the data. NKM provided brain tumor specimens for the project. RMH analyzed and interpreted microarray data under the supervision of JAH. SKS conceived the project, supervised the study, interpreted the results, and wrote the manuscript.

Our literature review showed a lack of *in vitro* GSC models to assess the effect of combined chemotherapy and radiation in the development of GBM recurrence. Hence, the aim of this work was to develop an *in vitro* model of GBM recurrence that tests both chemotherapy and radiation in GSC-enriched GBM cultures. We used clinically relevant doses of

chemotherapy, TMZ, and radiation in our model to recapitulate tumour biology evolution as expected in patients. We used known GSC markers such as CD133, CD15, Bmi1 and Sox2 and self-renewal assays, to assess the effects of chemoradiotherapy on sphere formation capacity of the GSCs post-treatment. We further characterized the effect of chemoradiotherapy on global gene expression of GSCs using microarray and developed a gene signature that identified an aggressive subtype of GBM with poor overall survival. Overall, this work developed a combined chemoradiotherapy model to generate GBM recurrence, which can be used as *in vitro* surrogate to study mechanisms of treatment-resistance in GBM.

A novel stem cell culture model of recurrent glioblastoma.

Maleeha A. Qazi^{a, b}, Parvez Vora^{a, c}, Chitra Venugopal^{a, c}, Nicole McFarlane^{a, c}, Minomi K. Subapanditha^{a, b}, Naresh K. Murty^c, John A. Hassell^{b, d}, Robin M. Hallett^{b, d}, Sheila K. Singh^{a- c}.

^aMcMaster Stem Cell and Cancer Research Institute, McMaster University, 1200 Main Street West, Hamilton, ON, Canada, L8S 4K1

Departments of ^bBiochemistry and Biomedical Sciences, and ^cSurgery, Faculty of Health Sciences, McMaster University, 1280 Main Street West, Hamilton, ON, Canada, L8S 4L8

^dMcMaster Centre for Functional Genomics, McMaster University, 1200 Main Street West, Hamilton, ON, Canada, L8N 3Z5

Corresponding Author:

Sheila K. Singh, MD, PhD, FRCS(C)

Scientist, McMaster Stem Cell and Cancer Research Institute

McMaster University, MDCL 5027, 1200 Main Street West

Hamilton, ON, Canada L8S 4K1

Phone: 1 905 521 2100 x75237, Fax: 1 905 521 9992, E-mail: ssingh@mcmaster.ca.

Abstract

Glioblastoma (GBM) is the most common and aggressive primary brain tumor in adults with average disease relapse at 9 months and median survival rarely extending beyond 15 months. Brain tumor stem cells (BTSCs) have been implicated in not only initiating GBM but also conferring resistance to therapy. However, it is not clear whether the BTSC population that initiates tumor growth is also responsible for GBM recurrence. In this study,

we have developed a novel in vitro treatment model to profile the evolution of primary treatment-naïve GBM BTSCs through chemoradiotherapy. We report that our in vitro model enriched for a CD15+/CD133- BTSC population, mirroring the phenotype of BTSCs in recurrent GBM. We also show that in vitro treatment increased stem cell gene expression as well as self-renewal capacity of primary GBMs. In addition, the chemoradiotherapy-refractory gene signature obtained from gene expression profiling identified a hyper-aggressive subtype of glioma. The delivery of in vitro chemoradiotherapy to primary GBM BTSCs models several aspects of recurrent GBM biology, and could be used as a discovery and drug-screening platform to uncover new biological drivers and therapeutic targets in GBM.

Keywords: GBM; brain tumor stem cell; chemotherapy; radiotherapy; CD15; CD133

Introduction

Glioblastoma (GBM), the most common primary brain tumor in adults, is a highly aggressive astrocytic tumor (WHO grade IV), with uniformly fatal prognosis[1]. GBM is pathologically characterized by nuclear pleomorphism, microvascular proliferation and necrosis, and displays great inter-tumoral cellular heterogeneity[2-4]. Despite multimodal therapy, consisting of surgical resection followed by chemo and radiotherapy, patients typically experience tumor relapse at 9 months and median survival remains around 15 months[5]. At the genetic level, this heterogeneity has been classified into molecular subgroups, based on differential transcriptome profiling of hundreds of GBMs by TCGA[1, 6]. At the cellular level, this heterogeneity can be explained by the existence of multiple cellular subpopulations of cancer cells that have acquired stem cell properties, variably

labeled in the literature as BTSCs (brain tumor stem cells) or GICs (glioblastoma initiating cells)[7, 8]. Since cell surface markers allow sorting of bulk GBM into cellular subpopulations, much research has focused on the application of proteins such as CD133[8], CD15[9], integrin alpha6[10] and L1CAM[11] to define functional BTSC subgroups. In addition, intracellular proteins such as RNA binding protein Musashi-1[12], transcription factor Sox2[13] and polycomb repressor Bmi1[14] that have a characterized functional role in driving normal neural stem cell (NSC) self-renewal, have also been investigated as putative BTSC markers[15, 16]. Although recent data suggests that CD133+ GBM BTSCs are chemo-[17] and radioresistant[18], no study has prospectively identified whether such BTSCs are causal of tumor relapse, and whether the same BTSC populations that drive tumor initiation also drive recurrence.

In vitro functional assays of BTSC self-renewal have been shown to correlate with patient survival[19] and are used to study resistance of GBM BTSCs to temozolomide (TMZ), the chemotherapeutic used to treat GBM, or to radiation[18, 20]. However, the combinatorial effect of TMZ and radiation on BTSC populations in GBM has not been clearly studied and whether this leads to selection of subclonal population from which recurrence may arise remains to be explored.

In this study, we have developed a novel *in vitro* BTSC model of GBM recurrence to profile the evolution of BTSC populations through therapy. We investigated the effect of *in vitro* chemoradiotherapy on primary human GBMs (P-GBM) harvested from patients at initial

diagnosis, identifying and characterizing the treatment-refractory BTSC population. We then compared it to the BTSC profile of clinically-treated recurrent human GBM specimens (R-GBM). By comparing *in vitro* treated P-GBM to R-GBM patient samples, we could 1. determine if our *in vitro* treatment protocol resulted in similar clonal evolution as seen in patients, and 2. establish a treatment-naïve vs. post-treatment GBM differential BTSC profile through the application of stem cell assays and marker expression. Lastly, a global gene expression analysis comparing P-GBMs to corresponding *in vitro* treatment-refractory BTSCs identified signaling networks underlying therapy resistance.

Materials and Methods

Dissociation and culture of GBM tissue: Human GBM brain tumors were obtained from consenting patients, as approved by the Hamilton Health Sciences/McMaster Health Sciences Research Ethics Board. Brief clinico-pathological information of each patient is included in Fig. 1a. Tumors were dissociated and cells resuspended in complete NSC medium as previously published [7, 8].

Real-time quantitative PCR: Total RNA was isolated using NorgenTotal RNA Purification kit. cDNA was synthesized by qScript cDNAsupermix (Quanta Biosciences) followed by real-time quantitative PCR using SsoAdvancedTM Universal SYBR[®]GreenSupermix (Bio-Rad). Samples were quantified using CFX ManagerTM software. Data were presented as the ratio of the gene of interest to *GAPDH*. Primer sequences used for each gene are provided in Supp. Table S1.

Flow cytometry analysis: The percentage expression of CD133 and CD15 was determined on a MoFlo XDP flow cytometer (Beckman Coulter) using anti-CD133-APC

(MiltenyiBiotec), anti-CD15-PE (Beckman Coulter) and matched isotype controls. Data was analyzed with Kaluza® Flow Analysis software.

Self-renewal assay: Once primary sphere formation was noted, spheres were dissociated to single cells and 200 cells/well were re-plated in 0.2mL of complete NSC media in a 96 well plate as previously published[8]. The low cell density prevents cell aggregates from forming and allows for the formation of a sphere from a single cell. The spheres were counted after 7 days of incubation.

In vitro treatment: Single cells were plated at a density of 2×10^6 cells per mL of complete NSC media. The *in vitro* chemoradiotherapy protocol had three treatment groups. The radiation-only group received 1Gy per day for five consecutive days. The combined chemoradiotherapy group Tx1 received five days of TMZ (Sigma-Aldrich) at $25 \mu\text{M}$ concurrently with 1Gy per day of radiation and Tx2 received an additional five days of TMZ at $50 \mu\text{M}$. The concentration of TMZ used in the study is adapted from clinically relevant doses received by GBM patients [21, 22]. Cells were treated with TMZ for 1 hour, after which media was replaced with fresh complete NSC media and cells were immediately exposed to X-rays for a total dose of 1Gy (Faxitron RX-650). Control cells received corresponding concentrations of DMSO for the same time periods. One week post-treatment, cells were analyzed using flow cytometry and stem cell assays, and RNA was extracted for RT-PCR and microarray analysis.

Illumina bead chip analysis: Briefly, 200ng of RNA isolated using Qiagen RNeasy Micro Kit from the treated samples were labeled using the Illumina TotalPrep-96 RNA Amplification kit (Ambion). 750ng cRNA was hybridized onto Human HT-12 V4

beadchips. BeadChips were stained as per Illumina protocol and scanned on the iScan (Illumina). Raw .IDAT files pre-processed using cubic spline normalization.

REMBRANDT data analysis: Publically available GBM sample data was downloaded from the Repository for Brain Neoplasia Data (REMBRANDT). The samples were clustered based on Control/Tx2 variable genes that were common to at least 2 of 3 GBM lines using non-negative matrix factorization (NMF)[23]. Survival analysis was completed in R and survival curves were graphed using Graphpad Prism 5.

Network analysis: Common Control/Tx2 variable genes to at least 2 of 3 GBM lines were mapped as genes onto nodes of the REACTOME functional interaction network[24, 25]. Markov clustering was used to subset the network and identify modules of interacting genes. Subsequently modules were annotated with significantly enriched pathways. All network analyses was carried out using Cytoscape (v2.8.2) and the Reactome FIs plugin (v2012).

Statistical analysis: All quantitative data presented are the mean \pm SEM. Samples used and respective n values are listed in the figure legends. The level of significance was determined by Student's two-tailed t-test or ANOVA using GraphPad Prism 5 software.

Results

Inter-tumoral heterogeneity in stem marker expression in P-GBMs

We determined the gene and surface protein expression levels of known BTSC markers using RT-PCR and flow cytometry respectively, (Fig. 1b-d) in three P-GBM samples: BTs 428, 458 and 465. All P-GBMs express *BM11* (Fig. 1b) and *SOX2* (Fig. 1c), genes known to play a role in maintaining GBM self-renewal. However, the expression was highly

variable across individual patient P-GBMs with BT428 and BT458 expressing 4-5 fold higher levels of *BM11* and up to 10 times lower level of *SOX2* as compared to BT465. Similarly, the cell surface expression of CD15 and CD133 varied considerably between P-GBM samples as BT428 and BT458 had higher numbers of CD133+ and CD15+ cells than BT465 (Fig. 1d). This variability was not unexpected considering the high inter-tumoral heterogeneity that exists in GBM[1]. Despite variable stem cell gene and protein expression levels, we found no significant difference in secondary sphere formation capacity between the three P-GBMs (Fig. 1e), illustrating the significance of functionally quantifying self-renewal capacity in addition to characterizing stem cell gene and protein expression. We also determined the MGMT promoter methylation status of our P-GBMs (Supp. Fig. S1). Both BT428 and BT465 harbor unmethylated MGMT promoter while BT458 has a partially methylated MGMT promoter. Based on the expression of 21 subtype specific genes as described in Verhaak *et al.* 2010[1] we subtyped the GBM samples used in this study (Supp. Table S3) and found that BT428 and BT465 belonged to Proneural subtype while BT458 belonged to Classical subtype.

In vitro chemoradiotherapy increases the expression of genes potentially driving self-renewal

In order to study the effect of *in vitro* chemoradiotherapy on *BM11* and *SOX2* expression, we designed an *in vitro* protocol combining TMZ and radiation treatment (Fig. 2a). The protocol divided into three treatment groups: Rad, Tx1 and Tx2 (Fig. 2b). We found that *in vitro* chemoradiotherapy significantly increased the expression of *BM11* in both Tx1 and Tx2 group in all P-GBMs tested by 2 to 3 fold except in BT465 Tx1 (Fig. 2c). Similarly, *in*

in vitro chemoradiotherapy significantly increased *SOX2* expression in both Tx1 and Tx2 treatment groups in all P-GBMs (Fig. 2d). In contrast, radiotherapy alone induced variable changes in *BMI1* and *SOX2* expression across the P-GBM samples (Supp. Fig. S2) validating that combined *in vitro* chemoradiotherapy provides a better model to study therapy resistance in GBM.

In vitro chemoradiotherapy enriches for the CD15+/CD133- cell population, mirroring the BTSC marker profile of R-GBMs

In addition to changes in *BMI1* and *SOX2* gene expression, we wanted to study the evolution of the CD15/CD133 flow profile of P-GBMs over the course of *in vitro* chemoradiotherapy (Fig. 3a). Radiation alone increased the CD133+ cell populations in all three P-GBMs, supporting previous studies identifying CD133+ BTSCs as radioresistant[18]. In both BT428 and BT458, the increase in the CD133+ cell population was characteristically restricted to the CD15-/CD133+ subpopulation. Only BT465 showed an increase in CD15+ cell population in response to radiation alone.

In contrast to flow profiles of P-GBMs post-radiation, combined chemoradiotherapy enriched exclusively for the CD15+/CD133- cell population (Fig. 3a). Both BT428 and BT458 expressed higher CD15+ in control groups and showed dramatic increases in the CD15+/CD133- population in Tx1 and Tx2 treatment groups. On the other hand, BT465 with its low fraction of CD15+ cells showed only a slight increase in the CD15+ cell population after treatment. All P-GBMs showed significant decrease in CD133+/CD15- subpopulations in the Tx2 group as compared to control.

In order to investigate the relevance of CD15⁺/CD133⁻ subpopulation enrichment in P-GBMs in response to *in vitro* chemoradiotherapy, we profiled R-GBMs for CD15 and CD133 cell surface expression levels. Intriguingly, R-GBMs were also characterized by a CD15^{high}/CD133^{low} subpopulation (Fig. 3b). In fact, both BT241 and BT566 had 3 fold higher levels of CD15⁺ cells than CD133⁺ cells, while BT618 exclusively presented a CD15⁺ cell population with less than 0.5% of cells expressing CD133. This characteristic CD15^{high}/CD133^{low} flow profile of R-GBMs was very similar to profiles obtained by *in vitro* chemoradiotherapy of P-GBMs (Fig. 3a, Tx2). Hence, *in vitro* chemoradiotherapy in Tx2 treatment group of P-GBMs generated flow profiles similar to those of patient-derived R-GBMs.

In vitro chemoradiotherapy increases self-renewal capacity of P-GBMs

Although we see an increased expression of both *BM11* and *SOX2* genes as well as an enrichment of the CD15⁺ cell population in response to *in vitro* chemoradiotherapy, we wanted to determine if the changes had a functional consequence on regulating self-renewal capacity of P-GBMs. Control and Tx2 treatment cells from each GBM sample were plated for secondary sphere formation assay one-week post treatment. We find that *in vitro* chemoradiotherapy increases the secondary sphere formation capacity of Tx2 group compared to DMSO controls (Fig. 3c). In fact, R-GBMs also exhibit higher self-renewal than P-GBMs (Fig. 3d), again validating that our *in vitro* chemoradiotherapy protocol is mimicking BTSC biology of R-GBMs. We tested whether *in vitro* chemoradiotherapy refractory cells were more resistant to subsequent exposure to TMZ and radiation. We

found that BT458 cells with previous chemoradiotherapy treatment presented higher cell survival when challenged with subsequent chemoradiotherapy and significantly increased sphere formation capacity as compared to challenged DMSO treated control cells (Supp. Fig. S3). This suggests that cell survival in response to *in vitro* chemoradiotherapy is not stochastic and rather cells acquire resistance to TMZ and radiation.

Gene expression profiling of treated P-GBMs reveals patterns of acquired resistance and identifies hyper-aggressive brain tumors

Our observations that acquired resistance to *in vitro* chemoradiotherapy appeared to model the biology of R-GBMs prompted us to do comprehensive global gene expression profiling of control and treated P-GBMs. For each of the 3 P-GBMs we identified the top 250 variably expressed genes between the control and Tx2 samples, which represented our best *in vitro* model of untreated and clinically treated GBM, and used these genes to cluster control, radiation, Tx1 and Tx2 treated GBMs (Fig. 4a). Analysis of the resulting clusters revealed a similar pattern of resistance acquisition in each GBM sample. Radiation-only treated samples were generally more similar to control GBM cultures, whereas both chemoradiotherapy-treated cultures were highly similar to each other. Importantly these data suggest that the radiation-only GBM group represent an intermediary step that occurs during acquisition of chemoradiotherapy resistance by GBM (Fig. 4a).

We next examined the 250-control/Tx2 variable genes for overlap between the three GBMs. 62 genes were common to at least 2 of the 3 GBMs (Fig. 4b), which we hypothesized represents a signature of chemoradiotherapy resistance in brain tumors

(henceforth called 62-RS). We completed unsupervised clustering using NMF of brain tumors that comprised the repository for brain neoplasia data (REMBRANDT, n=286) based on the expression of the 62-RS genes (Fig. 4c). This analysis revealed that REMBRANDT samples optimally stratified into 3 classes of brain tumors based on the expression of 62-RS genes. Intriguingly, patients whose tumors were assigned to class 2 experienced dramatically poorer survival than class 1 and 3 tumors. (Class 1 Vs 2, HR: 0.4, * $p < 0.0001$, Class 3v2, HR: 0.059, * $p = 0.0004$) (Fig. 4d). Therefore, the 62-RS identified using our *in vitro* chemoradiotherapy model of brain tumor could also be used to identify patients with ultra-high risk brain tumors.

To identify the biological programs measured by the 62-RS, we generated a protein interaction network (Fig. 4e) comprising of protein products and their interaction partners using the Reactome database. Clustering of the interaction network suggested that the 62-RS interacted in 6 sub-networks, or modules, each of which was associated with distinct biological processes (Supp. Table S4, Supp. Fig. S4). Although no pathways were significantly enriched in module 0 (FDR<0.05), module 0 comprised many genes involved in inflammation including CCL2, JUN, MGP, and LMO2. Module 1 was likely associated with proliferation, as it displayed enrichment in many proliferation-associated pathways, including mitosis as well as PLK1 and FOXM1 signaling. Module 2 was enriched in pathways associated with cell adhesion and angiogenesis, including focal adhesion, signaling through VEGFR, and the PDGFR signaling pathway. Although module 3 was only significantly enriched in a p53 related signaling pathway, it also comprised many

genes involved in cellular proliferation including CDC20, CCNB1 and CCNB2. Module 4 was also not significantly enriched in any pathways, but is likely associated with hypoxia as it contains HIF1A, ADM, and CA9, which are all either functionally involved, or markers of hypoxia in tumor cells. Finally, module 5 was enriched in pathways associated with chromosome stability and maintenance. Hence, together these data reveal that brain tumor resistance to chemoradiotherapy is multifactorial, and likely results in changes to multiple biological pathways, including proliferation, chromosome stability, angiogenesis, inflammation, hypoxia and cell adhesion.

Discussion

GBM is characterized by both genetic and cellular heterogeneity, which together drive the hierarchical organization of the tumor, its clonal evolution and subsequent therapeutic resistance. Tumor evolution over the course of disease progression and in response to therapy may generate genetically and functionally distinct BTSC clones throughout tumor progression[26, 27]. These chemo- and radio-resistant BTSC clones might substantially contribute to tumor recurrence. Adding to the complexity, this evolution is dynamic in spatial organization within the tumor mass, as well as temporally throughout the disease course. Ideally, sampling different parts of same tumor tissue or sampling tissue at different time-points might help in identifying the BTSC clonal subpopulation. Unfortunately, in case of GBM, re-sampling post-treatment or at the time of relapse may encounter problems: risk of infection, risk of neurological deficits and psychological deficits like depression[28, 29]. Therefore, matched R-GBM is a rare specimen, as patients do not always undergo additional surgical resections for their relapsed tumor. In the present study, we have

developed a benchtop model to study GBM recurrence and identify the evading treatment-refractory population in an individual patient with P-GBM (Fig. 5). This may constitute a unique model for studying the later stages of tumor progression from P-GBM to R-GBM. This *in vitro* model will be crucial for the investigation of genetic, epigenetic and cellular alterations, for the study of proliferation, migration and tumor recurrence and to define potential molecular markers for tumor progression. Ultimately, it will accelerate the development of personalized therapeutic strategies targeting BTSCs driving recurrent GBM.

The upregulation of stem cell genes, *BMI1* and *SOX2* is not a surprising finding. Previously, Bmi1 protein was shown to interact with DNA damage response machinery and confer radioresistance to irradiated GBM cells[30]. Additionally, loss of Sox2 is shown to delay tumor progression in GBMs through polo-like kinase 1 (PLK1), which possibly drives radio-resistance in GBM[31, 32]. Interestingly, our data identified PLK1 pathway as significantly variable signaling event in our Tx2 treatment group (Supp. Table S4). The involvement of these signaling pathways is not entirely novel; however it further validates this unique *in vitro* model to study GBM recurrence. Further studies are warranted to specifically elucidate the role of Bmi1 and Sox2 in GBM therapy resistance and tumor relapse.

The enrichment of CD15+/CD133- subpopulation in P-GBM after chemoradiotherapy is an exciting finding, which was further corroborated by the presence of a predominant

CD15^{high}/CD133^{low} subpopulation in R-GBM. Our findings add to the growing body of evidence that there is a hierarchy of self-renewing BTSCs, playing different roles in tumor initiation, progression and recurrence. While BTSCs with neural stem cell marker CD133 expression represent the tumor-initiating subpopulation, cells with neural progenitor cell marker CD15 may represent BTSCs driving tumor recurrence. Further studies investigating the molecular heterogeneity and defining the cellular hierarchy of BTSCs will lead to better understanding of the disease process.

Although previous studies have been conducted to examine the resistance of GBMs to TMZ and radiation, none looked at the combinatorial effects of chemoradiotherapy in modulating therapy resistance and tumor relapse, despite the fact that most GBM patients undergo combined therapy. Our work suggests that studying a therapy module in isolation may not inform on the complexity of the tumor recurrence. This is illustrated by the CD15/CD133 flow profile where radiation alone led to an enrichment of the CD133⁺/CD15⁻ population; if taken in isolation, this data would warrant attempted targeting of the CD133⁺ population in P-GBM, even if this cell population is not driving tumor recurrence after subsequent chemotherapy. Our data suggests that combined chemoradiotherapy further uniquely modulates GBM subpopulations, as in our model it leads to a subsequent enrichment of the CD15⁺/CD133⁻ subpopulation. Similarly, the gene expression of stem cell genes *BM11* and *SOX2* was only significantly increased after combined chemoradiotherapy, demonstrating the need to model disease progression through combined therapies with concurrent gene expression profiling, to define the state of therapy resistance. Only in a combined treatment

model can treatment-refractory cell populations and gene signatures be identified, which can then lead to development of informed combinatorial therapies not only in GBM, but also in other malignancies that exhibit heterogeneity.

Acknowledgements

Funding: Stem Cell Network Undergraduate Co-op Award and Canadian Institute of Health Research Canada Graduate Scholarship – Master’s Award (to M.A.Q.); Stem Cell Network Stem Cell Drug Discovery Award, Terry Fox Foundation New Investigator Award, Ontario Institute for Cancer Research Cancer Stem Cell Program, and Canada Research Chair Award (to S.K.S.).

Conflict of Interest: The authors declare no conflict of interests.

References

1. Verhaak RG, Hoadley KA, Purdom E, Wang V, Qi Y, Wilkerson MD, Miller CR, Ding L, Golub T, Mesirov JP, Alexe G, Lawrence M, O’Kelly M, Tamayo P, Weir BA, Gabriel S, Winckler W, Gupta S, Jakkula L, Feiler HS, Hodgson JG, James CD, Sarkaria JN, Brennan C, Kahn A, Spellman PT, Wilson RK, Speed TP, Gray JW, Meyerson M, Getz G, Perou CM, Hayes DN, Cancer Genome Atlas Research N (2010) Integrated genomic analysis identifies clinically relevant subtypes of glioblastoma characterized by abnormalities in PDGFRA, IDH1, EGFR, and NF1. *Cancer Cell* 17: 98-110 doi:10.1016/j.ccr.2009.12.020
2. Wechsler-Reya R, Scott MP (2001) The developmental biology of brain tumors. *Annual review of neuroscience* 24: 385-428 doi:10.1146/annurev.neuro.24.1.385

3. Zhu Y, Parada LF (2002) The molecular and genetic basis of neurological tumours. *Nature reviews Cancer* 2: 616-626 doi:10.1038/nrc866
4. Huse JT, Holland EC (2010) Targeting brain cancer: advances in the molecular pathology of malignant glioma and medulloblastoma. *Nature reviews Cancer* 10: 319-331 doi:10.1038/nrc2818
5. Stupp R, Mason WP, van den Bent MJ, Weller M, Fisher B, Taphoorn MJ, Belanger K, Brandes AA, Marosi C, Bogdahn U, Curschmann J, Janzer RC, Ludwin SK, Gorlia T, Allgeier A, Lacombe D, Cairncross JG, Eisenhauer E, Mirimanoff RO, European Organisation for R, Treatment of Cancer Brain T, Radiotherapy G, National Cancer Institute of Canada Clinical Trials G (2005) Radiotherapy plus concomitant and adjuvant temozolomide for glioblastoma. *The New England journal of medicine* 352: 987-996 doi:10.1056/NEJMoa043330
6. Cancer Genome Atlas Research N (2008) Comprehensive genomic characterization defines human glioblastoma genes and core pathways. *Nature* 455: 1061-1068 doi:10.1038/nature07385
7. Singh SK, Hawkins C, Clarke ID, Squire JA, Bayani J, Hide T, Henkelman RM, Cusimano MD, Dirks PB (2004) Identification of human brain tumour initiating cells. *Nature* 432: 396-401 doi:nature03128 [pii] 10.1038/nature03128
8. Singh SK, Clarke ID, Terasaki M, Bonn VE, Hawkins C, Squire J, Dirks PB (2003) Identification of a cancer stem cell in human brain tumors. *Cancer research* 63: 5821-5828

9. Son MJ, Woolard K, Nam DH, Lee J, Fine HA (2009) SSEA-1 is an enrichment marker for tumor-initiating cells in human glioblastoma. *Cell stem cell* 4: 440-452 doi:10.1016/j.stem.2009.03.003
10. Lathia JD, Gallagher J, Heddleston JM, Wang J, Eyler CE, Macswords J, Wu Q, Vasanji A, McLendon RE, Hjelmeland AB, Rich JN (2010) Integrin alpha 6 regulates glioblastoma stem cells. *Cell stem cell* 6: 421-432 doi:10.1016/j.stem.2010.02.018
11. Bao S, Wu Q, Li Z, Sathornsumetee S, Wang H, McLendon RE, Hjelmeland AB, Rich JN (2008) Targeting cancer stem cells through L1CAM suppresses glioma growth. *Cancer research* 68: 6043-6048 doi:10.1158/0008-5472.CAN-08-1079
12. Kaneko Y, Sakakibara S, Imai T, Suzuki A, Nakamura Y, Sawamoto K, Ogawa Y, Toyama Y, Miyata T, Okano H (2000) Musashi1: an evolutionally conserved marker for CNS progenitor cells including neural stem cells. *Developmental neuroscience* 22: 139-153 doi:17435
13. Graham V, Khudyakov J, Ellis P, Pevny L (2003) SOX2 functions to maintain neural progenitor identity. *Neuron* 39: 749-765
14. Fasano CA, Dimos JT, Ivanova NB, Lowry N, Lemischka IR, Temple S (2007) shRNA knockdown of Bmi-1 reveals a critical role for p21-Rb pathway in NSC self-renewal during development. *Cell stem cell* 1: 87-99 doi:10.1016/j.stem.2007.04.001
15. Abdouh M, Facchino S, Chatoo W, Balasingam V, Ferreira J, Bernier G (2009) BMI1 sustains human glioblastoma multiforme stem cell renewal. *The Journal of neuroscience : the official journal of the Society for Neuroscience* 29: 8884-8896 doi:10.1523/JNEUROSCI.0968-09.2009

16. Suva ML, Rheinbay E, Gillespie SM, Patel AP, Wakimoto H, Rabkin SD, Riggi N, Chi AS, Cahill DP, Nahed BV, Curry WT, Martuza RL, Rivera MN, Rossetti N, Kasif S, Beik S, Kadri S, Tirosh I, Wortman I, Shalek AK, Rozenblatt-Rosen O, Regev A, Louis DN, Bernstein BE (2014) Reconstructing and reprogramming the tumor-propagating potential of glioblastoma stem-like cells. *Cell* 157: 580-594 doi:10.1016/j.cell.2014.02.030
17. Liu G, Yuan X, Zeng Z, Tunici P, Ng H, Abdulkadir IR, Lu L, Irvin D, Black KL, Yu JS (2006) Analysis of gene expression and chemoresistance of CD133+ cancer stem cells in glioblastoma. *Molecular cancer* 5: 67 doi:10.1186/1476-4598-5-67
18. Bao S, Wu Q, McLendon RE, Hao Y, Shi Q, Hjelmeland AB, Dewhirst MW, Bigner DD, Rich JN (2006) Glioma stem cells promote radioresistance by preferential activation of the DNA damage response. *Nature* 444: 756-760 doi:10.1038/nature05236
19. Venugopal C, Li N, Wang X, Manoranjan B, Hawkins C, Gunnarsson T, Hollenberg R, Klurfan P, Murty N, Kwiecien J, Farrokhyar F, Provias JP, Wynder C, Singh SK (2012) Bmi1 marks intermediate precursors during differentiation of human brain tumor initiating cells. *Stem cell research* 8: 141-153 doi:10.1016/j.scr.2011.09.008
20. Beier D, Rohrl S, Pillai DR, Schwarz S, Kunz-Schughart LA, Leukel P, Proescholdt M, Brawanski A, Bogdahn U, Trampe-Kieslich A, Giebel B, Wischhusen J, Reifenberger G, Hau P, Beier CP (2008) Temozolomide preferentially depletes cancer stem cells in glioblastoma. *Cancer Res* 68: 5706-5715 doi:10.1158/0008-5472.CAN-07-6878
21. Hammond LA, Eckardt JR, Baker SD, Eckhardt SG, Dugan M, Forral K, Reidenberg P, Statkevich P, Weiss GR, Rinaldi DA, Von Hoff DD, Rowinsky EK (1999)

Phase I and pharmacokinetic study of temozolomide on a daily-for-5-days schedule in patients with advanced solid malignancies. *J Clin Oncol* 17: 2604-2613

22. Barazzuol L, Jena R, Burnet NG, Jeynes JC, Merchant MJ, Kirkby KJ, Kirkby NF (2012) In vitro evaluation of combined temozolomide and radiotherapy using X rays and high-linear energy transfer radiation for glioblastoma. *Radiation research* 177: 651-662

23. Brunet JP, Tamayo P, Golub TR, Mesirov JP (2004) Metagenes and molecular pattern discovery using matrix factorization. *Proceedings of the National Academy of Sciences of the United States of America* 101: 4164-4169 doi:10.1073/pnas.0308531101

24. Wu G, Stein L (2012) A network module-based method for identifying cancer prognostic signatures. *Genome biology* 13: R112 doi:10.1186/gb-2012-13-12-r112

25. Wu G, Feng X, Stein L (2010) A human functional protein interaction network and its application to cancer data analysis. *Genome biology* 11: R53 doi:10.1186/gb-2010-11-5-r53

26. Notta F, Mullighan CG, Wang JC, Poepl A, Doulatov S, Phillips LA, Ma J, Minden MD, Downing JR, Dick JE (2011) Evolution of human BCR-ABL1 lymphoblastic leukaemia-initiating cells. *Nature* 469: 362-367 doi:10.1038/nature09733

27. Dalerba P, Cho RW, Clarke MF (2007) Cancer stem cells: models and concepts. *Annual review of medicine* 58: 267-284 doi:10.1146/annurev.med.58.062105.204854

28. Barami K, Fernandes R (2012) Incidence, risk factors and management of delayed wound dehiscence after craniotomy for tumor resection. *Journal of clinical neuroscience : official journal of the Neurosurgical Society of Australasia* 19: 854-857 doi:10.1016/j.jocn.2011.09.025

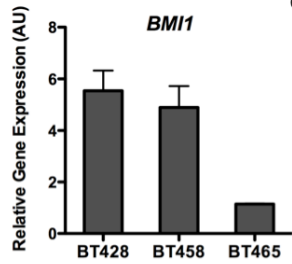
29. Chang SM, Parney IF, McDermott M, Barker FG, 2nd, Schmidt MH, Huang W, Laws ER, Jr., Lillehei KO, Bernstein M, Brem H, Sloan AE, Berger M, Glioma Outcomes I (2003) Perioperative complications and neurological outcomes of first and second craniotomies among patients enrolled in the Glioma Outcome Project. *Journal of neurosurgery* 98: 1175-1181 doi:10.3171/jns.2003.98.6.1175
30. Facchino S, Abdouh M, Chato W, Bernier G (2010) BMI1 confers radioresistance to normal and cancerous neural stem cells through recruitment of the DNA damage response machinery. *The Journal of neuroscience : the official journal of the Society for Neuroscience* 30: 10096-10111 doi:10.1523/JNEUROSCI.1634-10.2010
31. Tandle AT, Kramp T, Kil WJ, Halthore A, Gehlhaus K, Shankavaram U, Tofilon PJ, Caplen NJ, Camphausen K (2013) Inhibition of polo-like kinase 1 in glioblastoma multiforme induces mitotic catastrophe and enhances radiosensitisation. *European journal of cancer* 49: 3020-3028 doi:10.1016/j.ejca.2013.05.013
32. Lee C, Fotovati A, Triscott J, Chen J, Venugopal C, Singhal A, Dunham C, Kerr JM, Verreault M, Yip S, Wakimoto H, Jones C, Jayanthan A, Narendran A, Singh SK, Dunn SE (2012) Polo-like kinase 1 inhibition kills glioblastoma multiforme brain tumor cells in part through loss of SOX2 and delays tumor progression in mice. *Stem cells* 30: 1064-1075 doi:10.1002/stem.1081

CHAPTER 2 FIGURES AND TABLES

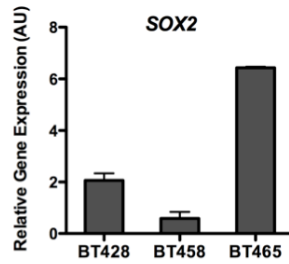
a

Specimen ID	Age/Gender	Diagnosis	Treatment	Disease Progression (Recurrence (R), Survival (S))
BT241	68/F	Recurrent/residual GBM	RT+TMZ	R: 12 months; S: 23 months
BT428	63/F	GBM	-	S: 14 months
BT458	81/M	GBM	-	S: 13 months
BT465	50/M	GBM	-	S: 16 months
BT566	55/F	Recurrent/residual GBM	RT+TMZ → TMZ	R: 9 months; S: 11 months
BT618	67/F	Recurrent/residual GBM	RT+TMZ	R: 10 months; S: 13 months

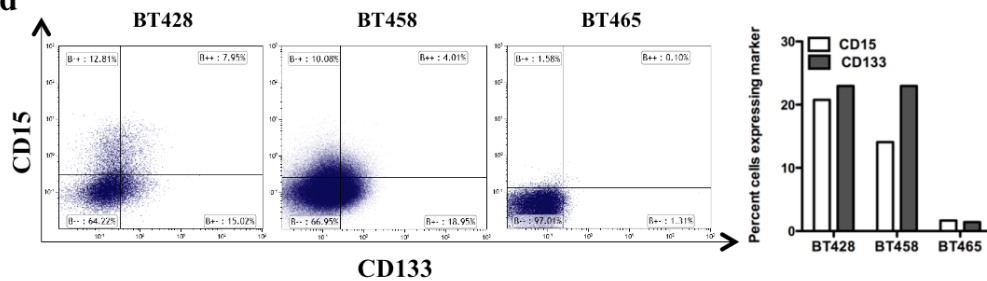
b



c



d



e

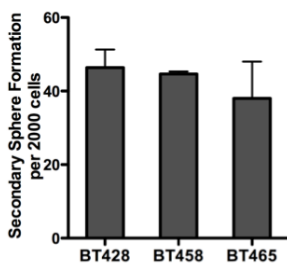
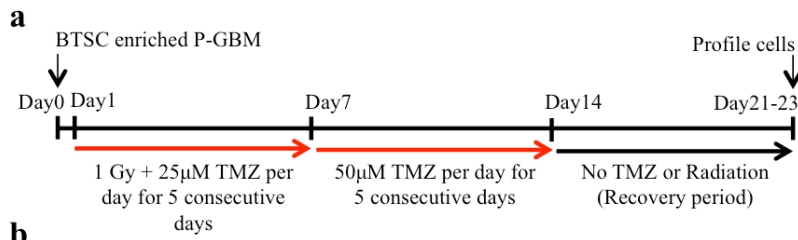


Figure 1: Inter-tumoral heterogeneity exists in *BMI1* and *SOX2* expression as well CD15 and CD133 cell surface expression in P-GBMs.

(a) GBM patient demographics. RT: radiation, 60 Gy. TMZ: temozolomide. → adjuvant temozolomide. (b) *BMI1* and (c) *SOX2* gene expression level was determined in three different P-GBM samples (n=2 for BT428, BT458 and BT465) with *GAPDH* expression as control. (d) Level of CD15 and CD133 cell surface protein expression was determined using flow cytometry in three P-GBM samples. The bar graph adjacent to the flow plots shows percent of CD15+ and CD133+ cells individually for each P-GBM sample. (e) Self-renewal capacity was determined using sphere formation assay with no significant difference in self-renewal between the three P-GBMs (n=3, p=0.5622). The bars represent mean±sem.



b

Treatment Group	Treatment
Control	No radiation + 2 weeks of DMSO
Rad	1 week of radiation + 1 week of DMSO followed by 1 week of DMSO
Tx1	1 week of radiation + 1 week of TMZ followed by 1 week of DMSO
Tx2	1 week of radiation + 1 week of TMZ followed by 1 week of TMZ

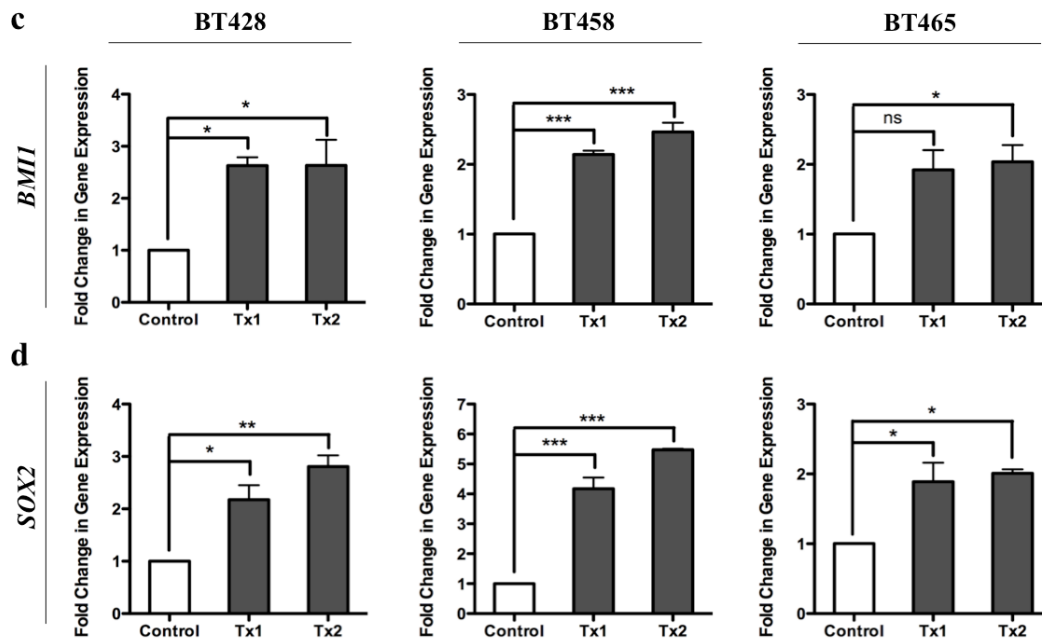


Figure 2: In vitro chemoradiotherapy increases the expression of BMI1 and SOX2 in P-GBMs.

(a) Timeline of the *in vitro* chemoradiotherapy protocol. Red arrows show the time frame during which radiation and TMZ was delivered to cells *in vitro*. (b) Four treatment groups were studied, labeled as control, Rad, Tx1 and Tx2. The treatment received by each group is described in the table. (c) *BMI1* expression level was determined in Tx1 and Tx2 groups and compared to control samples (n=3). Both Tx1 and Tx2 show significantly higher expression of *BMI1* except in BT465 Tx1 group (BT428, p<0.05; BT458, p<0.0001; BT465 Tx2, p<0.05). (d) *SOX2* expression level was determined in Tx1 and Tx2 groups and compared to control samples (n=3). Both Tx1 and Tx2 show significantly higher expression of *SOX2* in all P-GBMs (BT428, p<0.05; BT458, p<0.0001; BT465 Tx2, p<0.05). The bars represent mean±sem. ns: not significant, *P<0.05, **P<0.01, ***P<0.001.

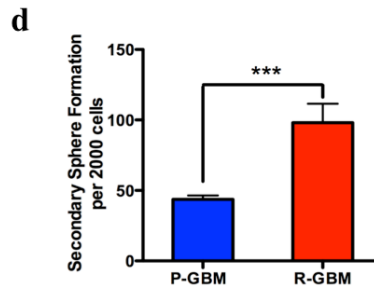
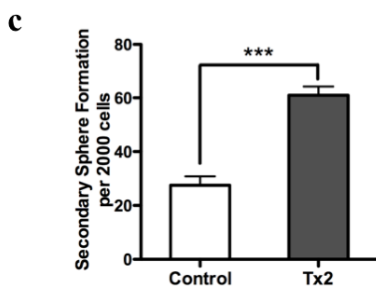
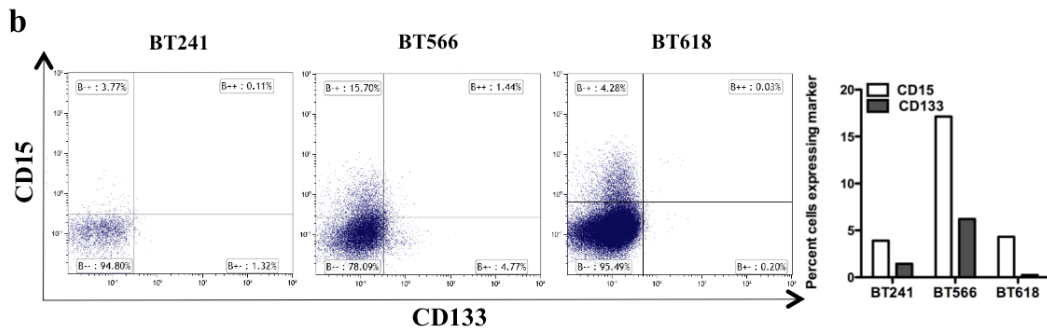
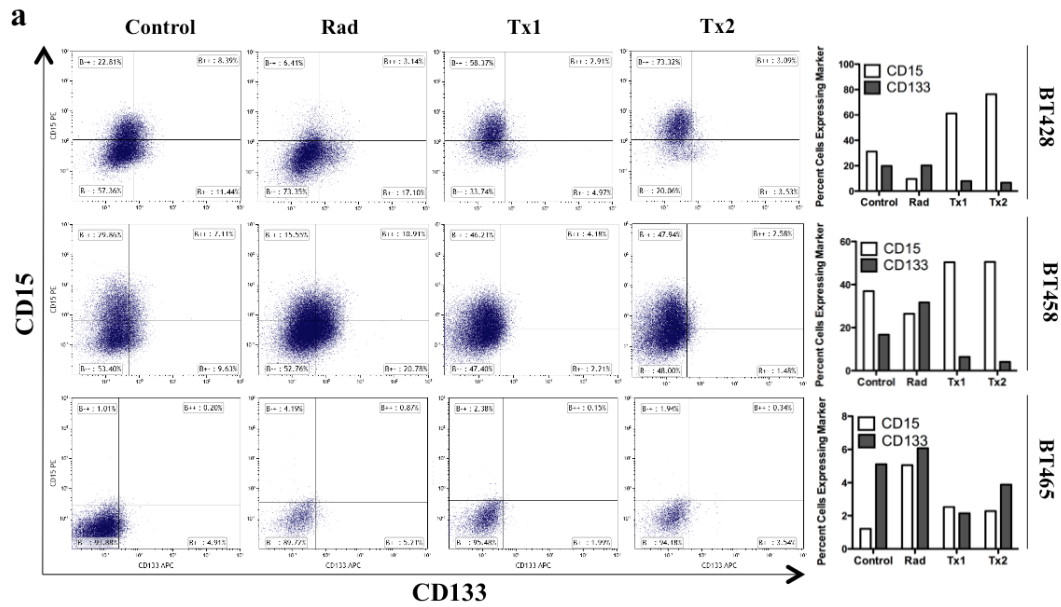


Figure 3: *In vitro* chemoradiotherapy enriches for CD15+/CD133- cell population in P-GBM and increases secondary sphere formation capacity, a profile similar to that of R-GBMs.

(a) Flow cytometry analysis was done on P-GBMs through the course of the *in vitro* chemoradiotherapy for all treatment groups. Rad group is enriched for CD133+/CD15- cell population, while both Tx1 and Tx1 have enriched CD15+ cell population as compared to controls. The bar graphs adjacent to the flow plots show the percent of CD15+ and CD133+ cells individually for each P-GBM. (b) Flow cytometry analysis of R-GBM for CD15 and CD133 levels show CD15 high and CD133 low profile for all three R-GBMs. The bar graph adjacent to the flow plots shows the percent of CD15+ and CD133+ cells individually for each R-GBM sample. (c) Control and Tx2 treatment cells from each P-GBM sample were plated for secondary sphere formation assay. Self-renewal capacity of Tx2 treatment group for all three P-GBMs is increased as compared to DMSO controls (n=3, p<0.001). (d) Secondary sphere formation capacity is significantly higher in R-GBMs (BT241, BT566 and BT618) as compared to P-GBMs (BT428, BT458 and BT465) (p=0.0002). The bars represent mean±sem. ***P<0.001.

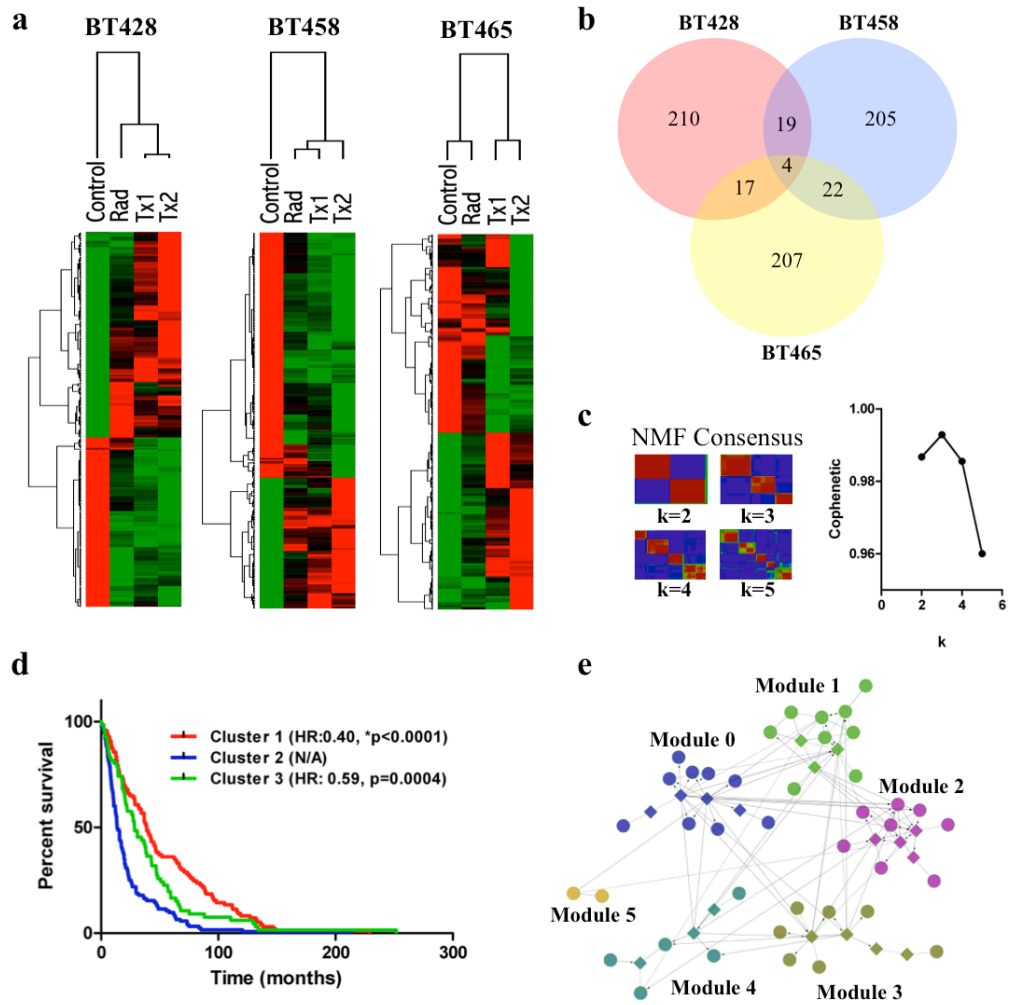


Figure 4: Transcriptional analysis of *in vitro* treated P-GBM cultures identifies pathways associated with resistance and hyper-aggressive subtypes of brain tumors.

(a) Hierarchical clustering of various GBM cultures based on the top 250 variably expressed genes in Control and Tx2 treated cultures. (b) Venn-diagram of overlapping Control/Tx2 variable genes among the three treated GBM cultures. (c, d) Survival analysis of the 3 brain tumor subtypes identified by NMF clustering of the REMBRANDT database using Control/Tx2 variable genes common to at least 2 of the 3 treatment experiments. (e) Network analysis of Control/Tx2 variable genes common to at least 2 of the 3 treatment experiments.

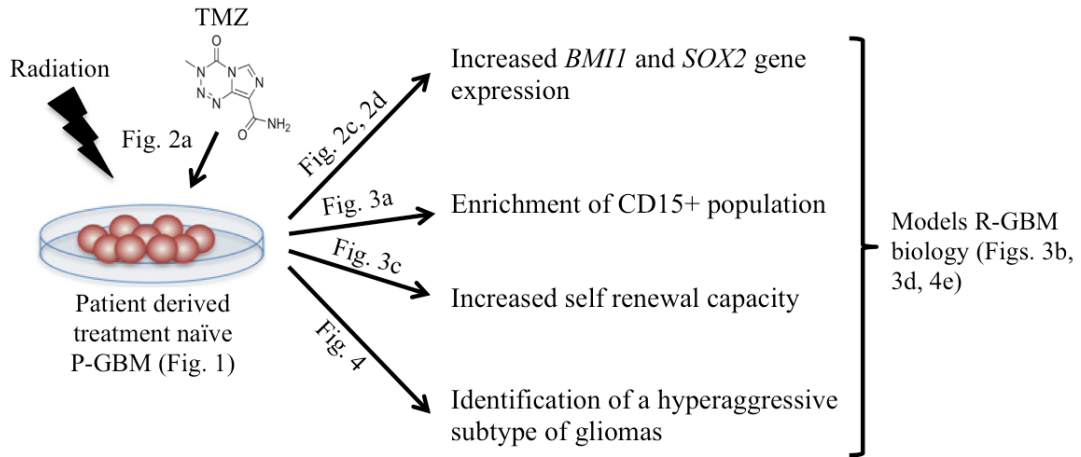


Figure 5: *In vitro* chemoradiotherapy of P-GBM models the biology of R-GBM.

In vitro treatment of BTSC enriched P-GBMs with radiation and TMZ leads to increase in expression of *BMII* and *SOX2*, enriches for CD15+ cell population and increases self-renewal capacity of P-GBMs. The global gene expression profile identifies a Tx2 specific 62-gene signature that clusters the REMBRANDT glioma dataset into an ultra-high risk brain tumor subgroup.

Supplementary Tables

Supplementary Table S1: Primer sequences used for RT-PCR experiments.

Gene	Forward Sequence	Reverse Sequence
<i>BM11</i>	GGAGGAGGTGAATGATAAAAGAT	AGGTTCTCCTCATAACATGACA
<i>SOX2</i>	TCAGGAGTTGTCAAGGCAGAGAAG	GCCGCCGCCGATGATTGTTATTAT
<i>GAPDH</i>	TGCACCACCAACTGCTTAGC	GGCATGGACTGTGGTCATGAG

Supplementary Table S2: MGMT promoter methylation specific primer sequences.

	Forward Sequence	Reverse Sequence
<i>Methylated</i>	TTTCGACGTTTCGTAGGTTTTC GC	GCACTCTCCGAAAACGAAACG
<i>Unmethylated</i>	TTTGTGTTTTGATGTTTGTAG GTTTTTGT	AACTCCACACTCTTCCAAAAACA AAACA

Supplementary Table S3: Molecular subtype of samples used.

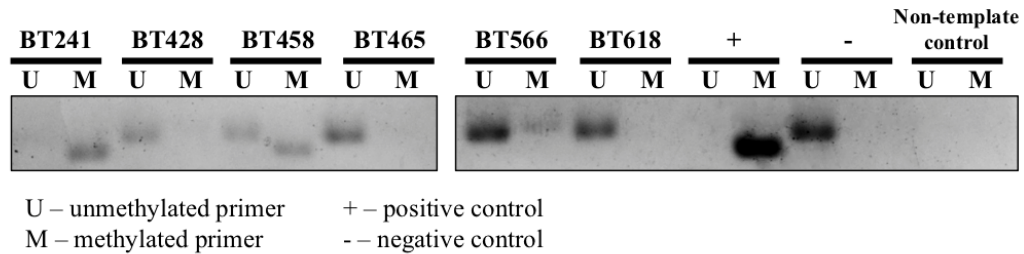
Specimen ID	Subtype
BT241	Mesenchymal
BT428	Proneural
BT458	Classical
BT465	Proneural
BT566	Mesenchymal
BT618	Mesenchymal

Supplementary Table S4: Significant network analysis pathways for common control/Tx2 variable genes.

The alphabet following pathway names identifies the source of the pathway. N: NCI – Nature pathways, R: REACTOME, K: KEGG, B: Bio-Carta. FDR: False discovery rate.

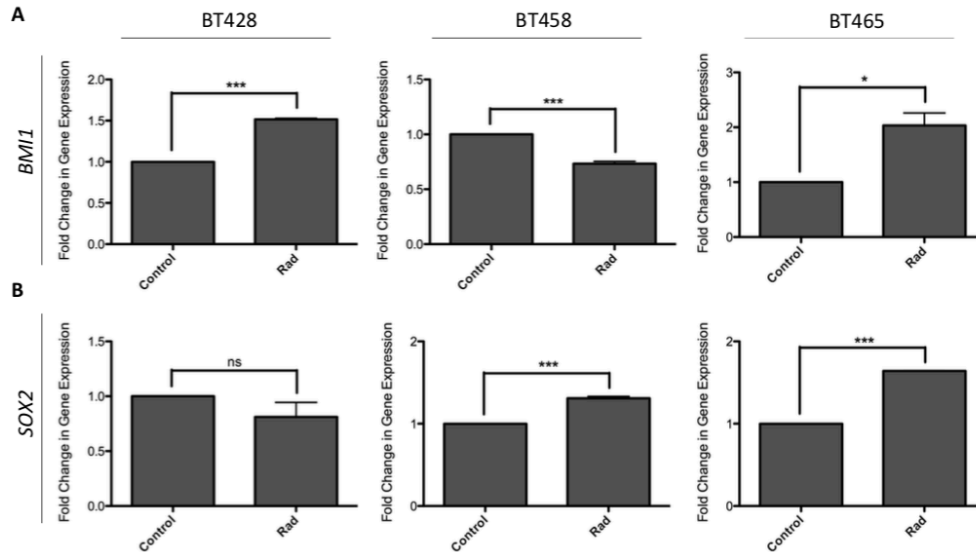
Module	Pathway	FDR
1	FOXM1 transcription factor network(N)	0.001
1	Regulation of mitotic cell cycle(R)	0.005
1	Mitotic G2-G2/M phases(R)	0.003
1	Oocyte meiosis(K)	0.005
1	Cell Cycle Checkpoints(R)	0.005
1	Cell cycle(K)	0.005
1	PLK1 signaling events(N)	0.023
1	Mitotic M-M/G1 phases(R)	0.025
1	HTLV-I infection(K)	0.032
1	p53 signaling pathway(K)	0.032
1	Antigen processing and presentation(K)	0.033
1	Progesterone-mediated oocyte maturation(K)	0.037
1	MHC class II antigen presentation(R)	0.046
2	PDGFR-alpha signaling pathway(N)	0.025
2	Cell adhesion molecules (CAMs)(K)	0.015
2	Osteopontin-mediated events(N)	0.020
2	rac1 cell motility signaling pathway(B)	0.022
2	Focal adhesion(K)	0.023
2	Beta3 integrin cell surface interactions(N)	0.021
2	Integrins in angiogenesis(N)	0.021
2	Axon guidance(R)	0.029
2	Signaling events mediated by VEGFR1 and VEGFR2(N)	0.026
2	Beta1 integrin cell surface interactions(N)	0.027
2	Pathways in cancer(K)	0.033
3	Direct p53 effectors(N)	0.018
5	Chromosome Maintenance(R)	0.005

Supplementary Figures



Supplementary Figure S1: MGMT promoter methylation status of GBM samples.

Methylation specific PCR for MGMT promoter from P-GBMs (BT428, BT458 and BT465) and R-GBMs (BT241, BT566 and BT618). BT428, BT465, BT566 and BT618 have unmethylated MGMT promoter. BT458 has partially methylated MGMT promoter. BT241 has hypermethylated MGMT promoter. Universally methylated DNA served as positive control and universally unmethylated DNA served as negative control.



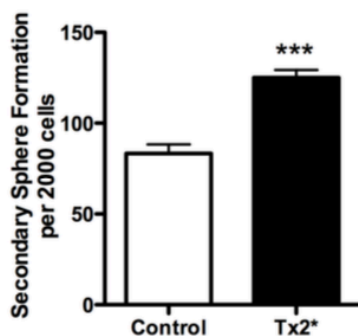
Supplementary Figure S2: *In vitro* radiotherapy changes the expression of *BMII* and *SOX2* in P- GBMs.

(A) *BMII* mRNA level was determined in Rad group and compared to control samples (n=3). BT428 and BT465 showed increase in *BMII* expression due to radiation but BT458 showed a decrease in *BMII* expression (BT428, $p < 0.0001$; BT458, $p = 0.0002$; BT465, $p = 0.0105$). (B) *SOX2* mRNA expression level was determined in Rad group and compared to control samples (n=3). BT458 and BT465 showed an increase in *SOX2* expression but no change was observed in BT428 (BT428, $p = 0.2295$; BT458, $p = 0.0002$; BT465 Tx2, $p < 0.0001$). The bars represent mean \pm sem. ns: not significant, * $P < 0.05$, ** $P < 0.01$, *** $P < 0.001$.

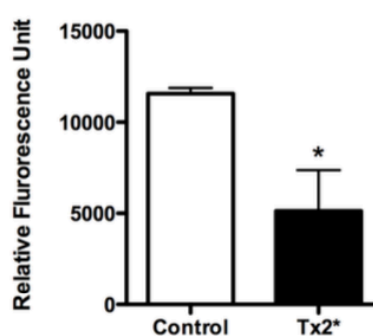
A

BT458	Cell Viability Post 1 st dose of chemoradiotherapy (Day 40)	Cell Viability Post Challenge Chemoradiotherapy (Day 5)
Control	68%	50%
Tx2*	63%	75%

B

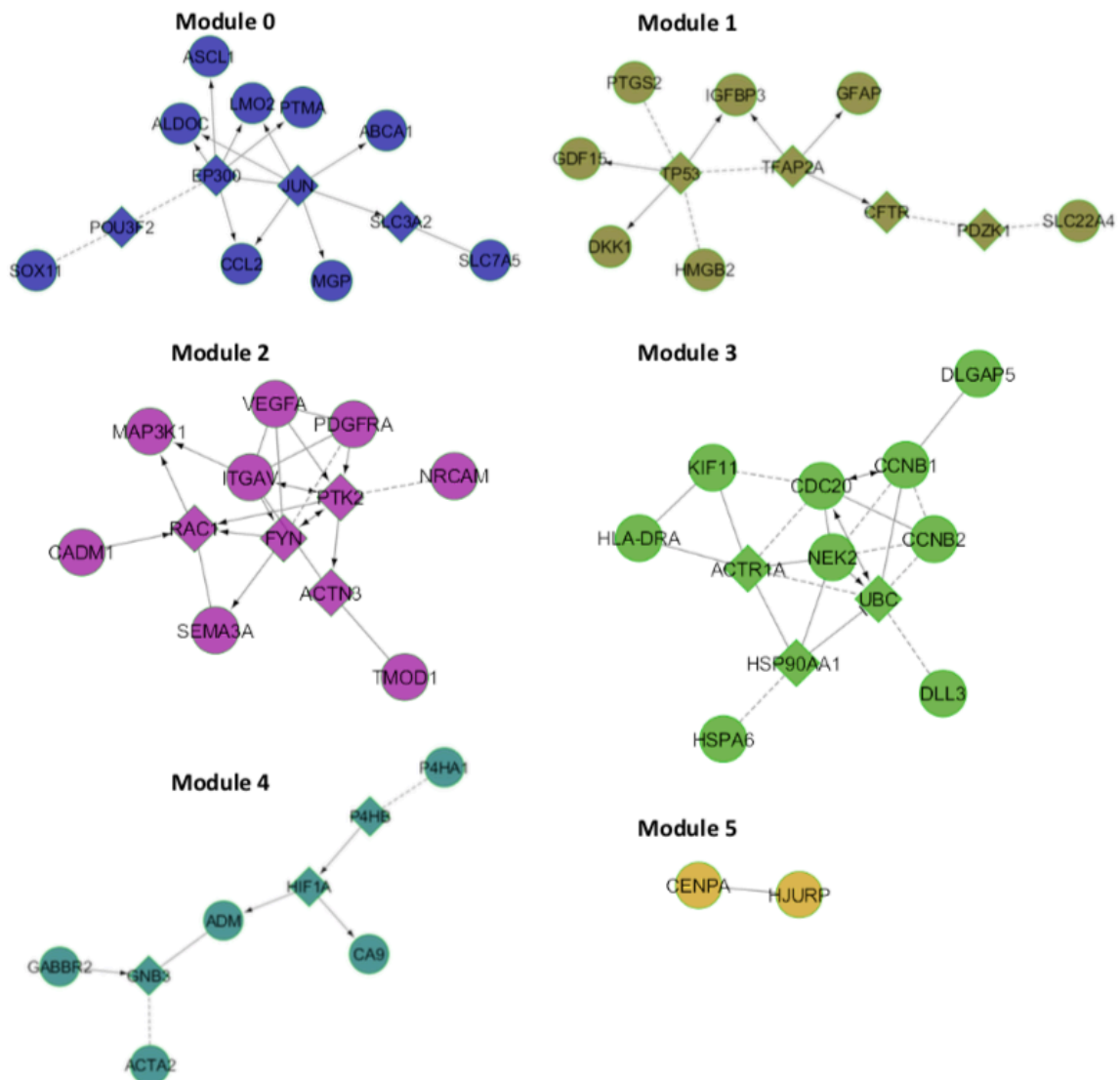


C



Supplementary Figure S3: *In vitro* chemoradiotherapy refractory BT458 cells are resistant to TMZ and radiation and have increased secondary sphere formation capacity but decreased proliferation capacity.

(A) Cell viability was determined following modified chemoradiotherapy on day 4 and after subsequent chemoradiotherapy challenge on day 5 for both control and Tx2* cells. Tx2* cells have higher cell viability following chemoradiotherapy challenge as compared to challenged control cells. (B) Secondary sphere formation of challenged Tx2* cells was higher than challenged control cells (n=6 technical replicates, p<0.0001). (C) Challenged control cells had higher proliferation capacity than challenged Tx2* cells (n=3 technical replicates, p=0.0461). *P<0.05, ***P<0.001.



Supplementary Figure S4: Modules for network analysis of common Control/ Tx2 variable genes.

The five modules identified from network analysis are presented here showing all interacting proteins in the module.

CHAPTER 3: Cotargeting ephrin receptor tyrosine kinases A2 and A3 in cancer stem cells reduces growth of recurrent glioblastoma

Preamble

This is a pre-copyedited, author-produced version of an article accepted for publication in *Cancer Research* following peer review. The version of record **Qazi MA**, Vora P, Venugopal C, Adams J, Singh M, Hu A, Gorelik M, Subapanditha MK, Savage N, Yang J, Chokshi C, London M, Gont A, Bobrowski D, Grinshtein N, Brown KR, Murty NK, Nilverbrant J, Kaplan D, Moffat J, Sidhu S, Singh SK. Cotargeting ephrin receptor tyrosine kinases A2 and A3 in cancer stem cells reduces growth of recurrent glioblastoma. *Cancer Research*, 78(17):5023-5037, 2018 is available online at: <http://http://cancerres.aacrjournals.org/content/78/17/5023>, DOI: 10.1158/0008-5472.CAN-18-0267.

MAQ designed the project, acquired and analyzed the data, interpreted the results, and wrote the manuscript. PV designed the project, analyzed the data, interpreted the results, and wrote the manuscript. CV designed the project, interpreted the results, and revised the manuscript. JA, MG, ML, and JN designed and characterized the antibody and wrote the manuscript under the supervision of SS, who also conceived the project. MS, NS and CC assisted with *in vivo* studies. AH acquired and analyzed CyTOF data. AG and NG acquired and analyzed phosphor-proteomic data under the supervision of DK. MKS acquired and analyzed flow cytometry data. DB assisted with *in vitro* studies. KRB analyzed and interpreted RNA-sequencing data under the supervision of JM, who also conceived the

project. NKM provided the brain tumour specimen for the project. SKS conceived and designed the project, supervised the study, interpreted the results, and wrote the manuscript.

Previous studies have assessed the role of ephrin receptors (EphR) in GBM. However, given functional redundancy between EphRs, no study had evaluated the role of all EphR in the context of GBM biology, especially in rGBM. Therefore, the aim of this work was to identify whether multiple EphRs drive the tumorigenic phenotype of rGBM as evaluated by functional *in vitro* and *in vivo* self-renewal assays. We found that co-expression of both EphA2 and EphA3 marked a highly tumorigenic subpopulation of GSCs in rGBM, that could act as potential therapeutic targets. Hence, we developed a bispecific antibody against both EphA2 and EphA3, characterized its mechanism of action, and evaluated its efficacy in rGBM using patient-derived xenograft models. This study highlighted the importance of concurrent evaluation of multiple GSC markers in GBM tumorigenesis and the need to develop poly-targeting approaches for the treatment of rGBM.

Co-targeting ephrin receptor tyrosine kinases A2 and A3 in cancer stem cells reduces growth of recurrent glioblastoma.

Running Title: Targeting EphA2 and EphA3 in recurrent GBM.

Maleeha A. Qazi¹, Parvez Vora¹, Chitra Venugopal¹, Jarrett Adams², Mohini Singh¹, Amy Hu², Maryna Gorelik², Minomi K. Subapanditha¹, Neil Savage¹, Jiahe Yang², Chirayu Chokshi¹, Max London², Alexander Gont³, David Bobrowski¹, Natalie Grinshtein³, Kevin R. Brown², Naresh K. Murty⁴, Johan Nilvebrant², David Kaplan³, Jason Moffat², Sachdev Sidhu², Sheila K. Singh^{1,4} *.

Affiliations:

¹Stem Cell and Cancer Research Institute, McMaster University, Hamilton, ON L8S 4L8 Canada

²The Donnelly Centre, University of Toronto, Toronto, ON M5S 3E1 Canada

³The Hospital for Sick Children, Toronto, ON M5G 1X8 Canada

⁴Department of Surgery, McMaster University, Hamilton, ON L8S 4L8 Canada

Corresponding author and lead contact:

Sheila K. Singh. M.D., Ph.D., FRCS(C)

Associate Professor of Pediatric Neurosurgery

Scientist, McMaster Stem Cell and Cancer Research Institute

MDCL 5027, Michael DeGroot Centre for Learning and Discovery,
1280 Main Street West, Hamilton, ON, L8S 4K1, Canada

P: 905 521 2100 x75237 F: 905 521 9992 Email: ssingh@mcmaster.ca

Conflict of Interest:

The authors declare no conflict of interest.

Author contributions

MAQ, PV: Conception and design, Collection and/or assembly of data, Data analysis and interpretation, Manuscript writing, Final approval of manuscript.

SKS, SS, JM, DK, CV, JA, KRB: Conception and design, Data analysis and interpretation, Manuscript writing, Final approval of manuscript.

MS, AH, MG, JY, MKS, CC, NS, ML, AG, DB, NG, JN: Collection and/or assembly of data, Data analysis and interpretation, Manuscript writing, Final approval of manuscript.

NKM: Acquisition of brain tumor samples, Manuscript writing, Final approval of manuscript.

Significance

Treatment of rGBM with a novel bispecific-antibody against EphA2 and EphA3 reduces tumor burden, paving the way for the development of therapeutic approaches against biologically relevant targets in rGBM.

Abstract

Glioblastoma (GBM) carries a dismal prognosis and inevitably relapses despite aggressive therapy. Many members of the Eph receptor tyrosine kinase (EphR) family are expressed by glioblastoma stem cells (GSC), which have been implicated in resistance to GBM therapy. In this study, we identify several EphR that mark a therapeutically targetable GSC population in treatment-refractory, recurrent GBM (rGBM). Using a highly specific EphR antibody panel and CyTOF (Cytometry by Time-Of-Flight), we characterized the expression of all 14 EphR in primary and recurrent patient-derived GSC to identify putative

rGBM-specific EphR. EphA2 and EphA3 co-expression marked a highly tumorigenic cell population in rGBM that was enriched in GSC marker expression. Knockdown of EphA2 and EphA3 together led to increased expression of differentiation marker GFAP and blocked clonogenic and tumorigenic potential, promoting significantly higher survival in vivo. Treatment of rGBM with a bispecific antibody (BsAb) against EphA2/A3 reduced clonogenicity in vitro and tumorigenic potential of xenografted recurrent GBM in vivo via downregulation of Akt and Erk and increased cellular differentiation. In conclusion, we show that EphA2 and EphA3 together mark a GSC population in rGBM and that strategic co-targeting of EphA2 and EphA3 presents a novel and rational therapeutic approach for rGBM.

Keywords

Recurrent glioblastoma, EphA2, EphA3, glioblastoma stem cells, poly-targeting, bispecific antibody.

Introduction

Glioblastoma (GBM) is the most malignant primary brain tumor in adults(1,2). Despite aggressive standard therapy consisting of surgical resection followed by radiation and chemotherapy, tumor re-growth and patient relapse remain inevitable. On average, patients face disease relapse at 7-9 months post-diagnosis and succumb to disease progression with a median survival of only 15 months(3,4). The dismal prognosis of GBM has been increasingly attributed to extensive genetic, epigenetic, cellular and functional heterogeneity (5-9), allowing for redundancy in signalling pathways and rendering single-agent therapy obsolete for long-term disease remission and cure. Moreover, the genomic

landscape of recurrent GBM has been shown to diverge significantly from the primary GBM, as actionable targets identified in primary, treatment naïve GBM are not present at recurrence. Rather, recurrent disease is instead driven by a different mutational and signalling profile (10-12). There is also accumulating evidence suggesting that GBMs may be instigated by stem cell like populations termed glioblastoma stem cells (GSCs) (13-16). Moreover, GSCs are thought to account for GBM recurrence after therapy as cells with GSC properties are resistant to radiation and chemotherapeutic agents (17-20). Together, this evidence implies that treatment of recurrent GBM should be informed by the identification of molecular targets specific to its evolved molecular landscape, and a poly-targeting approach could better address the advanced clonal heterogeneity that generates cellular escape from therapy, resulting in treatment resistance.

The EphR tyrosine kinase family, with 14 members, coordinates cell positioning, tissue and organ patterning during development, and is expressed in most adult stem cell niches and many cancers (21-23). Various members of the EphA/Ephrin-A and EphB/Ephrin-B subfamilies have been shown to play a role in GBM cell migration, invasion and angiogenesis (24-27). The expression of EphA2, EphA3, EphA4, EphA7 and EphB2 correlates with poor patient outcome in GBM, and each has a distinct role in GBM tumorigenicity, invasiveness, or maintenance of the GSC pool. In particular, EphA2 has been shown to drive tumorigenicity in GSCs, and infusion of EphrinA1-Fc into intracranial xenografts elicited strong tumor-suppressing effects (24). EphA2 overexpression has also been shown to promote invasiveness of GSCs *in vivo* in cooperation with the Akt signaling pathway(27,28). Similarly, EphA3 has also emerged as a GSC marker, which is

overexpressed in GBM and maintains GBM cells in a stem-like state (25). While these data validate EphA2 and EphA3 as therapeutic targets in brain tumors, the literature to date has only profiled or targeted single EphRs in treatment-naïve GBM and suggests single targeting of an EphR would leave other putative EphR driven GSC populations to seed tumor recurrence. Additionally, what has not been explored is the complex putative effects of multiple EphR family members dynamically activated or suppressed through therapy delivery and tumor progression.

In this study, we used an EphR profiler to simultaneously assess the protein expression of all EphRs in cells comprising primary and recurrent GBM, to identify the putative cooperative role of multiple EphRs in driving GBM tumorigenesis. Given the established importance of EphA2 and EphA3 individually in maintaining GSCs, we wanted to explore whether EphA2 and EphA3 together mark an even more potent tumorigenic cancer stem cell population in recurrent GBM. Considering the complex signaling pathways orchestrated by multiple EphRs, we also examined whether co-targeting of EphA2 and EphA3 using a bispecific antibody approach will impact the functional GSC pool more effectively than monotherapies.

Materials and Methods

Patient Tumors: Human GBM brain tumors were obtained from consenting patients, as approved by the Hamilton Health Sciences/McMaster Health Sciences Research Ethics Board (REB # 07366), in compliance with Canada's Tri-Council Policy Statement on the Ethical Conduct for Research Involving Humans and the International Ethical Guidelines for Biomedical Research Involving Human Subjects. GBM4 was a kind gift from Dr.

Hiroaki Wakimoto (Massachusetts General Hospital, Boston, MA). Patient demographics are presented in Supp. Table S1.

Dissociation and culture of GBM tissue: Human GBM tissue was dissociated and cells were maintained in NeuroCult complete media (StemCell Technologies; 10ng/mL bFGF, 20ng/mL EGF, and 2µg/mL Heparin) either as tumorspheres or grown adherently on poly-L-ornithine/laminin.

Eph Profiler: Receptor-selective Abs for all 14 Eph homologs were used to profile the expression of EphRs in primary and recurrent GBMs.

***In vitro* Chemoradiotherapy:** We treated primary GBM BT602 with radiation and temozolomide as described in Qazi et al.(20).

Flow cytometry analysis: The percentage expression of EphA2, EphA3, ephrinA1 and ephrinA5 was determined on a MoFlo XDP flow cytometer (Beckman Coulter) along with Summit 5.4 software using in-house anti-EphA2 Fab with Alexa Fluor 488 as secondary antibody (1:1000), in-house anti-EphA3 Fab with APC as secondary antibody, in-house anti-EphrinA1 Fab with AF488 as secondary antibody, and in-house anti-EphrinA5 Fab with APC as secondary antibody. Data was analyzed with Kaluza® Flow Analysis software.

CyTOF and viSNE analysis: Expression of EphRs along with a panel of stem cell markers implicated in GBM tumorigenesis were determined by CyTOF. Lanthanide metal tags were selected using Fluidigm's Maxpar Panel Designer and conjugated to commercial IgGs using Fluidigm's MAXPAR X8 antibody labeling kit following manufacturer's instructions (Fluidigm). In brief, commercial IgGs targeting MAP2 (¹⁵³Eu) (Fisher -13-

1500), CD133 (^{164}Dy) (Miltenyi - 130-090-851), CD15 (^{152}Sm) (BioLegend - 323002), SOX2 (^{176}Yb) (BD Biosciences - 561469), FOXG1 (^{145}Nd) (Abcam - AbF1774), ITGA6 (^{171}Yb) (R&D Systems – MAB1350), BMI1 (^{151}Eu) (R&D Systems - MAB3341), and human Fab'2 (Jackson Immunoresearch - 309-545-006) were conjugated directly to the X8 chelators through a thiol linkage. In house, synthetically-raised monoclonal Fabs used for analysis were pre-clustered to anti-Fab'2 IgGs conjugated with X8 chelator bound with one of the following isotopes: ^{154}Sm - EPHA1, ^{169}Tm - EPHA2, ^{147}Sm - EPHA3, ^{150}Nd - EPHA4, ^{162}Dy - EPHA5, ^{173}Yb - EPHA6, ^{156}Gd - EPHA7, ^{167}Er - EPHA8, ^{160}Gd - EPHA10, ^{159}Tb - EPHB1, ^{170}Er - EPHB2, ^{141}Pr - EPHB3, ^{158}Gd - EPHB4, ^{175}Lu - EPHB6. CyTOF acquisition was performed on CYTOF2 or HELIOS machine using standard settings by the UHN Flow and Mass Cytometry Facility. Acquisition was carried out on a HELIOS CyTOF system along with analysis platform, Cytobank and computational analysis software, viSNE to map the high-dimensional cytometry data for co-expression analysis.

Glioma patient database bioinformatics: To determine the clinical relevance of EphA2 and EphA3, we interrogated the REpository for Molecular Brain Neoplasia DaTa (REMBRANDT) dataset(29,30). Expression levels were compared between gliomas (oligodendroglioma, astrocytoma and GBM) and between GBM subtypes (proneural, classical and mesenchymal). For survival analysis, expression levels were categorized into high and low groups for both EphA2 and EphA3 using median value as a threshold. For EphA2^{high}/EphA3^{high} and EphA2^{low}/EphA3^{low} survival analysis, expression and patient data corresponding to EphA2 and EphA3 were obtained for The Cancer Genome Atlas (TCGA) low-grade glioma-glioblastoma dataset(6,29). Survival differences between the

EphA2^{high}/EphA3^{high} (N=193) and EphA2^{low}/EphA3^{low} (N=194) groups were compared using Kaplan-Meier analysis by the log-rank test in the R “survival” package (v2.42-3). In order to compute differential expression between EphA2^{high}/EphA3^{high} and EphA2^{low}/EphA3^{low} groups, hg38 read count data was obtained from the NCI Genomic Data Commons Data Portal (<https://portal.gdc.cancer.gov/>) for the TCGA LGG and GBM datasets. The counts were merged into a single matrix, annotated with Ensembl gene annotations, and filtered to remove transcripts lacking an Entrez Gene cross-reference. In total, expression data for 374 patients (183 EphA2^{high}/EphA3^{high} and 191 EphA2^{low}/EphA3^{low}) was processed using the Bioconductor packages edgeR and limma as follows. First, genes with less than 1 count per million (CPM) in at least 5% of the patients were filtered out, and then samples were normalized for read depth with the ‘calcNormFactors()’ function and converted to log2CPM with voom(). Finally, differentially expressed genes were identified using moderated t-tests.

Sphere formation and proliferation assay: After primary sphere formation was noted, spheres were dissociated to single cells and re-plated in 0.2 mL Neurocult complete media as previously published (13,31). Briefly, neurospheres were treated with Liberase Blendzyme® 3 and plated at 200 cells/well density for sphere formation assay and 1000 cells/well for proliferation assay in a 96 well microwell plate in 0.2 mL volume of Neurocult complete media. The spheres were counted 3 days later. Proliferation was measured using PrestoBlue® cell viability reagent (Thermo Fisher Scientific).

Lentiviral production and transduction: Lentiviral vectors expressing shRNA directed against EphA2 or EphA3 with the highest knock-down efficiency, or a control shGFP that

has no targets in the human genome were used in the *in vitro* and *in vivo* experiments (shEphA2-A: 5'CCATCAAGATGCAGCAGTATA3', shEphA3-B: 5'CCTTCCAATGAAGTCAATCTA3', shGFP: 5'ACAACAGCCACAACGTCTATA3'). Both shEphA2-A and shEphA3-B were used in combination for double KD of EphA2 and EphA3. Replication-incompetent lentiviruses were produced by cotransfection of the expression vector and packaging vectors pMD2G and psPAX2 in HEK 293FT cells. Viral supernatants were harvested 48 hours after transfection, filtered through a 0.45- μ m cellulose acetate filter, and precipitated using ultracentrifugation (25,000 rpm, 2 hours, 4°C). The viral pellet was resuspended in 1.0 mL of Neurocult basal media and stored at -80°C. EphA2 shRNA and EphA3 shRNA with the best relative knockdown efficiencies were utilized for all *in vitro* and *in vivo* studies.

Limiting dilution assay: Cells were plated at limiting dilution from 300 cells to 1 cell per well in 200 μ L of Neurocult complete media in a 96-well plate and 0.37 intercepts were calculated to determine the sphere-forming frequency(13). For *in vitro* LDA experiments, GBM cells were treated with 200nM of EphA2/A3 BsAb or control IgG (Jacksons AffiniPure Goat Anti-Huamn IgG, F(ab')₂ fragment specific).

Real-time quantitative PCR: Total RNA was isolated using NorgenTotal RNA Purification kit. cDNA was synthesized by iScript cDNAsupermix (Quanta Biosciences) followed by real-time quantitative PCR using SsoAdvanced™ Universal SYBR® GreenSupermix (Bio-Rad). Samples were quantified using CFX Manager™ software. Data is presented as the ratio of the gene of interest to GAPDH or bActin.

Cell cycle and apoptosis analysis: Cells were stained for DNA cell cycle using DNA Prep Reagent Kit (Beckman Coulter) and analyzed via flow cytometry (MoFlo XDP, Beckman Coulter). Annexin V conjugated to APC was used along with 7-AAD viability for analysis of apoptosis in cells of interest using flow cytometry.

RNA Sequencing and analysis: Illumina sequencing was performed by the Farncombe Metagenomics Facility (McMaster University). RNA integrity was first verified using the Agilent BioAnalyzer, followed by mRNA enrichment and library prep using the NEBNext Ultra Directional RNA Library Prep Kit along with the NEBNext Poly(A) mRNA Magnetic Isolation Module. Libraries were subject to further BioAnalyzer QC and quantified by qPCR. Sequencing was performed using the HiSeq Rapid v2 chemistry with single end 1x50 bp read length configurations to a target depth of approximately 6M reads per sample. Reads were aligned with the STAR v2.4.2a aligner using genome build hg38 and Gencode v25 transcript models. Read counts for each sample, output by STAR, were merged into a single matrix along with annotation information. Finally, the count matrix was filtered to only include protein-coding genes. Transcripts were removed that did not have at least 0.5 counts per million mapped reads in at least two samples, and the remaining reads were normalized using ‘TMM’ normalization in edgeR. Differential expression was determined moderated t-tests using limma (v3.32.10).

Orthotopic Xenografts: Animal studies were approved by and performed according to guidelines under Animal Use Protocols of McMaster University Central Animal Facility (AUP # 14-12-52). All intracranial injections were performed 2 mm anterior to the coronal suture, 3 mm lateral to midline in the right frontal lobe of 6-8 week old NOD-SCID or NSG

mice. rGBM BT241 cells were sorted based on expression of EphA2 and EphA3 and 6.5×10^3 cells were intracranially injected into NOD-SCID mice. A cohort of animals was sacrificed when EphA2⁺/EphA3⁺ engrafted mice from the experiment showed signs of tumor formation (head swelling, hunching, rough coat, weight loss) for IHC while a cohort of mice was left for survival studies. For *in vivo* LDA of EphA2⁻/EphA3⁻ and EphA2⁺/EphA3⁺ cells, 4×10^2 , 4×10^3 and 4×10^4 cells for each subpopulation of cells sorted using flow cytometry were intracranially injected into NOD-SCID mice. For EphA2 and EphA3 knockdown, 1×10^5 live cells of BT241 from control shGFP, shEphA2, shEphA3 and shEphA2/A3 cells were intracranially injected into NOD-SCID mice. A cohort of animals was sacrificed 4 weeks post-injection for IHC while a cohort of mice was left for survival studies. For BT972 knockdown experiments, 6×10^5 live cells from control shGFP and shEphA2/A3 were intracranially injected NOD-SCID mice. For EphA2/A3 BsAb treatment, 1×10^5 BT241 cells or 1×10^6 BT972 cells were intracranially injected into 6-8 week old NSG mice. Intracranial treatment with EphA2/A3 BsAb (in-house) or control IgG (Jacksons AffiniPure Goat Anti-Huamn IgG, F(ab')₂ fragment specific) was started 10-14 days later twice a week ($9.4 \mu\text{L}$ of EphA2/A3 BsAb or control IgG for a total of $30 \mu\text{g}/\text{dose}$) into the same burr hole created for the initial engraftment of the tumor cells. The EphA2/A3 BsAb or control IgG were intracranially infused using a Hamilton syringe at an infusion rate of $30 \mu\text{L}/\text{min}$. The intracranial treatment continued for twice a week until control mice succumbed to disease burden. Mice were perfused with 10% formalin and collected brains were sliced at 2mm thickness using brain-slicing matrix. Sections were paraffin-embedded and multiple immunohistochemical tests were performed (H&E, EphA2, EphA3 and

GFAP). Tumor area was quantified using ImageJ software taking into account the scale bar measurement on the scanned H&E images.

Western Blot and phosphor-proteomics: For western blotting, we used Santa-Cruz antibodies EphA2 (sc-924, 1:500) and EphA3 (sc-919, 1:1,000), and Cell Signaling antibodies pEphA2 (12677S, 1:1,000), pEphA3 (8862S, 1:1,000), Erk1/2 (4695S, 1:1,000), pERK1/2 (4377S, 1:1,000), Akt (4691S, 1:1,000), pAkt (4051S, 1:1,000). GAPDH was used as a loading control. For phosphor-proteomics, BT241 cells treated with control IgG or EphA2/A3 BsAb (200nm for 15 min) were collected in urea lysis buffer (20mM HEPES, 8M urea, phosphatase inhibitor tablet – 88667, Pierce) and lysed by pipetting and sonication. Following centrifugation, the lysate was treated with 1/10th of the volume of 45mM DTT (60°C, 20min), cooled on ice and then treated with 110mM iodoacetamide (room temperature in the dark, 15min). Samples were diluted to a final concentration of 2M urea and treated with 1/100th of the volume of 1mg/mL trypsin-TPCK (16h, dark, room temperature, rocking). Samples were treated with 1/20th the volume of 20% TFA and purified using Sep-Pak C18 columns (WAT051910, Sep-Pak). Samples were eluted in 40% acetonitrile/0.1% TFA, frozen and lyophilized. PTMScan phosphor-tyrosine mouse mAb kit (5636, Cell signalling) was used for immunoaffinity purification. Following a 2h incubation at 4°C, cells were washed 5 times in IAP buffer and 3 times in water prior to elution in 0.15% TFA. Samples were concentrated and purified using C18 stage tips (87784, Pierce) and eluted in 50% acetonitrile/0.1% TFA. Samples were analysed at the SPARC BioCentre (Hospital for Sick Children, Toronto, On, Canada) by LC-MS/MS on the Q Exactive™ Tandem Mass Spectrometer (ThermoFisher). Phospho-tyrosine peaks

were quantified using MaxQuant (Max Planck Institute of Biochemistry, Munich, Germany) and represented as a heat map of the intensity of the peptide in each condition over the max intensity (blue: lowest intensity, red: highest intensity).

Statistical Analysis: All quantitative data presented are the mean \pm SD. Samples used and respective n values are listed in the figure legends. The level of significance was determined by Student's two-tailed t-test or ANOVA using GraphPad Prism 5 software.

Results

EphRs are expressed heterogeneously in human GBMs and co-express with stem cell markers.

We profiled the surface protein expression of all 14 members of the Eph receptor family in primary, treatment-naïve GSCs (pGBMs: BT428, BT458, BT459, BT465, BT486, BT602 and BT648) and recurrent GSCs (rGBMs: BT241, BT566 and BT618) using our Eph profiler. The heterogeneous expression of all EphRs in human GSCs (Fig. 1A) suggest a variety of signaling paradigms that might drive oncogenesis in these patients. We observed that EphA2 was expressed at moderate to high levels and EphA3 was expressed at moderate levels across all GSC lines, and proceeded to characterize its expression in human neural stem and progenitor cells (NSPCs), pGBMs and rGBM by flow cytometry. Here we noted that EphA2 and EphA3 expression is enriched in rGBM compared to pGBM and NSPCs (Fig. 1B, Supp. Fig. S1A). As we had previously developed a stem cell culture model of GBM recurrence (20), we treated pGBM BT602 with our *in vitro* chemoradiotherapy protocol, and noted increased expression of both EphA2 and EphA3 post-treatment (Fig. 1C). We then profiled pGBMs and rGBMs for all EphRs along with a panel of GSC markers

including CD133, CD15, Bmi1, Sox2, Integrin- α 6 and FoxG1, using mass “cytometry time-of-flight” (CyTOF) assays. CyTOF, which employs antibodies labelled with lanthanide metals rather than fluorochromes, permits a greater degree of multiplexing than traditional flow cytometry and the simultaneous quantification of numerous cell surface targets. We find that although GBMs display heterogeneous expression of these markers at the single cell level (Fig. 1D, Supp. Fig. S1B), there is heightened intensity of EphA2 and EphA3 co-localizing with GSC marker expression (Fig. 1E, population in circle). In fact, BT241, a rGBM sample, co-expressed EphA2 and EphA3 with all GSC markers in a population twice as large as that of two pGBMs, BT459 and BT602 (1.30% in BT241 vs 0.52% and 0.43% in BT459 and BT602, respectively).

EphA2 and EphA3 are highly expressed in GBM, overrepresented in poor-outcome subgroups of GBM and have higher expression in rGBM.

Since previous studies implicated EphA2 and EphA3 as independent oncogenic drivers of GSCs (24,25), and our data suggested that EphA2 and EphA3 are expressed at higher levels at GBM recurrence we interrogated EphA2 and EphA3 expression REpository for Molecular BRAin Neoplasia DaTa (REMBRANDT) database. Both EphA2 and EphA3 are highly expressed in GBM compared to low-grade oligodendrogliomas and astrocytomas (Fig. 2A). In addition, EphA2 and EphA3 expression was higher in classical and mesenchymal subgroups of GBM, which have a slightly worse outcome (5) when compared to the better performing proneural subgroup (Fig. 2B). In The Cancer Genome Atlas (TCGA) GBM database, we found only six matched primary-recurrent GBM pairs, and found that in a subset of these patients, the expression of EphA2 and EphA3 is higher at

recurrence (Fig. 2C). High expression of EphA2 predicted poor survival in GBM patients (Fig. 2D), while high expression of EphA3 trended towards poor but non-significant patients survival (Fig. 2E). More importantly, in the TCGA low-grade glioma-glioblastoma database showed that patients with high expression of EphA2 and EphA3 had significantly poor survival as compared to patients with low expression of both EphA2 and EphA3, signifying that together EphA2 and EphA3 drive a poor prognosis in patients with gliomas (Fig. 2F). In fact, when we explored the genes associated with EphA2^{high}/EphA3^{high} patient subgroup, we discovered high expression of multiple genes known to promote GBM tumorigenesis such as the integrin receptors (ITGA1, ITGA5, ITGB3), integrin receptor ligand (POSTN), genes associated with tumor invasion (CHI3L1, IL13RA2, TWIST1, CD70, IL6), as well as genes known to mark GSCs (PROM1, CA9, LGR6) (Fig. 2G). Together, this data led us to the hypothesis that EphA2 and EphA3 may co-identify an even more potent GSC population in rGBMs than expression of either EphR alone.

EphA2 and EphA3 co-expression marks a highly tumorigenic GSC population in rGBM.

To reinforce the correlation between EphA2 and EphA3 co-expression in rGBM GSCs, we FACS-sorted rGBM cells into four pools, expressing either low EphA2 and EphA3 (EphA2-/EphA3-), high EphA2 only (EphA2+/EphA3-), high EphA3 only (EphA2-/EphA3+) and high EphA2 and EphA3 (EphA2+/EphA3+) (Fig. 3A), and then assessed their *in vitro* clonogenicity and intracranial tumorigenic capacity. As expected, the EphA2+/EphA3+ fraction contained the most clonogenic cells (Fig. 3B) compared to the EphA2-/EphA3- cells, with the EphA2+/EphA3- and EphA2-/EphA3+ cells presenting intermediate clonogenic capacity. We saw the same trend in the proliferation capacity of

these fractionated cell populations (Fig. 3C). We then assessed the expression of key GSC markers in EphA2-/EphA3- and EphA2+/EphA3+ rGBM fractions and found no difference in expression of CD133 or CD15 but a significantly higher expression of Bmi1 and Sox2 in EphA2+/EphA3+ cells compared to EphA2-/EphA3- cells (Fig. 3D). Despite very low percentage of EphA2+/EphA3- cell population and low sorting efficiency of rGBM BT241, we were able to sort cells for intracranial injections. We intracranially implanted mice with the sorted cell populations and found that EphA2+/EphA3+ cells give rise to much larger tumors compared to EphA2-/EphA3- cells, with EphA2+/EphA3- and EphA2-/EphA3+ cells giving rise to intermediate-sized tumors, replicating our *in vitro* clonogenic data (Fig. 3E). *In vivo* limiting dilution intracranial transplantation assays using EphA2-/EphA3- and EphA2+/EphA3+ cells confirmed that high EphA2 and EphA3 are the hallmark GSCs in rGBM and can be used for their enrichment (Fig. 3F; stem cell frequency: EphA2-/EphA3- 1/26,096 cells compared to EphA2+/EphA3+ 1/12,358 cells). EphA2+/EphA3+ cells were able to give rise to tumors with as few as 4,000 cells compared to 40,000 cells when implanting EphA2-/EphA3- cells. In addition, mice engrafted with EphA2+/EphA3+ cells had a shorter survival (median survival 53 days) as compared to single positive cells (median survival: EphA2+/A3- 57 days and EphA2-/EphA3+ 58 days) and significantly shorter than mice engrafted with EphA2-/EphA3- cells (median survival 64 days, Log-rank p value=0.03) (Fig. 3G). We wanted to investigate how the cell surface expression of EphA2 and EphA3 in EphA2+/EphA3+ cells change overtime. We performed time-course experiment and found that in just four weeks, EphA2+/EphA3+ sorted cells revert back to their original EphA2 and EphA3 surface expression distribution (Supp. Fig. S2). This

suggests that the tumorigenic potential of EphA2⁺/EphA3⁺ would be even higher than demonstrated in *in vivo* tumor formation and survival studies as EphA2⁺/EphA3⁺ cells rapidly establish the original subpopulations of cells including less tumorigenic EphA2⁺/EphA3⁻, EphA2⁻/EphA3⁺ and EphA2⁻/EphA3⁻ cells.

Loss of EphA2 and EphA3 inhibits clonogenicity and tumor formation capacity of rGBMs.

We next investigated the effect of EphA2 and EphA3 knockdown (KD) on *in vitro* clonogenicity and intracranial tumorigenic capacity of rGBMs. We used small-hairpin RNA (shRNA) to KD either EphA2 or EphA3 individually or in a combined fashion in two rGBM samples. We tested three separate shRNA against EphA2 (shEphA2-A, B and C) and two separate shRNA against EphA3 (shEphA3-B and C), and found shEphA2-A and shEphA3-B to be the most effective at reducing protein expression of EphA2 and EphA3, respectively as well as in reducing proliferation of rGBM cells (Supp. Fig. S3A-D). Therefore, in all subsequent studies, we used shEphA2-A and shEphA3-B to knockdown EphA2 and EphA3 expression, respectively in rGBM GSCs (Fig. 4A). We find that combined EphA2 and EphA3 KD led to loss in clonogenic capacity of rGBM cells as compared to control shGFP cells (Fig. 4B). In addition, proliferative capacity of cells was only significantly inhibited in cells with double-KD compared to control shGFP cells (Fig. 4C). The KD of EphA2 and EphA3 also affects the cell cycle of rGBM, decreasing the percentage of cells in DNA replication S phase and increasing percentage of cells in quiescent G0G1 phase (Fig. S3E). We also noted an increase in apoptosis of rGBM with shEphA2/A3, illustrating that EphA2 and EphA3 are integral to cell survival (Fig. S3F).

Furthermore, the combined EphA2 and EphA3 KD led to decreased expression of all GSC markers in rGBMs, suggesting loss of the undifferentiated, stem-like state (Fig. 4D). We next submitted control shGFP and shEphA2/A3 cells from rGBM BT241 for RNA-sequencing for global transcriptome profiling. We found that KD of both EphA2 and EphA3 leads to reduction in gene expression of markers of epithelial-mesenchymal transition and invasion (Fig. 4E), some of which we found to be correlated with the EphA2^{high}/EphA3^{high} patient samples (Fig. 2G), such as CHI3L1, SNAI1 and VIM. Additionally, KD of both EphA2 and EphA3 increased levels of GFAP in rGBM, indicating that the decrease in EphA2 and EphA3 directs rGBM cells to a more differentiated, astrocytic lineage (Fig. 4F). We next intracranially implanted these cells in mice and find that combined KD of EphA2 and EphA3 completely prevented the cells from forming tumors in just over half of the transplanted mice (3/5 mice formed tumors with shEphA2/A3 cells), while EphA2 KD formed tumors as large as control shGFP and EphA3 KD formed intermediate-sized tumors (Fig. 4G). We found similar results with KD of both EphA2 and EphA3 in another rGBM line, BT972 (Fig. 4H). These results corroborated with survival studies where mice engrafted with shEphA2/A3 cells had the longest survival (Fig. 4I, median survival 57 days, Log-rank p value=0.0003) as compared to control mice (median survival shGFP 44, shEphA2 45.5 and shEphA3 49.5 days). These results suggest that EphA2 and EphA3 should be co-targeted to inhibit rGBM clonogenicity, proliferation, invasion and tumorigenic capacity potentially through a differentiation mechanism to astrocytic cell type.

Co-targeting of EphA2 and EphA3 with bispecific antibody (BsAb) decreases EphA2 and EphA3 surface expression and limits Akt and Erk1/2 Pathway activation in rGBM.

Since our data suggests that EphA2 and EphA3 cooperate in maintaining a potent GSC population and tumorigenic potential of rGBMs, we designed a bispecific variable heavy domain (VHD) antibody that co-targets both EphA2 and EphA3 (EphA2/A3 BsAb; in-house) with high affinity (Fig. 5A and Supp. Fig. S4A). We wanted to next determine if binding of EphA2/A3 BsAb leads to internalization of the BsAb. We incubated EphA2 and EphA3 expressing cells lines with control IgG or EphA2/A3 BsAb at 4°C and 37°C for four hours (Fig. 5B and Supp. Fig. S4B). As expected, we observed a temperature-dependent reduction of surface EphA2/A3 BsAb binding, consistent with antibody dependent internalization and degradation of Eph receptor observed for Eph targeting agonists. To further determine whether the internalization of the EphA2/A3 BsAb leads to decreased surface expression of EphA2 and EphA3, we treated rGBM with EphA2/A3 BsAb for three days and performed CyTOF to identify surface co-expression of EphA2 and EphA3. We find that treatment with EphA2/A3 BsAb leads to a complete loss of surface EphA2 receptor expression and a ~50% decrease in EphA3 surface receptor levels (Fig. 5C and D), which was validated with western blot analysis for total EphA2 and EphA3 protein levels (Supp. Fig. S4C). After three-day treatment with EphA2/A3 BsAb, the EphA2/A3 BsAb itself has much lower levels of binding to rGBM consistent with the loss of EphA2+/EphA3+ target cell population (Supp. Fig. S4D).

We next wanted to determine the mechanism by which EphA2/A3 BsAb reduces surface EphA2 and EphA3 levels. At baseline, rGBMs do not display any phosphorylation of EphA2 or EphA3 (Supp. Fig. S5A and Fig. 5E, untreated lane), but it is induced in the presence of ephrinA1 ligand (Fig. 5E). We profiled the expression of ephrinA1 and ephrinA5 in rGBM and found very minimal expression in our cells (Fig. S5B). Upon further investigation, we found that ephrinA1 and ephrinA5, both of which activate EphA2 and EphA3, were highly expressed in the EphA2-/EphA3- cell fraction as compared to the tumorigenic EphA2+/EphA3+ cells (Fig. S5C). This possibly illustrates a bidirectional signaling mechanism between the non-GSC EphA2-/EphA3- cells and GSC EphA2+/EphA3+ cells which co-exist in a regulatory cancer stem cell niche (32).

We treated rGBM cells with EphA2/A3 BsAb and checked for phosphorylation of EphA2 and EphA3 as well as known downstream targets of Eph signaling using western blot. While we saw an apparent increase in both EphA2 and EphA3 phosphorylation upon EphA2/A3 BsAb treatment (Fig. 5E), given the sequence conservation of juxtamembrane pTyr sites between EphA2 and EphA3, we evaluated receptor phosphorylation at the peptide resolution. Indeed, phospho-proteomics on phosphorylated tyrosines revealed high levels of phosphorylated EphA2 peptides, but no phosphorylated EphA3 peptides were identified suggesting that phosphorylation induced by the EphA2/A3 BsAb was asymmetrically driven through EphA2 (Supp. Fig. S5D). Consistent with this we observed decrease in EphA2 protein levels after 60 min of treatment with EphA2/A3 BsAb (Fig. 5E) whereas EphA3 clearance was observed only after days of treatment and inequivalent to

that of EphA2 (Fig. 5D). To further explore the mechanistic regulation of EphA2/A3 BsAb on rGBM, we assessed the activation level of downstream targets such as Akt and Erk1/2. Although 5 minutes of treatment with EphA2/A3 BsAb leads to phosphorylation of EphA2, we found no difference in the activation of Akt and a slight decrease in activated Erk1/2 (Supp. Fig. S5E). After 15 minutes of treatment with EphA2/A3 BsAb, we observed a decrease in the activation of both Akt and Erk1/2 (Fig. 5E). Even after 60 minutes of treatment with EphA2/A3 BsAb, levels of pAkt and pERK1/2 remained lower (Fig. 5E). Interestingly, *in vitro* treatment of rGBM with EphA2/A3 BsAb does not lead to change in expression of other EphRs as shown by CyTOF profiling (Supp. Fig. S5F), demonstrating a lack of compensatory response in an otherwise redundant EphR family signaling. Hence, treatment of rGBM with EphA2/A3 BsAb rapidly clears the levels of EphA2 and slowly reduces the EphA3 receptor levels in rGBM.

EphA2/A3 BsAb inhibits clonogenicity, promotes differentiation and reduces tumorigenicity of rGBM.

To assess the functional effects of EphA2/A3 BsAb on rGBM, we performed secondary sphere formation and proliferation assays. Upon *in vitro* treatment of rGBMs with EphA2/A3 BsAb, we see a reduction in both the clonogenicity (Fig. 6A and B) and proliferation capacity (Fig. 6C) of rGBMs. In fact, the activity of the EphA2/A3 BsAb is not limited to EphA2⁺/EphA3⁺ cell fraction alone; rather the EphA2/A3 BsAb targets EphA2⁺/EphA3⁻ and EphA2⁻/EphA3⁺ cell fractions as well (Fig. S6A and B), illustrating the efficacy of EphA2/A3 BsAb against three subpopulations in rGBM. We performed an *in vitro* limiting dilution assay of rGBM cells pre-treated with EphA2/A3 BsAb and found

a significant decrease in stem cell frequency of rGBM treated with EphA2/A3 BsAb as compared to control cells (Fig. 6D; stem cell frequencies: BT241 control IgG treated 1/8 cells vs EphA2/A3 BsAb treated 1/13 cells; BT618 control IgG treated 1/37 cells vs EphA2/A3 BsAb treated 1/78 cells; BT972 control IgG treated 1/58 cells vs EphA2/A3 BsAb treated 1/99 cells). To understand the mechanism of action of the EphA2/A3 BsAb, we performed cell cycle analysis and apoptosis assays on rGBMs treated with EphA2/A3 BsAb as compared to control. We find that loss of clonogenicity was not caused by changes in cell cycle or apoptosis after treatment with EphA2/A3 BsAb (Supp. Fig. S6C and D). Hence, EphA2/A3 BsAb hinders clonogenicity in rGBM GSCs independent of cell cycle and perhaps in a non-cytotoxic way. To assess whether treatment with EphA2/A3 BsAb induced a differentiation-like phenotype in rGBM, we treated rGBM with EphA2/A3 BsAb for three consecutive days. We find that treatment with EphA2/A3 BsAb leads to an increase in the protein levels of GFAP and MAP2, suggesting that the EphA2/A3 BsAb acts in a similar way to EphA2/A3 KD by directing rGBMs to cellular differentiation (Fig. 6E and F, Supp. Fig. S6E).

To test the efficacy of EphA2/A3 BsAb against rGBMs, we intracranially treated mice engrafted with rGBM (BT241 and BT972) with twice-weekly doses of 30 μ g/dose of EphA2/A3 BsAb until control mice succumbed to disease burden. Although treatment schedule had not been optimized due to limited knowledge of half-life of the EphA2/A3 BsAb, we still found a 30%, although non-significant, decrease in tumor volume in mice treated with EphA2/A3 BsAb as compared to control IgG (Fig. 6G and H) for both models

of rGBM. We performed immunohistochemistry on EphA2/A3 BsAb treated tumors to determine if any residual EphA2⁺ and EphA3⁺ population survives post-treatment. Given the EphA2/A3 BsAb dosage limitations as described above, we saw only a slight decrease in EphA2 and EphA3 levels in EphA2/A3 BsAb-treated tumors (Fig. 6I). Similar to the CyTOF results for *in vitro* treatment with EphA2/A3 BsAb, we again see an increase in GFAP-positive cells in tumors treated with EphA2/A3 BsAb, suggesting that the EphA2/A3 BsAb does indeed drive the differentiation of rGBM toward the astrocytic lineage (Fig. 6J). Thus, despite intracranial dose limits, our novel EphA2/A3 BsAb shows initial efficacy against rGBMs that are driven by EphA2⁺/EphA3⁺ GSCs.

Discussion

GBM is a lethal disease that is refractory to standard surgery and chemoradiotherapy, with the majority of patients facing tumor re-growth and uniformly fatal outcomes upon disease progression post-therapy. Intratumoral heterogeneity (ITH) at the cellular, genetic and functional level is increasingly appreciated as a key determinant of treatment failure, and poor patient survival also correlates with increased frequency of GSCs, which are also implicated in the development of treatment resistance. Meta-analysis of recent clinical trials for GBM patients has also predicted the failure of monotherapy to target the well-documented complexity of ITH in GBM, highlighting the need to develop innovative and informed polytherapeutic strategies for this highly complex disease.

In this work, we report the first effective application of a bispecific antibody in a preclinical, patient-derived xenograft model of recurrent GBM, thereby promoting the concept of poly-

targeting of multiple GSC pools that may escape therapy to drive disease recurrence. We describe the role of EphA2 and EphA3 receptors in cooperatively driving pathogenesis of recurrent human GBM. We report that rGBMs have enhanced expression of both EphA2 and EphA3 and we show that co-expression of EphA2 and EphA3 is directly correlated to the highly tumorigenic *in vitro* and *in vivo* capacity of these GSCs. Furthermore, loss of EphA2 and EphA3 expression in rGBM leads to drastic decrease in self-renewal capacity of these cells and the ability to establish intracranial rGBMs. This decrease in tumorigenicity is mediated through a loss of expression of stem cell genes and a gain in expression of differentiation markers. We therefore developed a BsAb against EphA2 and EphA3 for targeting of this potent GSC population in rGBM. The mechanism of action of the EphA2/A3 BsAb was mediated through phosphorylation and subsequent internalization and degradation of EphA2 receptor and decrease in surface EphA3 levels, which together led to the down-regulation of both Akt and Erk pathways. Intracranial administration of EphA2/A3 BsAb led to a reduction in tumor burden of established rGBMs.

Previous studies of Eph receptors in GBM had individually identified EphA2 and subsequently EphA3 as markers of cancer stem cells in human GBM(24,25). However, similar to other studies in GBM, discovery of molecular targets such as EphRs has been limited to characterization in primary, de novo GBMs, with little focus on recurrent GBM biology. Recent studies have shown that rGBM presents a different molecular landscape, with unique clonal events driving therapy-resistant populations(12,33). The lack of adequate models combined with limited strategies for target discovery in rGBM could

explain the failure of new therapies in prolonging GBM patient survival, which are largely derived from the study of primary GBM alone. Our current investigation focused on the identification of EphRs that marked a GSC population in recurrent GBM. With the Eph profiler, we elucidated the differential expression of all 14 EphR in recurrent and primary GSC lines. We then found that EphA2 and EphA3 were enriched in rGBM. Further characterization of EphR expression in GBM using CyTOF showed that EphA2 and EphA3 co-expressed with multiple known GSC markers, and that this co-expression was enhanced in rGBM, possibly identifying EphA2/A3 co-expressing cells as a stem-cell like population in rGBM. Upon analyzing a large GBM dataset (Rembrandt), we identified high expression of EphA2 and EphA3 as being characteristic of the poor-performing classical and mesenchymal subgroups of GBM and also predicted lower survival in GBM. Importantly, despite the few recurrent GBM samples present in the TCGA dataset, we identified trends of higher expression of EphA2 and EphA3 in recurrent GBM as compared to primary GBM (all samples and paired-samples). Altogether, this illustrated that EphA2 and EphA3 together may mark a tumorigenic GSC population exclusive to recurrent GBM.

Conclusive evidence of the idea that co-expression of EphA2 and EphA3 marked a rGBM GSC population came from fractionating rGBM into EphA2-/EphA3-, EphA2+/EphA3-, EphA2-/EphA3+ and EphA2+/EphA3+ populations. The highest *in vitro* clonogenic potential and *in vivo* tumorigenic potential was associated with combined high EphA2/EphA3 expression (EphA2+/EphA3+). The EphA2/EphA3 co-expressing population also had the highest expression of known GSC markers, Bmi1 and Sox2,

validating our CyTOF data. The fact that cell population that co-expresses both EphA2 and EphA3 may drive rGBM GSC was reinforced by the fact that knockdown of both EphA2 and EphA3 was required to significantly reduce *in vitro* tumorigenicity of rGBM. In fact, intracranial injection of rGBM with double EphA2/EphA3 knockdown abrogated tumor initiation in half of the mice, while single EphA2 or EphA3 knockdown still lead to initiation of tumors in all mice. Additionally, knockdown of both EphA2 and EphA3 led to a significant increase in astrocytic differentiation marker GFAP, suggesting the decrease in tumorigenicity is driven by an increase in differentiation of GBM cells. For the first time, we show that two EphR together mark and drive a highly potent GSC population in recurrent GBM, where loss of EphA2 and EphA3 together promotes differentiation of GBM.

Considering that GBM presents with extensive ITH, it is no surprise that we identified multiple GSC populations cooperating in driving tumorigenesis of GBM. Despite that, new therapies continue to focus on single targets and rely on monotherapies to promote patient survival. Since multiple cellular populations promote tumorigenic phenotype, single population targeting by monotherapies allows other cellular populations to escape therapy and seed disease recurrence. Our work aims to change that paradigm by presenting evidence of multiple GSC pools in recurrent GBM that may be co-targeted for improved patient outcome. Other ephrin poly-targeting strategies have been described in GBM, notably an EphA2, A3 and B2-targeting agent composed of ephrinA5 ligand linked to a cytotoxin which demonstrated efficacious cell killing *in vitro* (34). This ligand-based

polytargeting strategy is however limited by a lack of target specificity, as ephrin ligands can be expected to bind a multitude of EphRs in many cells and tissues, such that off-target effects and resultant *in vivo* toxicity are likely. We proposed a more precise poly-targeting strategy through the development of a bispecific antibody against both EphA2 and EphA3 driven GSC population in recurrent GBM. The treatment of rGBM with EphA2/A3 BsAb reduced clonogenicity and proliferative capacity of the cells, mediated through a reduction in EphA2 and EphA3 levels which in turn down regulated Akt and Erk1/2, known oncogenic pathways in GBM. The attenuation of EphA2 and EphA3 by EphA2/A3 BsAb also resulted in partial differentiation as evidenced by increase in GFAP and MAP2 levels, mimicking the effect of knockdown of these receptors.

Although we had limited knowledge of the pharmacokinetics and pharmacodynamics of the EphA2/A3 BsAb, we tested the efficacy of EphA2/A3 BsAb in reducing established recurrent GBM xenografts through twice weekly intracranial doses of the EphA2/A3 BsAb and noted a reduction in tumor growth, a decrease in EphA2 and EphA3 expression and an increase in GFAP levels. Additionally, studies by Brown *et al.* have shown that intracranial delivery of therapy for GBM patients is safe and well tolerated (35), with intraventricular infusion showing greater efficacy against multi-nodal, infiltrative tumors as compared to intracavitary infusion(36,37). This demonstrates that our current intracranial therapy delivery model of the BsAb will be a viable option for patients with recurrent GBM. Critical to our approach was the development and validation of autonomous VHD capable of selectively targeting and modulating GBM-specific tumor

antigens with high affinity. While mass transport of VHD-Fc through the BBB is unlikely in its current format, the size (~13 kDa) and single chain format the of the VHD is ideal for the engineering of fusion proteins that enable mass transport(38-40). Optimization of the modality for systemic delivery, biodistribution and therapeutic efficacy remain important goals for further therapeutic development. The EphA2/A3 BsAb hence dually targets a highly tumorigenic, multi-target driven GSC population in recurrent GBM through the promotion of a differentiation phenotype. The mechanism of action of the BsAb is through phosphorylation and internalization of the EphA2 receptor, leading to its degradation, whereas the decrease in EphA3 at the cell surface appears to be phosphorylation-independent. The latter finding is not surprising, as anti-EphA3 antibodies in clinical trials for advanced hematologic malignancies induce reduction of EphA3 levels and subsequent apoptosis and activation of antibody-dependent cell mediated cytotoxicity in treated leukemia cells, with no evidence of phosphorylation of EphA3; thus the mechanism of EphA3 receptor reduction at the cell surface remains unknown (41). Future optimization of the EphA3-depleting features of our EphA2/A3 BsAb by exploring unique epitopes or valencies could perhaps further enhance the reduction of tumor burden, to the degree observed in our knockdown studies.

Therapeutic monoclonal antibodies have several major limitations in their mode of action, including redundancy of molecular pathways leading to tumor cell survival, effects of the microenvironment, and activation of inhibitory receptors. To overcome the functional redundancy among pro-tumorigenic signaling pathways we empirically applied a bi-

specific antibody modality to target heterogeneous GSC populations, while also blocking the activity of the pro-tumorigenic non-GSC populations that comprise the tumor niche. Comprehensive profiling of the entire EphR family in recurrent human GBM and in-depth functional characterization of GSC populations that contribute to ITH have together generated a novel, empiric poly-targeted therapy that offers a new and promising treatment paradigm for patients with recurrent GBM.

Acknowledgments:

M.A.Q. is supported by the Canadian Institute of Health Research Canada Graduate Scholarship - Doctoral. This study was funded by Terry Fox Research Institute Program Project Grant awarded to J.M., S.S., and S.K.S. We thank Mr. Mohammad Ali Malik for assisting with animal work and assembly of data.

References

1. Louis DN, Ohgaki H, Wiestler OD, Cavenee WK, Burger PC, Jouvet A, et al. The 2007 WHO Classification of Tumours of the Central Nervous System. *Acta Neuropathol.* 2007;114:97–109.
2. Louis DN, Perry A, Reifenberger G, Deimling von A, Figarella-Branger D, Cavenee WK, et al. The 2016 World Health Organization Classification of Tumors of the Central Nervous System: a summary. *Acta Neuropathol.* 2016;131:803–20.
3. Stupp R, Hegi ME, Mason WP, van den Bent MJ, Taphoorn MJ, Janzer RC, et al. Effects of radiotherapy with concomitant and adjuvant temozolomide versus radiotherapy alone on survival in glioblastoma in a randomised phase III study: 5-year analysis of the EORTC-NCIC trial. *Lancet Oncology.* Elsevier Ltd;

- 2009;10:459–66.
4. Stupp R, Taillibert S, Kanner A, Read W, Steinberg D, Lhermitte B, et al. Effect of Tumor-Treating Fields Plus Maintenance Temozolomide vs Maintenance Temozolomide Alone on Survival in Patients With Glioblastoma: A Randomized Clinical Trial. *JAMA*. 2017;318:2306–16.
 5. Verhaak RGW, Hoadley KA, Purdom E, Wang V, Qi Y, Wilkerson MD, et al. Integrated genomic analysis identifies clinically relevant subtypes of glioblastoma characterized by abnormalities in PDGFRA, IDH1, EGFR, and NF1. *Cancer Cell*. 2010;17:98–110.
 6. Brennan CW, Verhaak RGW, McKenna A, Campos B, Nounshmehr H, Salama SR, et al. The somatic genomic landscape of glioblastoma. *Cell*. 2013;155:462–77.
 7. McLendon R, Friedman A, Bigner D, Van Meir EG, Brat DJ, M Mastrogiannis G, et al. Comprehensive genomic characterization defines human glioblastoma genes and core pathways. *Nature*. 2008;455:1061–8.
 8. Patel AP, Tirosh I, Trombetta JJ, Shalek AK, Gillespie SM, Wakimoto H, et al. Single-cell RNA-seq highlights intratumoral heterogeneity in primary glioblastoma. *Science*. American Association for the Advancement of Science; 2014;344:1396–401.
 9. Meyer M, Reimand J, Lan X, Head R, Zhu X, Kushida M, et al. Single cell-derived clonal analysis of human glioblastoma links functional and genomic heterogeneity. *Proc Natl Acad Sci USA*. National Acad Sciences; 2015;:201320611.
 10. Kim J, Lee I-H, Cho HJ, Park C-K, Jung Y-S, Kim Y, et al. Spatiotemporal

- Evolution of the Primary Glioblastoma Genome. *Cancer Cell*. 2015;28:318–28.
11. Johnson BE, Mazar T, Hong C, Barnes M, Aihara K, McLean CY, et al. Mutational analysis reveals the origin and therapy-driven evolution of recurrent glioma. *Science*. American Association for the Advancement of Science; 2014;343:189–93.
 12. Wang J, Cazzato E, Ladewig E, Frattini V, Rosenbloom DIS, Zairis S, et al. Clonal evolution of glioblastoma under therapy. *Nat Genet*. Nature Research; 2016;48:768–76.
 13. Singh SK, Clarke ID, Terasaki M, Bonn VE, Hawkins C, Squire J, et al. Identification of a cancer stem cell in human brain tumors. *Cancer Research*. 2003;63:5821–8.
 14. Son MJ, Woolard K, Nam D-H, Lee J, Fine HA. SSEA-1 is an enrichment marker for tumor-initiating cells in human glioblastoma. *Cell Stem Cell*. 2009;4:440–52.
 15. Lathia JD, Gallagher J, Heddleston JM, Wang J, Eyler CE, Macsworlds J, et al. Integrin alpha 6 regulates glioblastoma stem cells. *Cell Stem Cell*. 2010;6:421–32.
 16. Suva ML, Rheinbay E, Gillespie SM, Patel AP, Wakimoto H, Rabkin SD, et al. Reconstructing and reprogramming the tumor-propagating potential of glioblastoma stem-like cells. *Cell*. 2014;157:580–94.
 17. Bao S, Wu Q, McLendon RE, Hao Y, Shi Q, Hjelmeland AB, et al. Glioma stem cells promote radioresistance by preferential activation of the DNA damage response. *Nature*. 2006;444:756–60.
 18. Liu G, Yuan X, Zeng Z, Tunici P, Ng H, Abdulkadir IR, et al. Analysis of gene expression and chemoresistance of CD133+ cancer stem cells in glioblastoma. *Mol*

- Cancer. 2006;5:67.
19. Chen J, Li Y, Yu T-S, McKay RM, Burns DK, Kernie SG, et al. A restricted cell population propagates glioblastoma growth after chemotherapy. *Nature*. Nature Publishing Group; 2012;:1–6.
 20. Qazi MA, Vora P, Venugopal C, McFarlane N, Subapanditha MK, Murty NK, et al. A novel stem cell culture model of recurrent glioblastoma. *J Neurooncol*. Springer US; 2016;126:57–67.
 21. Pasquale EB. Eph-Ephrin Bidirectional Signaling in Physiology and Disease. *Cell*. 2008;133:38–52.
 22. Genander M, Frisén J. Ephrins and Eph receptors in stem cells and cancer. *Current Opinion in Cell Biology*. Elsevier Ltd; 2010;22:611–6.
 23. Nakada M, Hayashi Y, Hamada JI. Role of Eph/ephrin tyrosine kinase in malignant glioma. *Neuro-Oncology*. 2011;13:1163–70.
 24. Binda E, Visioli A, Giani F, Lamorte G, Copetti M, Pitter KL, et al. The EphA2 Receptor Drives Self-Renewal and Tumorigenicity in Stem-like Tumor-Propagating Cells from Human Glioblastomas. *Cancer Cell*. Elsevier Inc; 2012;22:765–80.
 25. Day BW, Stringer BW, Al-Ejeh F, Ting MJ, Wilson J, Ensbey KS, et al. EphA3 Maintains Tumorigenicity and Is a Therapeutic Target in Glioblastoma Multiforme. *Cancer Cell*. Elsevier Inc; 2013;23:238–48.
 26. Nakada M, Anderson EM, Demuth T, Nakada S, Reavie LB, Drake KL, et al. The phosphorylation of ephrin-B2 ligand promotes glioma cell migration and invasion. *Int J Cancer*. 2009;:NA–NA.

27. Wykosky J. EphA2 as a Novel Molecular Marker and Target in Glioblastoma Multiforme. *Molecular Cancer Research*. 2005;3:541–51.
28. Miao H, Gale NW, Guo H, Qian J, Petty A, Kaspar J, et al. EphA2 promotes infiltrative invasion of glioma stem cells in vivo through cross-talk with Akt and regulates stem cell properties. *Oncogene*. 2014.
29. Bowman RL, Wang Q, Carro A, Verhaak RGW, Squatrito M. GlioVis data portal for visualization and analysis of brain tumor expression datasets. *Neuro-Oncology*. 2017;19:139–41.
30. Madhavan S, Zenklusen J-C, Kotliarov Y, Sahni H, Fine HA, Buetow K. Rembrandt: helping personalized medicine become a reality through integrative translational research. *Molecular Cancer Research*. 2009;7:157–67.
31. Singh SK, Hawkins C, Clarke ID, Squire JA, Bayani J, Hide T, et al. Identification of human brain tumour initiating cells. *Nature*. 2004;432:396–401.
32. Plaks V, Kong N, Werb Z. The cancer stem cell niche: how essential is the niche in regulating stemness of tumor cells? *Cell Stem Cell*. 2015;16:225–38.
33. Kim H, Zheng S, Amini SS, Virk SM, Mikkelsen T, Brat DJ, et al. Whole-genome and multisector exome sequencing of primary and post-treatment glioblastoma reveals patterns of tumor evolution. *Genome Res*. Cold Spring Harbor Lab; 2015;:gr.180612.114.
34. Ferluga S, Tomé CML, Herpai DM, D'Agostino R, Debinski W. Simultaneous targeting of Eph receptors in glioblastoma. *Oncotarget*. 2016;7:59860–76.
35. Brown CE, Badie B, Barish ME, Weng L, Ostberg JR, Chang W-C, et al. Bioactivity

- and Safety of IL13R α 2-Redirected Chimeric Antigen Receptor CD8⁺ T Cells in Patients with Recurrent Glioblastoma. *Clin Cancer Res.* 2015;21:4062–72.
36. Brown CE, Alizadeh D, Starr R, Weng L, Wagner JR, Naranjo A, et al. Regression of Glioblastoma after Chimeric Antigen Receptor T-Cell Therapy. *N Engl J Med.* Massachusetts Medical Society; 2016;375:2561–9.
37. Priceman SJ, Tilakawardane D, Jeang B, Murad JP, Park AK, Chang W-C, et al. Regional Delivery of Chimeric Antigen Receptor-Engineered T Cells Effectively Targets HER2⁺ Breast Cancer Metastasis to the Brain. *Clin Cancer Res.* 2017;:clincanres.2041.2017.
38. Dufès C, Robaian Al M, Somani S. Transferrin and the transferrin receptor for the targeted delivery of therapeutic agents to the brain and cancer cells. *Therapeutic Delivery.* 2013;4:629–40.
39. Nikanjam M, Blakely EA, Bjornstad KA, Shu X, Budinger TF, Forte TM. Synthetic nano-low density lipoprotein as targeted drug delivery vehicle for glioblastoma multiforme. *Int J Pharm.* 2007;328:86–94.
40. Zhang B, Sun X, Mei H, Wang Y, Liao Z, Biomaterials JC, et al. LDLR-mediated peptide-22-conjugated nanoparticles for dual-targeting therapy of brain glioma. Elsevier.
41. Swords RT, Greenberg PL, Wei AH, Durrant S, Advani AS, Hertzberg MS, et al. KB004, a first in class monoclonal antibody targeting the receptor tyrosine kinase EphA3, in patients with advanced hematologic malignancies: Results from a phase I study. *Leuk Res.* 2016;50:123–31.

CHAPTER 3 FIGURES AND TABLES

Figure 1

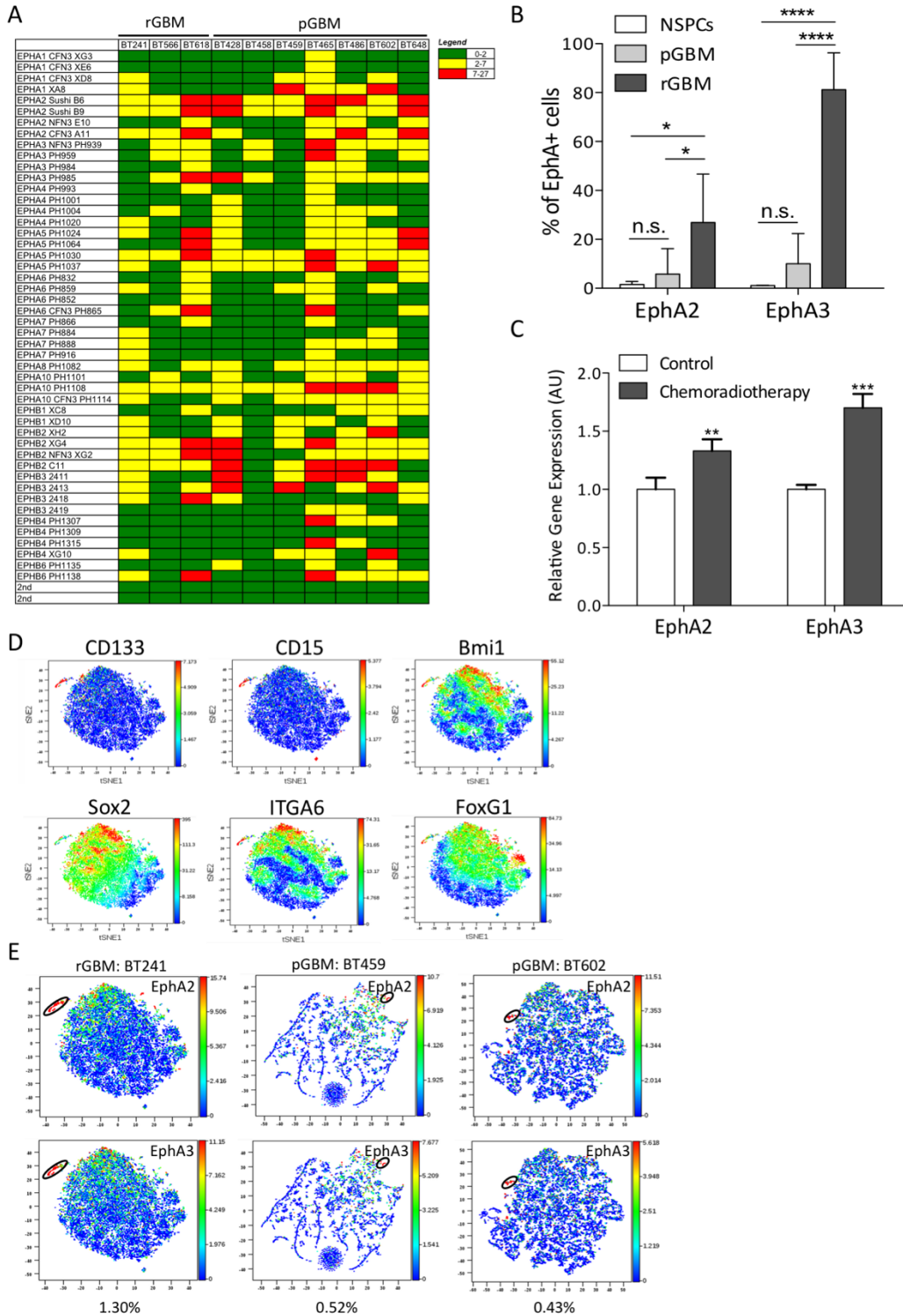


Figure 1: EphA2 and EphA3 have higher expression in recurrent GBM and co-express with glioblastoma stem cell (GSC) markers.

(A) Using the EphR profiler, we identified the expression of all 14 Eph receptors across ten primary (BT428, BT458, BT459, BT465, BT486, BT602, BT648) and recurrent (BT241, BT566, BT618) GSC lines. (B) Using flow cytometry, we determined the surface expression of EphA2 and EphA3 in human neural stem/progenitor cells (NSPC) (n=2), pGBM (n=6) and rGBM (n=3). All samples are biological replicates (EphA2: NSPCs vs pGBM p=0.8871, NSPCs vs rGBM p=0.0157, pGBM vs rGBM p=0.0115; EphA3: NSPCs vs pGBM p=0.5542, NSPCs vs rGBM p<0.0001, pGBM vs rGBM p<0.0001). (C) pGBM (BT602) was treated with *in vitro* chemoradiotherapy and the gene expression of EphA2 and EphA3 was determined. (D) CyTOF-based expression of GSC markers CD133, CD15, Sox2, Bmi1, ITGA6 and FoxG1 in BT241. (E) Co-expression of EphA2 (top) and EphA3 (bottom) with GSC markers in rGBM (BT241) and pGBMs (BT459 and BT602). The black circle represents the cellular population that co-expresses EphA2, EphA3 and all six GSC markers, with the percentage of cells listed at the bottom of each panel. Data is represented as mean±SD. (n.s. not significant, *p<0.05, ***p<0.001, ****p<0.0001).

Figure 2

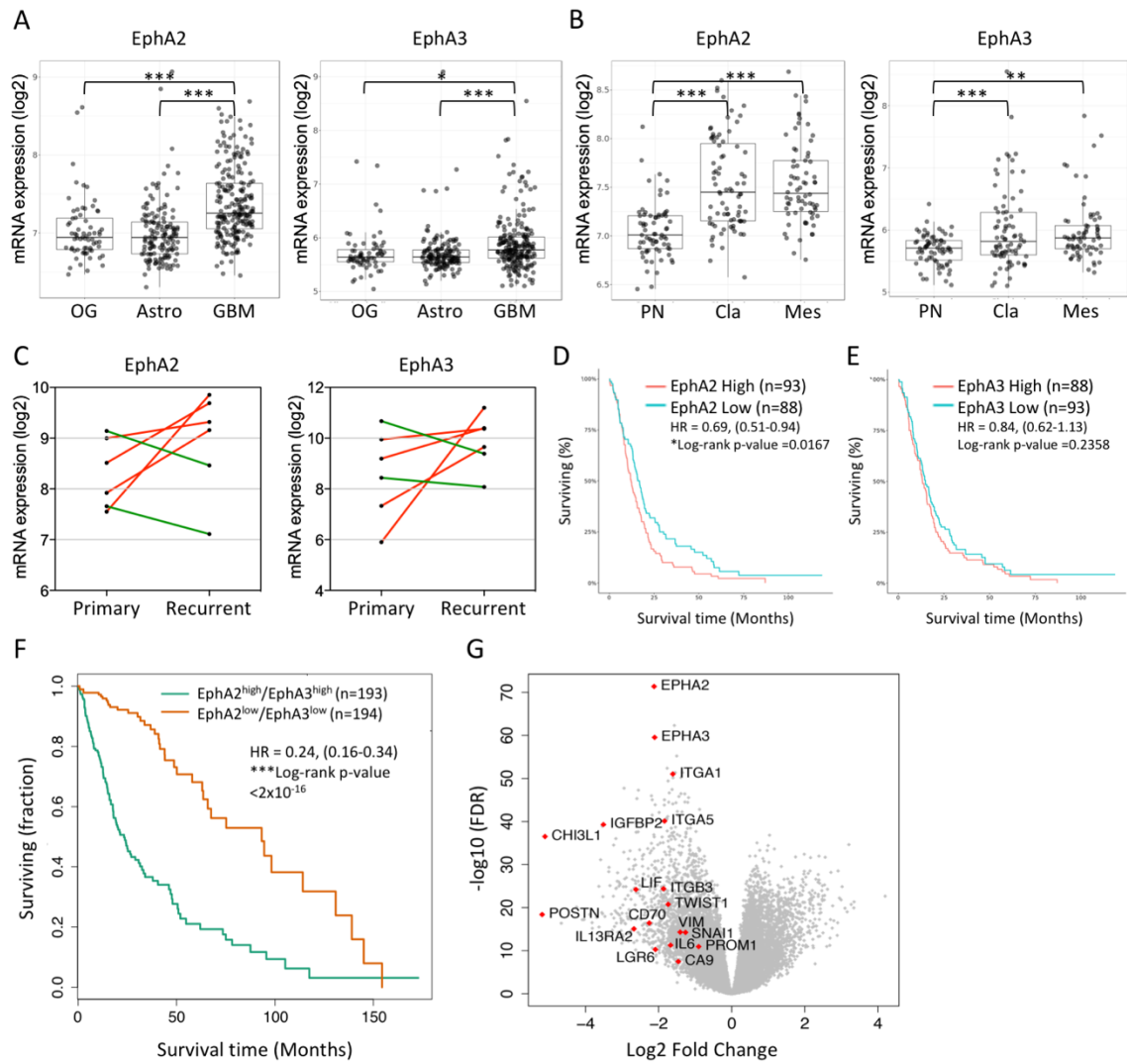


Figure 2: High EphA2 and EphA3 co-expression correlates with poor brain tumor patient survival.

(A) EphA2 and EphA3 have higher expression in GBM (grade IV) compared to low grade gliomas, oligodendroglioma (OG) and astrocytoma (Astro) in Rembrandt glioma database. (B) EphA2 and EphA3 have higher expression in classical (Cla) and mesenchymal (Mes) subgroups of GBM compared to proneural (PN) subgroup (Rembrandt). (C) EphA2 (left) and EphA3 (right) gene expression in paired primary GBM patient samples and their corresponding recurrent GBM tissues (TCGA, n=6 matched primary-recurrent GBM tissue pairs). A subset of GBM patients show increased expression of EphA2 and EphA3 in their recurrent tissue as compared to primary GBM. (D and E) Higher expression of EphA2 is associated with poor survival in GBM patients, while high expression of EphA3 trends towards poor but not statistically significant survival in GBM patients (Rembrandt). (F) Interrogation of the TCGA low-grade glioma-glioblastoma dataset indicates significant survival advantage for patients expressing low levels of both EphA2 and EphA3 (EphA2^{low}/EphA3^{low}) as compared to patients expressing high levels of both EphA2 and EphA3 (EphA2^{high}/EphA3^{high}). (G) Analysis of the differentially expressed genes from patient subpopulations in (F) shows high expression of genes involved in cell invasion, epithelial-mesenchymal transition and stemness in the EphA2^{high}/EphA3^{high} patient tissue. (*p<0.05, **p<0.01, ***p<0.001).

Figure 3

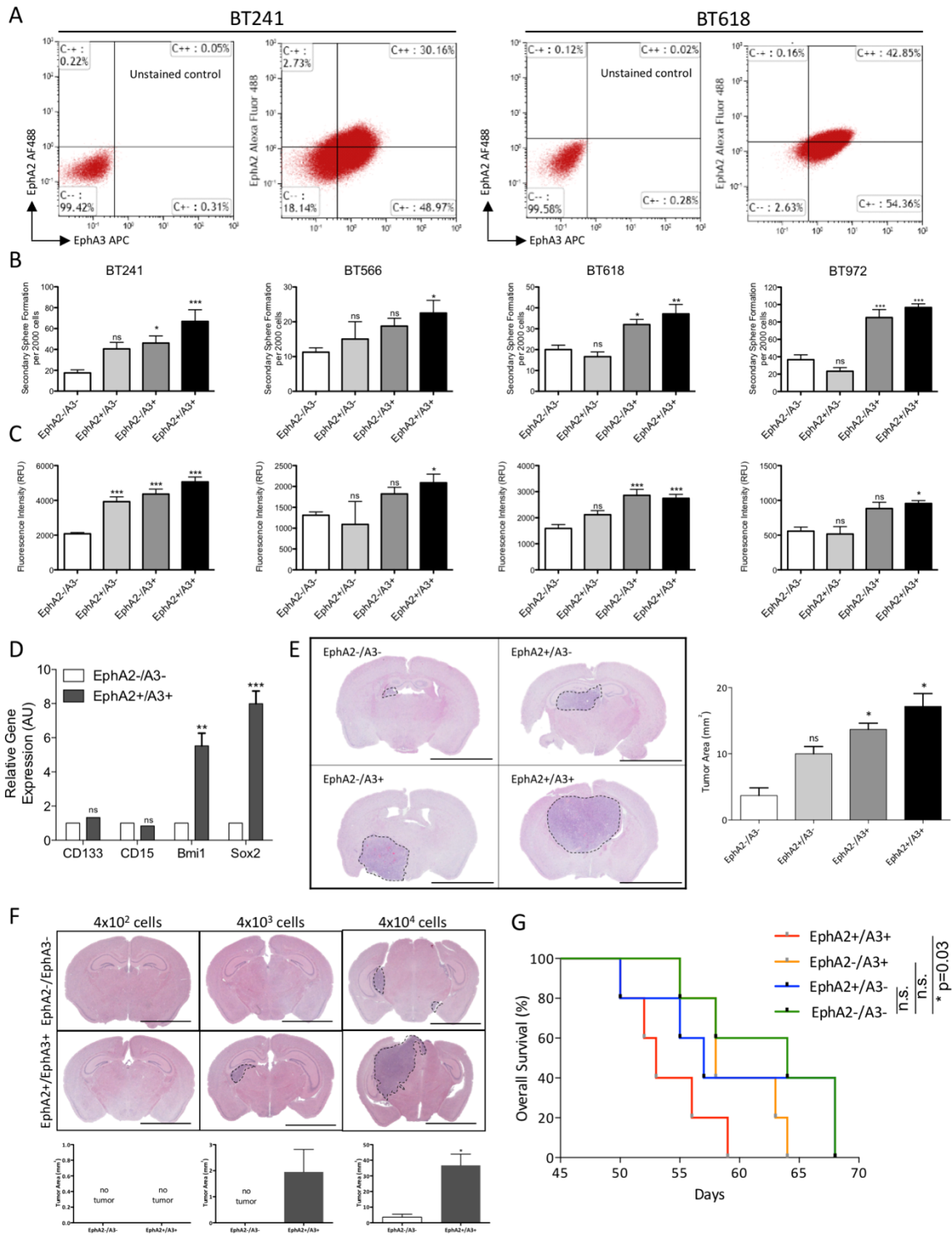


Figure 3: Co-expression of EphA2 and EphA3 marks a highly clonogenic and tumorigenic cell population in recurrent GBM.

(A) Flow profile of EphA2 and EphA3 in two rGBM samples, BT241 and BT618. (B) Secondary sphere formation assay of rGBMs sorted based on expression of EphA2 and EphA3, where EphA2⁺/A3⁺ exhibits the highest clonogenic capacity in four rGBMs. (C) Proliferation assay of rGBMs sorted based on the expression of EphA2 and EphA2, where EphA2⁺/EphA3⁺ has higher proliferation capacity than other cell populations. (D) Gene expression of GSC markers Bmi1 and Sox2 is higher in sorted EphA2⁺/EphA3⁺ compared to EphA2⁻/EphA3⁻ rGBM cell populations, while no difference is found in the expression of CD133 and CD15. (E) H&E staining of mice brains engrafted with rGBM BT241 cells sorted based on EphA2 and EphA3 expression, with total tumor area presented in bar graph on the right (n=2). (F) *In vivo* limiting dilution assay of mice engrafted with different numbers of EphA2/EphA3⁻ and EphA2⁺/EphA3⁺ cell, showing EphA2⁺/A3⁺ can form tumors at lower cell number. Bar graphs at the bottom show total tumor area of each panel (n=2). G. Kaplan-Meier survival curves for mice engrafted with BT241 EphA2⁻/A3⁻, EphA2⁺/A3⁻, EphA2⁻/A3⁺, EphA2⁺/EphA3⁺ (median survival: 53, 57, 58 and 64 days, respectively; n=5). Tumor area is presented in the bottom panel for each cell dose. Data is represented as mean±SD. (ns – not significant, *p<0.05, **p<0.01, ***p<0.001). Scale bar represents 5mm.

Figure 4

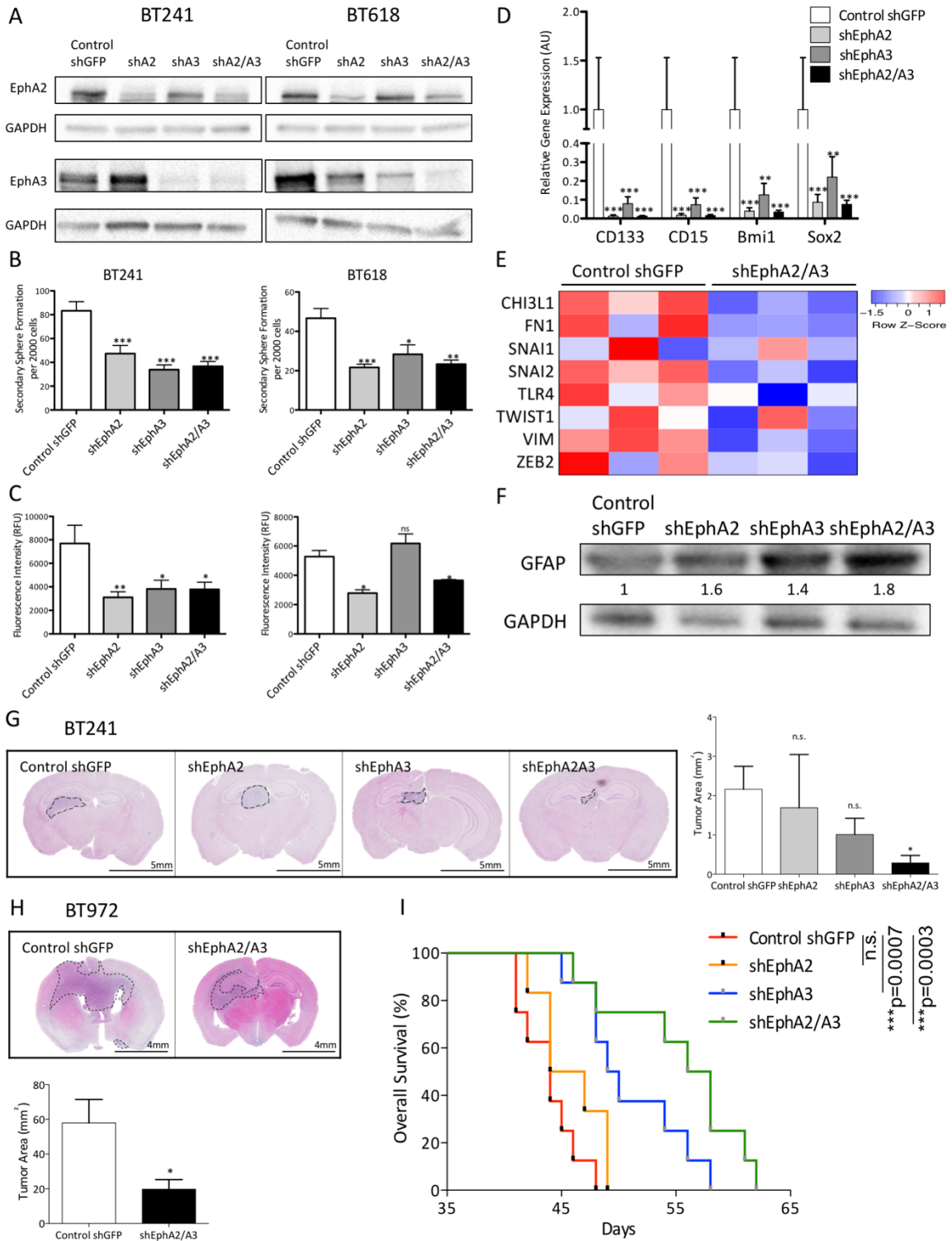


Figure 4: EphA2 and EphA3 knockdown in rGBM inhibits clonogenicity, decreases GSC and mesenchymal marker expression and prolongs survival.

(A) Western blot showing the expression of EphA2 and EphA3 after shRNA mediated knockdown (KD) of either EphA2 or EphA3 or both EphA2/A3 as compared to control shGFP in two rGBMs. (B) Secondary sphere formation assay of rGBM with KD against EphA2 and EphA3 shows decrease sphere formation capacity of shEphA2/A3 cells. (C) Proliferation assay of rGBMs with KD against EphA2 and EphA3 shows decreased proliferation capacity of shEphA2/A3 cells. (D) Gene expression of GSC markers CD133, CD15, Bmi1 and Sox2 is significantly decreased in rGBMs with KD against EphA2 and EphA3. (E) RNA sequencing results show decrease in expression of genes associated with mesenchymal and infiltrative cell type in rGBM BT241 shEphA2/A3 cell population as compared to control shGFP cells. (F) Western blot showing the expression of GFAP after shRNA mediated KD of either EphA2 or EphA3 or both EphA2/A3 in rGBM BT241. (G and H) H&E staining of mouse brains engrafted with rGBM BT241 control shGFP, shEphA2, shEphA3 or shEphA2/A3 cells, and rGBM BT972 control shGFP or shEphA2/A3 cells. Total tumor area is presented in the bar graph for BT241 on the right (n=5, except shGFP n=7) and for BT972 on the bottom (n=4) of the brain images. (I) Kaplan-Meier survival curves for mice engrafted with rGBM BT241 control shGFP, shEphA2, shEphA3 or shEphA2/A3 (median survival: 44, 45.5, 49.5, 57 days, respectively; n=8, except shEphA2 n=6). Data is represented as mean±SD. (*p<0.05, **p<0.01, ***p<0.001).

Figure 5: Treatment of rGBM with EphA2/A3 BsAb decreases EphA2 and EphA3 expression and decreases activation of Akt and Erk1/2.

(A) CyTOF analysis showing binding of BsAb to EphA2⁺ and EphA3⁺ cells in BT241. (B) Treatment of rGBM BT241 with EphA2/A3 BsAb at 4°C vs 37°C for 4 hours shows that the BsAb gets internalized as demonstrated by reduced BsAb binding signal at 37°C. Treatment with EphA2/A3 BsAb for three consecutive days (200nM) decreases EphA2 (C) and EphA3 (D) surface expression as shown by CyTOF. Median intensity of EphA2 and EphA3 is shown in the top right corner of their representative plots. (E) Western blot showing protein levels of total and phosphorylated EphA2 and EphA3 and multiple proteins involved in downstream signalling of the EphRs when treated with Ephrin A1 ligand (15 min) or 200nM of control IgG or EphA2/A3 BsAb for 15 or 60 minutes in rGBMs BT241 and BT618.

Figure 6

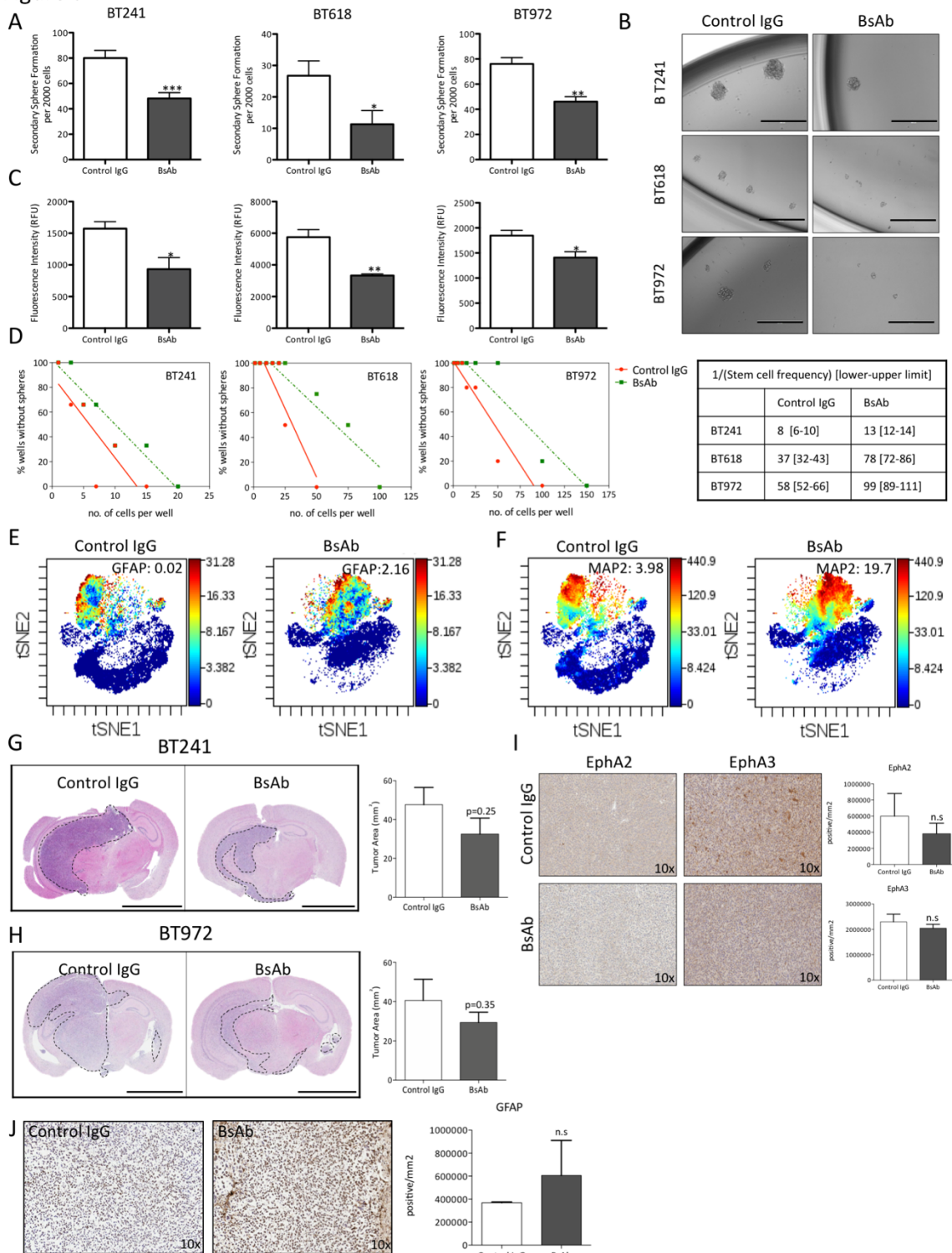


Figure 6: Treatment of rGBM with EphA2/A3 BsAb inhibits *in vitro* clonogenicity, increases differentiation and reduces tumor burden.

(A) Secondary sphere formation assay of rGBM treated with 200nM EphA2/A3 BsAb show a decrease in clonogenic capacity as compared control IgG treated cells (B) rGBM treated with 200nM EphA2/A3 BsAb have fewer and smaller spheres (scale bar represents 400 μ m). (C) Proliferation assay of rGBMs treated with EphA2/A3 BsAb shows decreased proliferation compared to control IgG-treated cells. (D) Limiting dilution assay of rGBM pre-treated with 200nM of EphA2/A3 BsAb for 3-days. The table on the right shows the stem cell frequencies and upper and lower limits. Protein expression of GFAP (E) and (F) MAP2 using CyTOF in BT241 after 3-day treatment with 200nM of EphA2/A3 BsAb. The number in the top right corner of each plot represents median intensity. (G and H) H&E staining of mouse brains engrafted with rGBMs BT241 or BT972, treated with 30 μ g intracranial biweekly dose of control IgG or EphA2/A3 BsAb, until control mice succumbed to disease burden. Total tumor area is presented in the bar graphs on the right of each IHC panel (BT241: n=6, BT972: n=5). (I) EphA2 (left) and EphA3 (right) staining on BT241, control IgG or EphA2/A3 BsAb treated tumors. Bar graphs on the right represents average positive staining per mm² of tumor area for both EphA2 and EphA3 (n=3). (J) GFAP staining on BT241, control IgG or EphA2/A3 BsAb treated tumors. Bar graph on the right represents average positive staining per mm² of tumor area. Data is represented as mean \pm SD. (n.s not significant, *p<0.05, **p<0.01, ***p<0.001). Scale bar on IHC images represent 4mm.

Supplementary Figures and Tables

Table S1: Patient Demographics			
Sample	Age	Sex	GBM Type
BT428	63	F	primary
BT458	81	M	primary
BT459	60	F	primary
BT465	50	M	primary
BT486	54	F	primary
BT602	56	F	primary
BT648	69	M	primary
BT799	77	F	primary
BT954	65	M	primary
BT993	52	F	primary
MBT06	50	F	primary
GBM4			primary
BT241	67	F	recurrent
BT566	55	F	recurrent
BT618	67	F	recurrent
BT972	53	M	recurrent

Figure S1

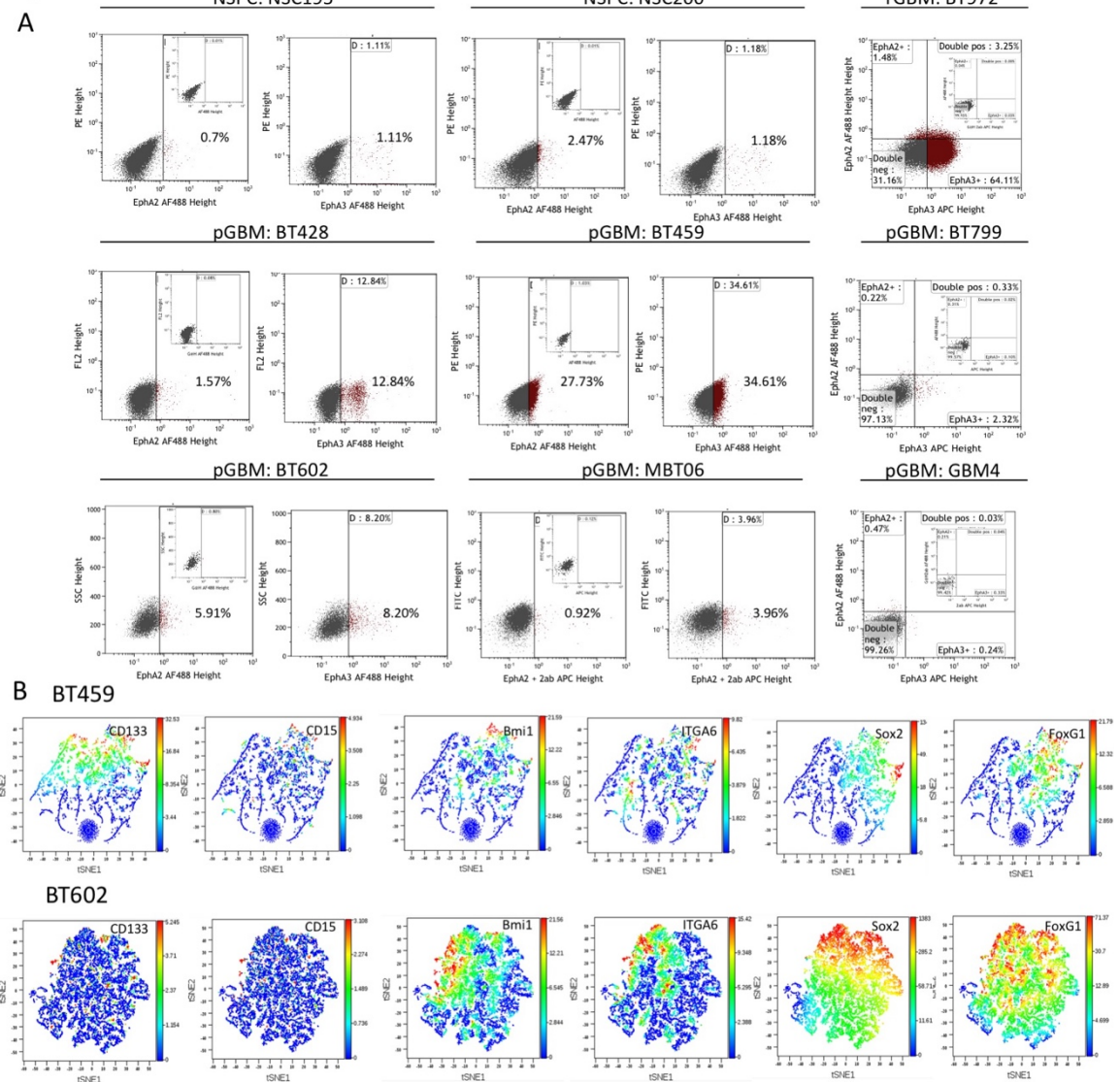


Figure S1: Protein expression of EphA2, EphA3, CD133, CD15, Bmi1, Sox2, FoxG1 and ITGA6 in GBM.

(A) Surface expression of EphA2 and EphA3 in neural stem progenitor cells (NSPCs), primary GBMs (pGBM) and recurrent GBMs (rGBM). (B) CyTOF based expression of stem cell markers CD133, CD15, Bmi1, ITGA6, Sox2 and FoxG1 in BT459 and BT602.

Figure S2

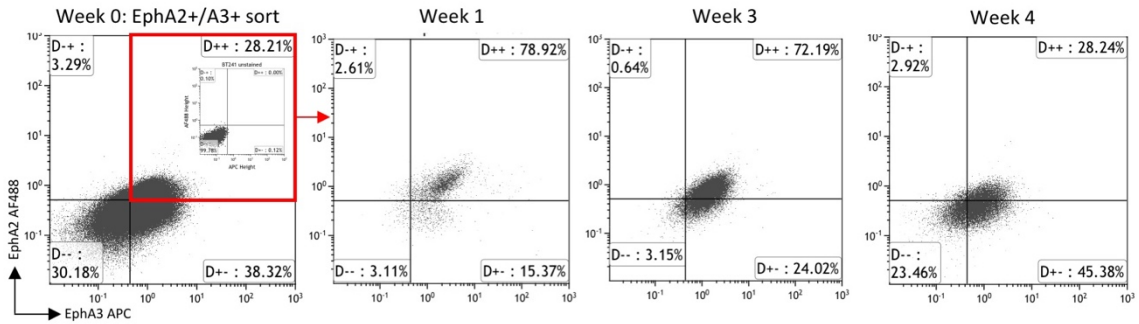


Figure S2: Characterization of EphA2+/EphA3+ sorted cell population overtime for changes in EphA2 and EphA3 surface expression.

EphA2+/A3+ cells were sorted from rGBM BT241. The expression of EphA2 and EphA3 was characterized over 4 weeks time course.

Figure S3

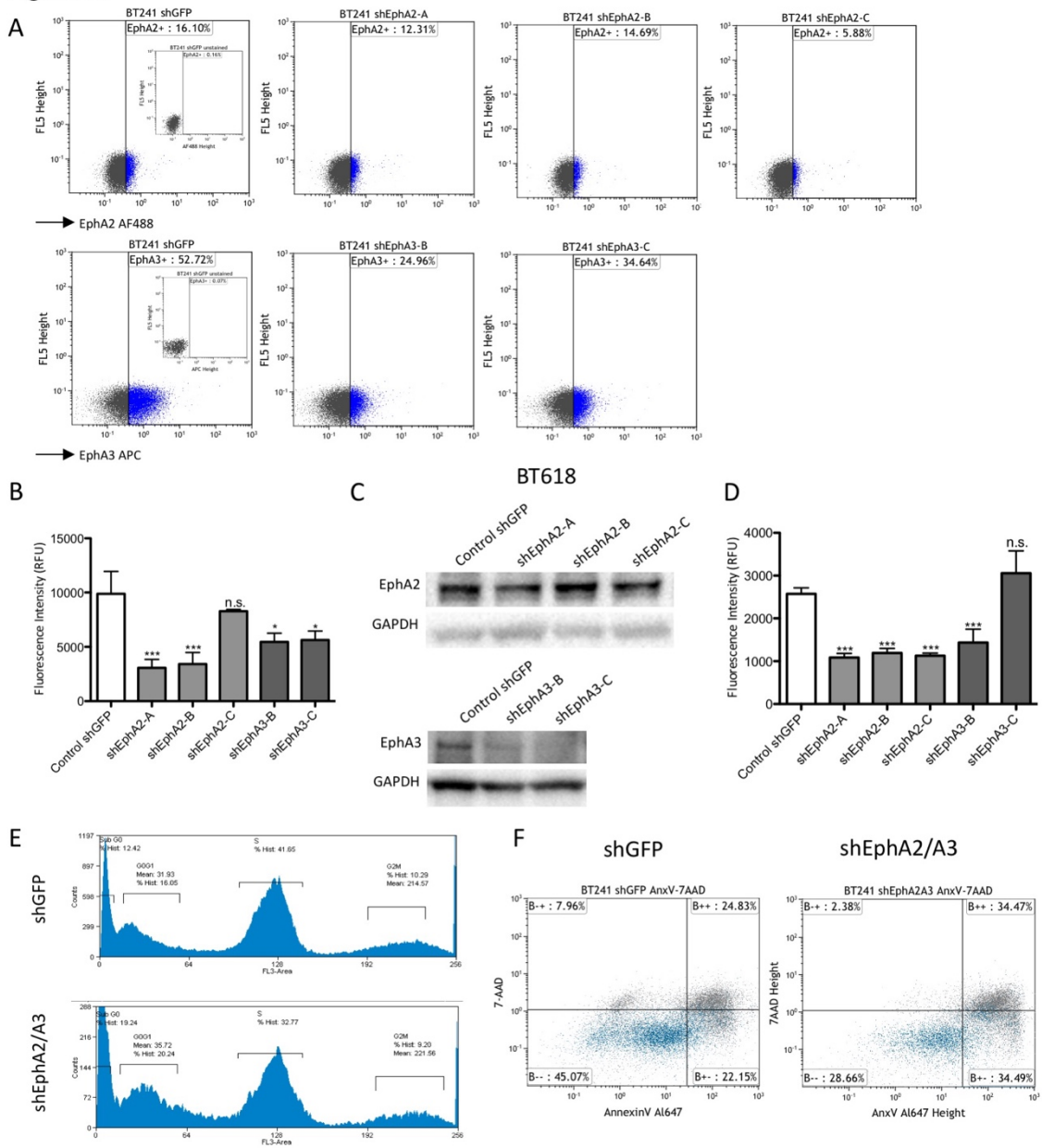


Figure S3: Knockdown of EphA2 and EphA3 alters cell cycle and increases apoptosis in recurrent GBM.

(A) Flow cytometry plots for knock down of EphA2 and EphA3 using multiple shRNAs to assess for knockdown efficiency and (B) effect on proliferation of rGBM BT241 cells. (C) Western blot demonstrating knockdown of EphA2 and EphA3 using multiple shRNAs and (D) effect on proliferation in rGBM BT618. (E) Cell cycle analysis of BT241 after EphA2/A3 knockdown compared to control shGFP cells shows decrease in S phase cell population and an increase in G0G1 phase cell population. (F) Apoptosis analysis with Annexin V shows an increase in apoptosis after knockdown of EphA2 and EphA3 in BT241. (n.s. not significant, * $p < 0.05$, *** $p < 0.001$).

Figure S4

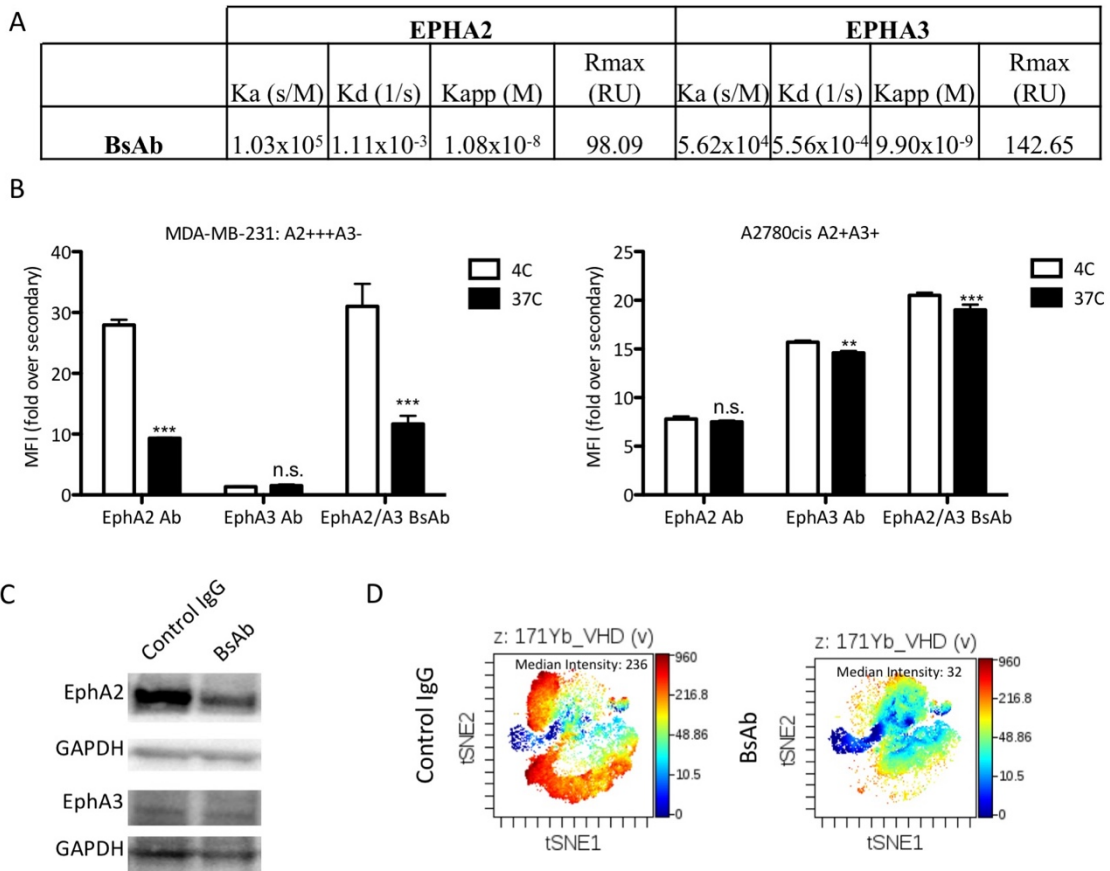


Figure S4: High affinity EphA2/A3 BsAb is internalized, leading to decreased expression of EphA2 and EphA3.

(A) Association constant (K_a), dissociation constant (K_d), apparent constant (K_{app}) and maximum binding capacity (R_{max}) of EphA2/A3 BsAb to EphA2 and EphA3 receptors.

(B) Internalization of EphA2/A3 BsAb at 37°C compared to at 4°C in high EphA2 expressing and EphA3 negative breast cancer line MDA-MB231, and EphA2 and EphA3 expressing cisplatin-resistant ovarian cancer line, A2780cis. EphA2 Ab and EphA3 Ab are the EphA2 and EphA3 targeting components of the EphA2/A3 BsAb, respectively.

(C) Western blot showing decrease in protein levels of EphA2 and EphA3 in BT241 following 3 days of treatment with EphA2/A3 BsAb.

(D) After 3-day treatment with EphA2/A3 BsAb (200nM), the binding of the BsAb to BT241 also decreases. (n.s. not significant, ** $p < 0.01$, *** $p < 0.001$).

Figure S5: Recurrent GBMs express low levels of ephrin A1/A5 ligands, and treatment with EphA2/A3 BsAb leads to EphA2 phosphorylation but does not alter other EphR expression.

(A) rGBM BT566 and BT972 do not present baseline phosphorylation of EphA2 or EphA3. (B) Using flow cytometry, we find low surface protein levels of ephrinA1 (EFNA1) in multiple GBM lines and low levels of ephrinA5 (EFNA5) in BT241. (C) mRNA expression by RT-PCR shows heightened expression of ephrinA1 and ephrinA5, putative ligands for EphA2 and EphA3, in the EphA2-/EphA3- cell population of BT241. (D) p-proteomics data shows phosphorylated peptides of EphA2 but not EphA3 after 15 min treatment with EphA2/A3 BsAb. (E) Western blot showing effect of 5 min treatment with EphA2/A3 BsAb in rGBM BT241. (F) CyTOF plots showing expression of all EphRs (except EphA2 and EphA3) following 3 days of treatment with EphA2/A3 BsAb. (***) $p < 0.001$.

Figure S6

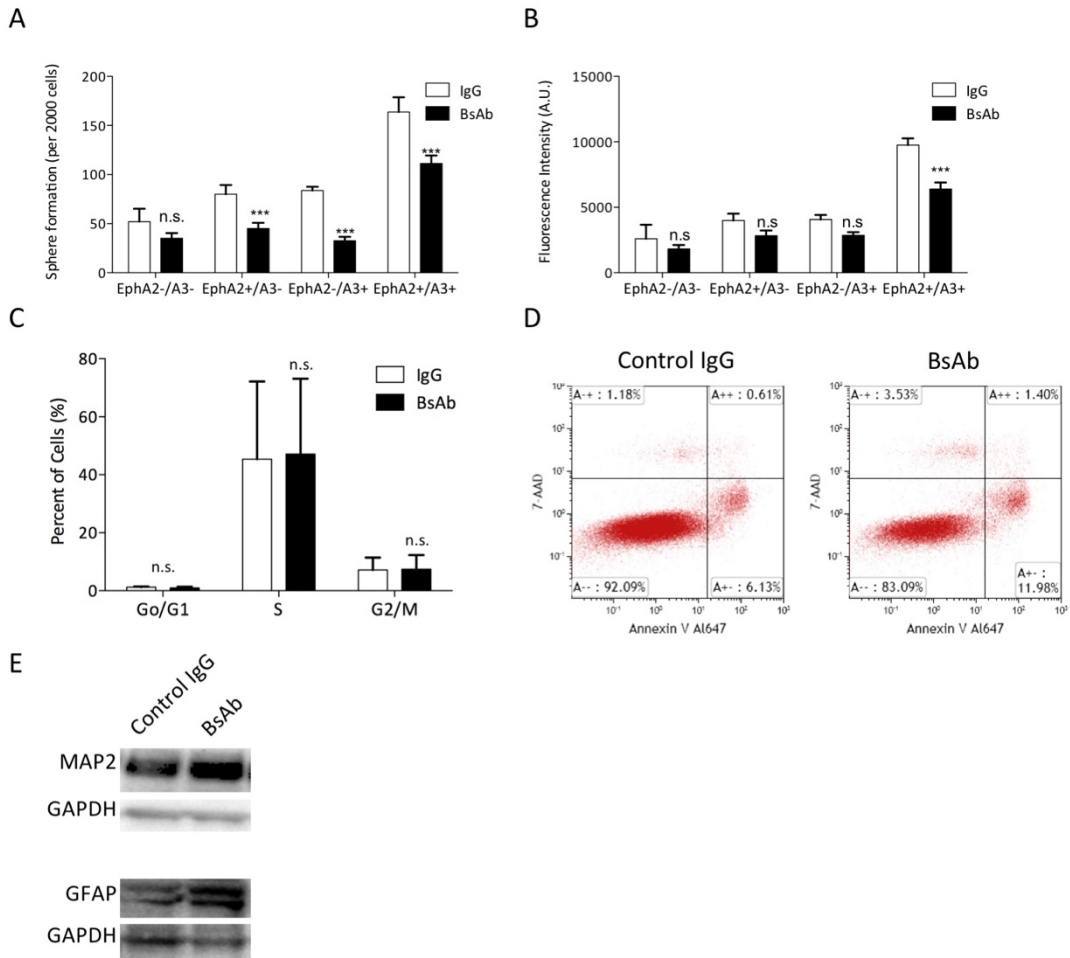


Figure S6: EphA2/A3 BsAb also targets EphA2+/EphA3- and EphA2-/EphA3+ cell populations, does not affect cell cycle or apoptosis, and leads to increased expression of GFAP and MAP2.

We treated cells sorted based on expression of EphA2 and EphA3 with EphA2/A3 BsAb and performed sphere formation (A) and proliferation (B) assays. Treatment with BsAb decreases sphere formation and proliferation capacity of EphA2+/EphA3- and EphA2-/EphA3+ cell populations as well but not of EphA2-/EphA3- cells. (C) Treatment of rGBM with EphA2/A3 BsAb for 3 days does not affect cell cycle and only leads to a small increase in apoptotic cells (D). (E) Western blot showing increased MAP2 and GFAP levels in rGBM BT241 treated with EphA2/A3 BsAb for 3 days. (n.s. Not significant, *** $p < 0.001$).

CHAPTER 4: Intratumoral heterogeneity: Pathways to treatment resistance and relapse in human glioblastoma

Preamble

This is a pre-copyedited, author-produced version of an article accepted for publication in *Annals of Oncology* following peer review. The version of record **Qazi MA**, Vora P, Venugopal C, Sidhu S, Moffat J, Swanton C, Singh SK. Intratumoral Heterogeneity: Pathways to Treatment Resistance and Relapse in Human Glioblastoma. *Annals of Oncology*, 28(7):1448-1456, 2017 is available online at: <https://doi.org/10.1093/annonc/mdx169>, DOI:10.1093/annonc/mdx169.

MAQ prepared the manuscript and created the figures. PV and VC helped with literature review and edited the manuscript. SS, JM and CW provided critical intellectual content. SKS supervised and edited the manuscript.

In this review, we explored the role of intratumoral heterogeneity (ITH) in mediating resistance to therapy in GBM. We begin with presenting a review of data that demonstrates the presence of extensive ITH in primary GBM and how it contributes to treatment failure. We next present the presence of ITH in recurrent GBM and highlight the differences in cellular and molecular biology of primary and recurrent GBM as demonstrated through genomic and transcriptomic data, such that recurrent GBM can now be described as a distinct biological entity. We next explore how the cancer stem cell hypothesis may explain the presence of functional ITH in GBM. Lastly, we propose the need to develop models

that recapitulate the changing landscape of GBM biology, especially over the course of treatment. We also describe new technological advances that when incorporated with models of recurrent GBM will enable researchers to demarcate ITH in the context of therapy resistance and identify clinically and functionally relevant therapeutic targets.

Sections of this review have also been used in the introduction chapter of this thesis.

Intratumoral Heterogeneity: Pathways to Treatment Resistance and Relapse in Human Glioblastoma

Maleeha A. Qazi^{1,2}, Parvez Vora^{1,3}, Chitra Venugopal^{1,3}, Sachdev S. Sidhu⁴, Jason Moffat⁴, Charles Swanton⁵, and Sheila K. Singh^{1,2,3}

¹Stem Cell and Cancer Research Institute, McMaster University, Hamilton, ON, Canada

²Department of Biochemistry and Biomedical Sciences, McMaster University, Hamilton, ON, Canada

³Department of Surgery, McMaster University, Hamilton, ON, Canada

⁴Donnelly Centre and Department of Molecular Genetics, University of Toronto, ON, Canada

⁵The Francis Crick Institute, University College London Institute, London, UK

^aCorresponding Author Contact Information:

Sheila K. Singh MD PhD FRCS(C), MDCL 5027, McMaster University Stem Cell and Cancer Research Institute, 1280 Main Street West, Hamilton, ON, L8S 4K1, CANADA.

T: 905 521 2100 x75237 F: 905 521 9992 Email: ssingh@mcmaster.ca

Abstract

Intratumoral heterogeneity (ITH) has increasingly being described for multiple cancers as the root cause of therapy resistance. Recent studies have started to explore the scope of ITH in glioblastoma (GBM), a highly aggressive and fatal form of brain tumor, to explain its inevitable therapy resistance and disease relapse. In this review, we detail the emerging data that explores the extensive genetic, cellular and functional ITH present in GBM. We discuss current experimental models of human GBM recurrence and suggest harnessing

new technologies (CRISPR-Cas9 screening, CyTOF, cellular barcoding, single cell analysis) to delineate GBM ITH and identify treatment-refractory cell populations, thus opening new therapeutic windows. We will also explore why current therapeutics have failed in clinical trials and how ITH can inform us on developing empiric therapies for the treatment of recurrent GBM.

Key words: glioblastoma, intratumoral heterogeneity, brain tumor initiating cells, recurrence, resistance, models, polytherapy, immunotherapy

Introduction

Glioblastoma (GBM), a highly aggressive astrocytic tumor (WHO grade IV), is the most common primary brain tumor in adults[1, 2]. Despite multimodal therapy consisting of surgical resection, radiation, and chemotherapy with the alkylating agent temozolomide (TMZ), the disease rapidly progresses and leads to relapse at 8-9 months post diagnosis, with an average survival of only 15 months[3-5]. This poor prognosis for GBM has been attributed to extensive cellular and genetic heterogeneity existing not only between patients, but also at an intratumoral level[6-9]. A molecular GBM classification by The Cancer Genome Atlas (TCGA) has offered insights into genetic regulation of GBM with identification of molecular subgroups with putative prognostic significance[10, 11]. The four subgroups of GBM described by TCGA, namely classical, neural, pro-neural and mesenchymal, were identified using transcriptional profiling data of bulk tumor specimens and based on dominant genes expressed in each group[11]. Despite extensive genomic and transcriptomic profiling of GBM by the TCGA to delineate molecular groups, most tumors were found to harbor alterations in common oncogenic pathways (receptor tyrosine kinase

(RTK) signaling through mutations/amplifications in receptors such as EGFR and PDGFRA; mutations in downstream partners of Akt pathway such as PI3K and PTEN; apoptosis signaling through mutations in p53; and cell cycle control signaling through alterations in CDKs) [10, 12]. Overall, the impact on treatment and prognosis of GBM subgroups has been limited by the fact that the genetic landscape of tumors is continually evolving through space and time[13-15], generating an almost unimaginable degree of cellular complexity and heterogeneity within a single tumor[16-18]. Such intratumoral heterogeneity (ITH) is increasingly believed to be one of the key determinants of therapy failure in GBM.

Intratumoral heterogeneity in GBM

Although the classification of GBM into four distinct molecular subgroups by TCGA attempted to address the challenge of heterogeneity in GBM[11], recent studies show that the GBM subgroups are flexible and vary spatially and temporally within the same tumor. A study by Patel *et al*[9] showed that at single cell RNA-sequencing resolution, a single tumor consisted of a heterogeneous mixture of cells representing all of the different GBM subgroups. When examining the pro-neural subgroup, which had the best survival of all GBM subgroups, the authors showed that patients with pro-neural tumors that also bore markers of other subgroups had poorer survival, especially if the relative representation of the alternative subgroups was high in the tumor[9], emphasizing the role ITH may play in therapy resistance. Another study by Reinartz *et al* [19] show that single cell derived GBM subclones have distinct genetic identity and maintain differential drug resistance profile. Initial reports of ITH in GBM identified coactivation of multiple RTK such as EGFR, Met

and PDGFR, which required poly-targeting approach of RTKs to abrogate downstream signaling and cell viability[20]. Similarly, Szerlip *et al* showed heterogeneous amplification of EGFR and PDGFRA within GBM cell subpopulations[21]. Inhibition of both RTKs was required to attenuate the activity of downstream target PI3K (phosphoinositide-3-kinase) and inhibit tumor growth. Additionally, multiple aberrations in EGFR, identified through single-cell genome sequencing, have been found to co-exist in GBM and in fact some EGFR variants (EGFRvIII and EGFR carboxy-terminal deletions) tend to exist in mutually exclusive subclonal populations[22]. Although factors such as CNS penetration of agents, target selection and limitations in patient selection based on biomarker presence also contributed to therapy failure with RTK inhibitors in clinical trials, the observation of extensive ITH in GBM suggests the need for combinatorial therapies to address the challenge of therapy failure.

Further clouding the molecular subgrouping of GBM is the idea of spatial heterogeneity, which confounds our diagnostic and therapeutic efforts since previous genomic studies relied on a single regional biopsy to subgroup a patient. By sampling geographically distinct regions of single tumors, Sottoriva *et al*[23] showed that genome-wide GBM ITH can be decomposed to reveal spatial and temporal tumor evolution, and based on gene expression levels, tumor fragments from the same patient may be classified into different GBM subgroups. These studies together inform not only on the extensive genomic heterogeneity that exists in GBM, but also present heterogeneity as a possible asset to evade therapy and generate resistance (Table 1). Consequently, ITH may then give rise to

subclonal populations of cells with selectable traits that can respond to and escape any given stress, including therapy[24].

Intratumoral heterogeneity in recurrent GBM

From an evolutionary perspective, the divergent development of subpopulations of cancer cells within the same tumor is likely at the root of therapy failure, the development of treatment resistance, and ultimately, recurrence of the malignancy (Figure 1). A study by Johnson *et al*[25] showed that low grade gliomas and their paired recurrences only shared a few early mutations and were highly divergent. They also found that in 43% of profiled GBM cases, at least half of the mutations in the initial tumor were undetected at recurrence, suggesting that therapy acts as a selection pressure or bottleneck for tumor evolution from minority cell populations present at time of initial diagnosis. Moreover, they also discovered that therapy might in itself drive the emergence of treatment-resistant subclones, as secondary GBMs from low-grade gliomas were found to be hypermutated and bearing a TMZ-induced mutagenesis signature.

The clonal evolution of primary GBM to recurrence was further demarcated through whole-genome and multisector exome sequencing studies of primary GBM and matched recurrences, which suggested both clonal and ancestral origins of GBM recurrence after therapy[26]. Verhaak and colleagues confirmed that while some GBM recurrences bore ancestral p53 driver mutations detectable in the primary GBM, many other recurrences were driven by branched subclonal divergent mutations not present in the primary GBM[26]. A case study by Swanton and colleagues[15] again showed that the driver clonal

mutation in a primary GBM was lost in the recurrence, which itself was dominated by a subclone from the primary GBM. Another study of the spatiotemporal evolution of the primary GBM epigenome to recurrence further consolidated the extent to which genomic instability and ITH are driven by therapy[27]. Further studies to explain patterns of GBM recurrence discovered that a spatially local recurrence of GBM was marked by a high retention of initial tumor mutations, following a linear evolution model, while a spatially distant recurrence retained fewer mutations from the initial tumor and followed a branched evolution model of recurrence[28]. In the recent study by Wang *et al.*, which comprises the largest longitudinal analysis of both genomic and transcriptomic data from GBM patients through therapy, the authors again show that 63% of patients change expression-based subtyping[29]. In addition, they identified mutational landscapes that corresponded exclusively to the primary or the recurrent GBM as well mutations shared between the two. Interestingly, EGFR and EGFRvIII, both common targets for clinical trials, were largely reserved to the initial tumor and not the recurrence. Their data also suggests that the evolutionary divergent cellular populations that seed relapse existed years before diagnosis. By determining how both genetic and epigenetic events are clonally selected during GBM progression and constructing phylogenetic and phylo-epigenetic trees of GBM patients at diagnosis and recurrence, these studies documented both linear and branched divergent subclonal evolution, suggesting that targeted monotherapies based on the tumor genome at diagnosis are doomed to failure [30].

Meta-analysis of all recent clinical trials for GBM patients has also predicted the failure of

monotherapy to target the now well documented complexity of ITH in GBM [31], stressing the importance of multimodal therapy whenever clinically feasible, and highlighting the need to develop innovative and informed polytherapeutic strategies for this highly complex disease. The sum of the recent emerging literature on ITH and GBM, including single cell sequencing studies and longitudinal genomic profiling of GBM progression, has mapped multiple iterations of the clonal hierarchies that exist in GBM, and it is clear that spatial and temporal evolution are at play. However, whereas some models suggest that truncal mutations present in the primary tumor, such as PI3KCa or IDH mutations or FGFR-TACC3 fusion events, may inform therapies more effectively than private events such as EGFR amplifications which are exclusive to only a few regions of the tumor[32], other models suggest that subclonal divergent events present exclusively at recurrence (arising either from rare clones that are not detected in the primary tumor or from mutational events that arise only after chemoradiotherapy) warrant a closer examination of the recurrent tumor to find efficacious therapeutic targets[25, 29]. In the end, the pattern of clonal evolution will likely vary from patient to patient, and only large population-based studies of the clonal maps of hundreds of sequenced GBMs will eventually discern reproducible cohorts of patients that recur in a similar manner. In any case, intratumoral genetic heterogeneity in clonal cell populations represents the root of therapy failure, the driver of development of treatment resistance, and ultimately results in recurrence of the malignancy.

A recent study by Meyer *et al*[33] demonstrated that clonal populations derived from single cells have variable response to TMZ as well other drugs, linking genomic heterogeneity to

functional heterogeneity. These single-cell derived clonal populations also presented with differential EGFR expression and O-6-methylguanine-DNA methyltransferase (MGMT) promoter methylation status, a biomarker for TMZ resistance. Furthermore, study by Parker *et al.* showed that ITH is not only evident for MGMT promoter methylation but also for several other genes of the DNA repair pathways, which could explain discordance in MGMT promoter methylation status and response to TMZ in some patients with GBM[34]. Similar reports of clonal populations derived from single GBM cells show distinct phenotypic and proliferative characteristics in both *in vitro* and *in vivo* model systems[19, 35]. This study suggests that functional heterogeneity in GBM is not only a derivative of genetic mutations but epigenetic mechanisms might also be playing a role, as cells from a single genetic background showed diverse expression of important GBM genes and differential functional response to drug treatment. At the cellular level, functional GBM heterogeneity can then be explained by the existence of multiple cellular subpopulations of cancer cells that have acquired stem cell properties of self-renewal and multi-lineage differentiation, variably labeled in the literature as BTICs (brain tumor initiating cells) or GICs (glioblastoma initiating cells)[36-39].

Brain tumor initiating cells may drive GBM recurrence

BTIC models[37, 40] combined with genomic deep-sequencing technologies have begun to resolve the extent of ITH in GBM. BTICs may arise from the dysregulation of genes that govern self-renewal, the cardinal property of stemness that allows a stem cell, at each cell division, to generate an identical copy of itself and a cell of the same or different phenotype[41]. The BTIC model of GBM is thought to recapitulate the functional

heterogeneity that exists within a tumor, as a BTIC has been shown to give rise to all the cellular subpopulations within a tumor[37, 42], including endothelial cells[43-46] but not immune cell infiltrates, which may arise from bone-marrow derived macrophages or brain-resident microglia[47]. Cancer may thus be thought of as a disease of unregulated self-renewal[6], as this property combined with the ability to assume a quiescent state to evade chemo and radiotherapy, together with enhanced DNA repair pathways, may allow BTICs to evade therapy. CD133, a known cell surface marker of BTICs, has been the focus of many studies as CD133+ populations not only initiated tumors *in vivo*, but are also known to be resistant to chemotherapy [48] and radiotherapy [49]. CD133+ cells maintain their radiotherapy-resistant phenotype through the activation of DNA damage checkpoint pathway, allowing the cells to repair radiation induced DNA damage by arresting cell cycle[49]. Resistance to TMZ seen in CD133+ cells seems to be mediated through multiple mechanisms including higher expression of MGMT to maintain DNA repair mechanism and increased expression of anti-apoptotic genes and ABC transporters such as BCRP1 in CD133+ cell population[50]. The small molecule compound pyrvinium has been shown to inhibit self-renewal and eradicate the CD133+ GBM BTIC population that may persist throughout the course of treatment by generating a cellular hierarchy that contributes to ITH and the acquisition of drug resistance[51].

Although CD133 marks a more tumorigenic population in GBM, it does not mark the entire BTIC population in GBM as subsequent studies have shown that in some GBM samples, CD133- cells are also able to initiate tumors in xenograft models[52]. This led to the

identification of additional markers of BTICs in GBM such as CD15[53], integrin alpha6[54] and L1CAM[55]. In addition, intracellular proteins such as RNA binding protein Musashi-1[56], transcription factors Sox2[57], Oct4[58] and FoxG1[59], and polycomb repressor Bmi1[60, 61] that have a characterized functional role in driving normal neural NSC self-renewal, have also been investigated as putative BTIC markers. Additional neurodevelopmental transcriptions factors such as Oct3, Sall2 and Olig2 have also been identified to play a role in GBM BTIC maintenance[58].

Future studies should now address whether BTICs are causative in tumor relapse and whether the same BTIC populations that drive tumor initiation also drive GBM recurrence.

Models to study intratumoral heterogeneity in GBM recurrence

Recent clonal evolution studies have relied largely on genome-wide sequencing alone, using the mutational profiles of bulk tumor populations to deduce the evolutionary trajectory followed by GBM through therapy. No studies have conclusively revealed how functional cell populations evolve through therapy in GBM to determine whether a pre-existing clone is driving therapy relapse in GBM, or therapy itself drives the emergence of a new population(s) that seeds the relapse. Studies so far have demonstrated that early somatic mutations in dominant clones drive tumor growth, whereas later mutations acquired during the course of treatment in heterogeneous low-frequency subclonal populations may aid in tumor recurrence and relapse. Current *in vitro* and *in vivo* models of GBM rely on primary tumor specimens at diagnosis to identify pathways that drive tumorigenesis, and extrapolate possible mechanisms of therapy resistance from the study

of the treatment-naïve tumor specimen. However, these studies show that recurrent GBM is a divergent disease and therefore should be profiled in conjunction with the primary tumor to fully capture the evolutionary mechanisms driving therapy resistance and tumor relapse (Figure 1).

Although the CD133+ population has already been identified as both chemoresistant [50] and radioresistant[49], with recurrence having higher expression of CD133[62], the combinatorial effect of TMZ and radiation on GBM BTIC populations has not been clearly studied to prospectively define whether these treatments lead to selection of subclonal populations from which recurrence may arise. Animal models of GBM also fail to capture the progression of GBM from a primary treatment-naïve disease to a recurrent treatment-refractory disease. In fact, most genetically engineered mouse models of GBM have relied on mutations identified in a primary GBM patient cohort from studies by TCGA [animal models of GBM reviewed in [63]]. Although genetically engineered mouse models have allowed researchers to explore the signaling pathways modulated by each mutation and how they impact tumor growth, studying each mutation in isolation prevents researchers from identifying the interdependence of multiple signaling pathways in GBM, their combinatorial role in disease progression and, most importantly, how the tumor will respond to therapy and escape treatment to seed relapse.

Patient-derived xenograft (PDX) models of GBM combat some shortcomings of genetically engineered mouse models by allowing the study of human GBM with its

complete mutational profile in tumor initiation and disease progression. In fact, xenografts of GBM in immunodeficient mice have been shown to recapitulate the histopathological features of the parental GBM tumor, making PDX models a good surrogate for the study of GBM (Figure 2a) [37]. However, PDX models also lack validated protocols to study the progression of the disease through treatment and disease relapse.

To address the limitations of current *in vitro* and *in vivo* models of GBM, the focus must shift to the development of models that capture the evolving GBM population at tumor initiation and maintenance and, more importantly, through therapy and at recurrence (Figure 2b). Unlike previous studies that evaluated the independent effects of either chemotherapy or radiotherapy on GBM cells, Qazi *et al* used BTIC-enriched GBM cultures to characterize chemoradiotherapy resistant cells[64]. They developed and optimized a combined chemoradiotherapy protocol for *in vitro* GBM cultures based on clinically relevant doses of TMZ and radiation. Delivery of chemoradiotherapy to primary, treatment naïve GBM BTICs leads to increased expression of important stem cell genes (Bmi1 and Sox2), enriches for a CD15+ (a BTIC marker) population similar to that observed in patient-derived recurrent GBMs, and increases self-renewal capacity of the cells. In addition, gene expression profiles of *in vitro* chemoradiotherapy-treated GBM identified a previously unknown, hyper-aggressive subgroup of gliomas with significantly poor survival. This *in vitro* model captures aspects of recurrent GBM biology that would have been unidentified had the therapies been studied individually, and generates GBM recurrences in the laboratory, as patients with GBM recurrence are often palliative,

disallowing repeat surgery for tissue sampling.

Extending these models to further delineate the role of ITH and subclonal selection upon recurrence in GBM, lentivector-mediated clonal tracking technology [65] can further delineate clonal dynamics of GBM recurrence. The concept of cellular heterogeneity is not cancer exclusive; rather normal cellular systems also display heterogeneity with the presence of multiple clonal subpopulations. A 2004 study by John Dick and colleagues showed that within the normal hematopoietic system, the hematopoietic stem cell (HSC) pool is highly functionally heterogeneous[66]. In the field of cancer research, cellular DNA barcoding technology can be used to answer pertinent tumor biology questions such as how the tumor evolves over the progression of the disease, how growth kinetics determine heterogeneity of tumor cells, and how tumor cells respond to therapy. To fully appreciate the complexity of a tumor population, studying tumor cells at single cell or clonal resolution is essential for the identification of drivers of tumor initiation, evolution and therapy resistance. Such studies have been undertaken in both leukemias and solid tumors (lung[67], breast[68] and colon[69]).

Although research has identified the presence of genomic heterogeneity in GBM and genetic subclones in primary and recurrent tumors, no studies have identified how clonal subpopulations present within GBM play a role in therapy resistance. Analysis of clonal dynamics in GBM following chemoradiotherapy will lead to the identification of clones that govern tumor recurrence, and will allow us to determine whether a pre-existing tumor

clone or a divergent subclonal population that arises after therapy administration dominantly comprises recurrent GBMs. Use of such analyses will inform our understanding of the tumor biology of the primary GBM, and identify the pattern of recurrence in model systems to develop personalized therapeutics before the patient relapses.

The identification of all clonal subpopulations is indeed limited by our ability to perform multiple, sectional biopsies on patients with GBM. Multiple invasive brain surgeries pose risks for the patients as it may lead to further neurological complications. In addition, GBM is a highly invasive disease and despite total tumor resectioning, malignant cells might still be left behind in the patient's brain that can regenerate the tumor leading to relapse. However, recent technological advances are allowing researchers to explore and dissect GBM ITH through powerful new methods in validated model systems. With the advancement of genome wide CRISPR-Cas9 screening, identification of targets that are essential to recurrent GBM in maintaining tumorigenicity and therapy resistance will pave new directions for the development of therapeutics for GBM. A recent study by Toledo *et al.* identified PKMYT1, a protein kinase, as essential to BTICs for completion of mitosis and therefore a candidate therapeutic target for GBM [70]. Another advancing technology that can be harnessed to understand GBM ITH is through the use of CyTOF (time-of-flight mass cytometry), which uses heavy metal tagged antibodies for highly multi-parametric single-cell proteomics [71]. Considering the heterogeneous landscape of GBM at the individual cell level, CyTOF lends itself to exploring the biological pathways governing multiple subpopulations of cells and identifying new markers for therapeutic targeting. The

analysis of hundreds of proteins at single-cell level through a therapy model will lead to identification of key proteins and signaling pathways that underlie therapy resistance in GBM. Combining these technologies with single cell RNA sequencing[9] and phosphoproteomics [72] will only enrich the breadth of information acquired on GBM ITH and inform researchers on the complexity of cell signaling within the tumor, leading to the identification of key signaling nodes for therapeutic targeting (Figure 2b). Together these technologies can help researchers not only capture the ITH of GBM biology but perhaps also identify the “Achilles’ Heel” of GBM recurrence, which can then be targeted through empirically developed therapeutics.

The development of clinically relevant models of GBM recurrence combined with advanced techniques will afford the opportunity to identify novel targets specific to recurrent GBM (Figure 2c). Most current targets identified for therapeutics are derived from primary GBM specimens, despite the fact that recurrent GBM is a unique entity that is driven by biological programs distinct from its parent primary tumor. Models of recurrent GBM thus become paramount to bring efficacious therapeutics to the clinic in order to improve GBM patient prognosis.

Therapeutic Implications of Intratumoral Heterogeneity

Taking into account the evolutionary dynamics of tumor populations, the therapeutic implications of ITH are of great importance for GBM therapy. The ongoing selection of cell populations through the course of disease development and particularly after the start of therapy suggests the need to study the evolving tumor biology throughout its disease

course. The addition of new mutations and evolving tumor landscape as expected at recurrence in GBM would possibly require targeting of multiple clonal mutations in order to achieve prolonged therapeutic benefits (Figure 1). A primary limitation of the TCGA data is in its single biopsy study design, where the four subgroups gave an illusion of clonality. The clonal or subclonal nature of driver events would have to be clearly defined before targeted intervention by undertaking multiple tumor-sectional studies as well as developing models that recapitulate the underlying tumor biology that drives therapy resistance and recurrence in GBM. *In vivo* therapy-adapted models of GBM combined with new methodologies for the study of complex biological systems will allow researchers to explore this complex biology in a systematic way and begin to uncover novel targets with potential therapeutic benefits for patients with GBM recurrence (Figure 2).

Clinical trials in GBM with targeted therapies to date have failed to show significant improvement in patient survival. Myriad reasons can explain treatment failure in GBM, including inability to obtain a complete resection, challenges of drug delivery and crossing the blood brain barrier, limitations in clinical trial design and execution, and multidrug acquired resistance[73, 74]. RTK targeting has been a prime focus of clinical trials for GBM with EGFR, PDGFR and VEGF as prominent GBM specific targets. However, these trials have been confounded by the use of monotherapies against single RTKs (erlotinib for EGFR, imatinib for PDGFR and bevacizumab for VEGF), as efficacy of single agents is highly unlikely to succeed considering the complex and overlapping networks of RTKs with different driver RTKs in cellular subpopulations of GBM. In addition, therapy with

single agents leads to selection of subclonal GBM populations, enriching for a therapy-resistant clone that then gives rise to recurrent GBM [72]. Targeting of EGFRvIII, a highly GBM-specific mutation, has also failed in trials, as the mutation has been shown to be present heterogeneously within the tumor population [75] and single targeting of EGFRvIII likely lead to the selection of wildtype EGFR-expressing populations that maintain tumor growth [76]. Immunotherapeutic approaches have recently gained momentum in the treatment of GBM as they promise better specificity and greater efficacy [77]. However, effective target identification for these therapies has been limited by the fact that large cohorts of genomic and transcriptomic studies have only included primary tumor specimens, with limited information on recurrent, treatment-refractory cell populations. To identify the converging and cooperative signaling pathways that maintain GBM growth through therapy and lead to recurrence, it will be critical to acquire large cohorts of datasets on recurrent GBM (genomic, transcriptomic and proteomic) and to combine these with experimental models to study GBM at subclonal levels through the use of multi-parametric technologies and/or single-cell analyses. The use of combining different modalities to treat GBM has been demonstrated to improve progression-free survival (3 months) and overall survival (5 months) through the use of tumour-treating fields that disrupt cell division in combination with TMZ for newly-diagnosed GBM patients[78]. Hence, polytherapeutic approaches that target multiple signaling pathways in recurrent GBM, along with multi-modal therapy approaches would allow for the elimination of the most tumorigenic populations that drive treatment resistance.

Conclusion

GBM is a highly heterogeneous disease at the genetic, transcriptomic and functional level. Research within the past decade has shown the complex biology underlying GBM tumorigenesis and efforts have been made to characterize the disease further. Although initial studies by the TCGA were helpful in starting to dissect the immense heterogeneity found in GBM, it was soon realized that this heterogeneity is not only inter-tumoral but also intra-tumoral, with each tumor presenting a complex heterogeneous milieu of cell biology. ITH identified in GBM can in turn explain poor prognosis and inevitable tumor relapse. The resistance of GBM to current aggressive chemoradiotherapy can be attributed to the tumor's extensive cellular heterogeneity and the presence of multiple subclonal populations that invariably either respond to or escape therapy, regenerating treatment-refractory recurrent tumor. Current models for the study of GBM fail to directly address the problem of GBM recurrence and continue to focus efforts on understanding primary, treatment-naïve tumor biology. Clearly, new models of GBM must address both spatial and temporal ITH, and must broaden analysis beyond a single treatment-naïve sample at diagnosis to capture the evolution of recurrent, treatment-resistant disease. A detailed understanding of the evolutionary dynamics of tumor progression will provide insight into the associated molecular genetic mechanisms underlying GBM recurrence.

Models that incorporate chemoradiotherapy in the study of GBM will pave the path for a comprehensive understanding of GBM biology, pathways of therapy resistance and cell population dynamics in recurrence. The identification of pathways governing therapy resistance in clonal subpopulations will allow clinicians to offer patients therapeutics that

selectively target the specific subclonal populations that drive GBM recurrence in each individual patient, leading to improved prognosis and outcomes.

Disclosure

The authors have declared no conflicts of interest.

References

1. Louis DN, Ohgaki H, Wiestler OD et al. The 2007 WHO Classification of Tumours of the Central Nervous System. *Acta Neuropathol* 2007; 114(2):97–109.
2. DeAngelis LM. Brain tumors. *N Engl J Med* 2001; 344(2):114–123.
3. Stupp R, Mason WP, Van Den Bent MJ. Radiotherapy plus concomitant and adjuvant temozolomide for glioblastoma. *N Engl J Med* 2005; 352(10):987–996.
4. Hegi ME, Diserens A-C, Gorlia T et al. MGMT gene silencing and benefit from temozolomide in glioblastoma. *N Engl J Med* 2005; 352(10):997–1003.
5. Stupp R, Hegi ME, Mason WP et al. Effects of radiotherapy with concomitant and adjuvant temozolomide versus radiotherapy alone on survival in glioblastoma in a randomised phase III study: 5-year analysis of the EORTC-NCIC trial. *Lancet Oncology* 2009; 10(5):459–466.
6. Wechsler-Reya R, Scott MP. The developmental biology of brain tumors. *Annu. Rev. Neurosci.* 2001; 24(1):385–428.
7. Zhu Y, Parada LF. The molecular and genetic basis of neurological tumours. *Nat Rev Cancer* 2002; 2(8):616–626.
8. Huse JT, Holland EC. Targeting brain cancer: advances in the molecular

- pathology of malignant glioma and medulloblastoma. *Nat Rev Cancer* 2010; 10(5):319–331.
9. Patel AP, Tirosh I, Trombetta JJ et al. Single-cell RNA-seq highlights intratumoral heterogeneity in primary glioblastoma. *Science* 2014; 344(6190):1396–1401.
 10. McLendon R, Friedman A, Bigner D et al. Comprehensive genomic characterization defines human glioblastoma genes and core pathways. *Nature* 2008; 455(7216):1061–1068.
 11. Verhaak RGW, Hoadley KA, Purdom E et al. Integrated genomic analysis identifies clinically relevant subtypes of glioblastoma characterized by abnormalities in PDGFRA, IDH1, EGFR, and NF1. *Cancer Cell* 2010; 17(1):98–110.
 12. Brennan CW, Verhaak RGW, McKenna A et al. The somatic genomic landscape of glioblastoma. *Cell* 2013; 155(2):462–477.
 13. Szerlip NJ, Pedraza A, Chakravarty D. Intratumoral heterogeneity of receptor tyrosine kinases EGFR and PDGFRA amplification in glioblastoma defines subpopulations with distinct growth factor response. 2012.
 14. Sottoriva A, Spiteri I, Piccirillo SGM et al. Intratumor heterogeneity in human glioblastoma reflects cancer evolutionary dynamics. *Proc. Natl. Acad. Sci. U.S.A.* 2013; 110(10):4009–4014.
 15. Favero F, McGranahan N, Salm M et al. Glioblastoma adaptation traced through decline of an IDH1 clonal driver and macroevolution of a double minute chromosome. *Ann. Oncol.* 2015:mdv127.

16. Yap TA, Gerlinger M, Futreal PA et al. Intratumor heterogeneity: seeing the wood for the trees. *Sci Transl Med* 2012; 4(127):127ps10–127ps10.
17. Hiley C, de Bruin EC, McGranahan N, Swanton C. Deciphering intratumor heterogeneity and temporal acquisition of driver events to refine precision medicine. *Genome Biol.* 2014; 15(8):453.
18. McGranahan N, Swanton C. Biological and Therapeutic Impact of Intratumor Heterogeneity in Cancer Evolution. *Cancer Cell* 2015; 27(1):15–26.
19. Reinartz R, Wang S, Kebir S et al. Functional Subclone Profiling for Prediction of Treatment-Induced Intratumor Population Shifts and Discovery of Rational Drug Combinations in Human Glioblastoma. *Clin. Cancer Res.* 2016. doi:10.1158/1078-0432.CCR-15-2089.
20. Stommel JM, Kimmelman AC, Ying H et al. Coactivation of receptor tyrosine kinases affects the response of tumor cells to targeted therapies. *Science* 2007; 318(5848):287–290.
21. Szerlip NJ, Pedraza A, Chakravarty D et al. Intratumoral heterogeneity of receptor tyrosine kinases EGFR and PDGFRA amplification in glioblastoma defines subpopulations with distinct growth factor response. *Proc. Natl. Acad. Sci. U.S.A.* 2012; 109(8):3041–3046.
22. Francis JM, Zhang C-Z, Maire CL et al. EGFR variant heterogeneity in glioblastoma resolved through single-nucleus sequencing. *Cancer Discov* 2014; 4(8):956–971.
23. Sottoriva A, Spiteri I, Piccirillo SGM et al. Intratumor heterogeneity in human

- glioblastoma reflects cancer evolutionary dynamics. *Proc. Natl. Acad. Sci. U.S.A.* 2013; 110(10):4009–4014.
24. Notta F, Mullighan CG, Wang JCY et al. Evolution of human BCR-ABL1 lymphoblastic leukaemia-initiating cells. *Nature* 2011; 469(7330):362–367.
 25. Johnson BE, Mazor T, Hong C et al. Mutational analysis reveals the origin and therapy-driven evolution of recurrent glioma. *Science* 2014; 343(6167):189–193.
 26. Kim H, Zheng S, Amini SS et al. Whole-genome and multisector exome sequencing of primary and post-treatment glioblastoma reveals patterns of tumor evolution. *Genome Res.* 2015:gr.180612.114.
 27. Mazor T, Pankov A, Johnson BE et al. DNA Methylation and Somatic Mutations Converge on the Cell Cycle and Define Similar Evolutionary Histories in Brain Tumors. *Cancer Cell* 2015; 28(3):307–317.
 28. Kim J, Lee I-H, Cho HJ et al. Spatiotemporal Evolution of the Primary Glioblastoma Genome. *Cancer Cell* 2015; 28(3):318–328.
 29. Wang J, Cazzato E, Ladewig E et al. Clonal evolution of glioblastoma under therapy. *Nat. Genet.* 2016; 48(7):768–776.
 30. Ramaswamy V, Taylor MD. The Amazing and Deadly Glioma Race. *Cancer Cell* 2015; 28(3):275–277.
 31. Scorsetti M, Navarria P, Pessina F, Ascolese AM. Multimodality therapy approaches, local and systemic treatment, compared with chemotherapy alone in recurrent glioblastoma. *BMC ...* 2015.
 32. Lee J-K, Wang J, Sa JK et al. Spatiotemporal genomic architecture informs

- precision oncology in glioblastoma. *Nat. Genet.* 2017; 54:3988.
33. Meyer M, Reimand J, Lan X et al. Single cell-derived clonal analysis of human glioblastoma links functional and genomic heterogeneity. *Proc. Natl. Acad. Sci. U.S.A.* 2015:201320611.
 34. Parker NR, Hudson AL, Khong P et al. Intratumoral heterogeneity identified at the epigenetic, genetic and transcriptional level in glioblastoma. *Sci Rep* 2016; 6(1):22477.
 35. Soeda A, Hara A, Kunisada T et al. The evidence of glioblastoma heterogeneity. *Sci Rep* 2015; 5:7979.
 36. Singh SK. Identification of a Cancer Stem Cell in Human Brain Tumors. *Cancer Research* 2003:1–9.
 37. Singh SK, Hawkins C, Clarke ID et al. Identification of human brain tumour initiating cells. *Nature* 2004; 432(7015):396–401.
 38. Clarke MF, Fuller M. Stem Cells and Cancer: Two Faces of Eve. *Cell* 2006; 124(6):1111–1115.
 39. Dalerba P, Cho RW, Clarke MF. Cancer Stem Cells: Models and Concepts. *Annu. Rev. Med.* 2007; 58(1):267–284.
 40. Singh SK, Clarke ID, Terasaki M et al. Identification of a cancer stem cell in human brain tumors. *Cancer Research* 2003; 63(18):5821–5828.
 41. Reynolds BA, Weiss S. Generation of Neurons and Astrocytes from Isolated Cells of the Adult Mammalian Central Nervous System. *Science* 1992; 255(5052):1707–1710.

42. Hemmati HD, Nakano I, Lazareff JA et al. Cancerous stem cells can arise from pediatric brain tumors. *Proc. Natl. Acad. Sci. U.S.A.* 2003; 100(25):15178–15183.
43. Soda Y, Marumoto T, Friedmann-Morvinski D et al. Transdifferentiation of glioblastoma cells into vascular endothelial cells. *Proc. Natl. Acad. Sci. U.S.A.* 2011; 108(11):4274–4280.
44. Ricci-Vitiani L, Pallini R, Biffoni M et al. Tumour vascularization via endothelial differentiation of glioblastoma stem-like cells. *Nature* 2010; 468(7325):824–828.
45. Wang R, Chadalavada K, Wilshire J et al. Glioblastoma stem-like cells give rise to tumour endothelium. *Nature* 2010; 468(7325):829–833.
46. Chroscinski D, Sampey D, Maherali N, Reproducibility Project: Cancer Biology. Registered report: tumour vascularization via endothelial differentiation of glioblastoma stem-like cells. *Elife* 2015; 4:139.
47. Quail DF, Bowman RL, Akkari L et al. The tumor microenvironment underlies acquired resistance to CSF-1R inhibition in gliomas. *Science* 2016; 352(6288):aad3018–aad3018.
48. Chen J, Li Y, Yu T-S et al. A restricted cell population propagates glioblastoma growth after chemotherapy. *Nature* 2012:1–6.
49. Bao S, Wu Q, McLendon RE et al. Glioma stem cells promote radioresistance by preferential activation of the DNA damage response. *Nature* 2006; 444(7120):756–760.
50. Liu G, Yuan X, Zeng Z et al. **Analysis of gene expression and chemoresistance of CD133+ cancer stem cells in glioblastoma.** *Mol Cancer* 2006; 5(1):67.

51. Venugopal C, Hallett R, Vora P et al. Pyrvinium targets CD133 in human glioblastoma brain tumor-initiating cells. *Clin. Cancer Res.* 2015:clincanres.3147.2014.
52. Hau P, Proescholdt M, Lohmeier A et al. CD133+ and CD133- Glioblastoma-Derived Cancer Stem Cells Show Differential Growth Characteristics and Molecular Profiles. *Cancer Research* 2007; 67(9):4010–4015.
53. Son MJ, Woolard K, Nam D-H et al. SSEA-1 is an enrichment marker for tumor-initiating cells in human glioblastoma. *Cell Stem Cell* 2009; 4(5):440–452.
54. Lathia JD, Gallagher J, Heddleston JM et al. Integrin alpha 6 regulates glioblastoma stem cells. *Cell Stem Cell* 2010; 6(5):421–432.
55. Bao S, Wu Q, Li Z et al. Targeting cancer stem cells through L1CAM suppresses glioma growth. *Cancer Research* 2008; 68(15):6043–6048.
56. Kaneko Y, Sakakibara S, Imai T et al. Musashi1: an evolutionally conserved marker for CNS progenitor cells including neural stem cells. *Dev. Neurosci.* 2000; 22(1-2):139–153.
57. Graham V, Khudyakov J, Ellis P, Pevny L. SOX2 functions to maintain neural progenitor identity. *Neuron* 2003; 39(5):749–765.
58. Suva ML, Rheinbay E, Gillespie SM et al. Reconstructing and reprogramming the tumor-propagating potential of glioblastoma stem-like cells. *Cell* 2014; 157(3):580–594.
59. Manoranjan B, Wang X, Hallett RM et al. FoxG1 Interacts with Bmi1 to Regulate Self-Renewal and Tumorigenicity of Medulloblastoma Stem Cells. *STEM CELLS*

- 2013; 31(7):1266–1277.
60. Fasano CA, Dimos JT, Ivanova NB et al. shRNA Knockdown of Bmi-1 Reveals a Critical Role for p21-Rb Pathway in NSC Self-Renewal during Development. *Cell Stem Cell* 2007; 1(1):87–99.
 61. Abdouh M, Facchino S, Chato W et al. BMI1 sustains human glioblastoma multiforme stem cell renewal. *J. Neurosci.* 2009; 29(28):8884–8896.
 62. Tamura K, Aoyagi M, Ando N et al. Expansion of CD133-positive glioma cells in recurrent de novo glioblastomas after radiotherapy and chemotherapy. *Journal of Neurosurgery* 2013; 119(5):1145–1155.
 63. Chen L, Zhang Y, Yang J et al. Vertebrate animal models of glioma: understanding the mechanisms and developing new therapies. *Biochim. Biophys. Acta* 2013; 1836(1):158–165.
 64. Qazi MA, Vora P, Venugopal C et al. A novel stem cell culture model of recurrent glioblastoma. *J Neurooncol* 2016; 126(1):57–67.
 65. Lu R, Neff NF, Quake SR, Weissman IL. tracking single hematopoietic stem cells in vivo using high-throughput sequencing in conjunction with viral genetic barcoding. *Nature Biotechnology* 2011; 29(10):928–933.
 66. Mazurier F, Gan OI, McKenzie JL et al. Lentivector-mediated clonal tracking reveals intrinsic heterogeneity in the human hematopoietic stem cell compartment and culture-induced stem cell impairment. *Blood* 2004; 103(2):545–552.
 67. Bhang H-EC, Ruddy DA, Krishnamurthy Radhakrishna V et al. Studying clonal dynamics in response to cancer therapy using high-complexity barcoding. *Nat.*

- Med. 2015; 21(5):440–448.
68. Nguyen LV, Cox CL, Eirew P et al. DNA barcoding reveals diverse growth kinetics of human breast tumour subclones in serially passaged xenografts. *Nat Commun* 2014; 5:5871.
 69. Kreso A, O'Brien CA, van Galen P et al. Variable clonal repopulation dynamics influence chemotherapy response in colorectal cancer. *Science* 2013; 339(6119):543–548.
 70. Toledo CM, Ding Y, Hoellerbauer P et al. Genome-wide CRISPR-Cas9 Screens Reveal Loss of Redundancy between PKMYT1 and WEE1 in Glioblastoma Stem-like Cells. *Cell Reports* 2015; 13(11):2425–2439.
 71. Bendall SC, Simonds EF, Qiu P et al. Single-cell mass cytometry of differential immune and drug responses across a human hematopoietic continuum. *Science* 2011; 332(6030):687–696.
 72. Wei W, Shin YS, Xue M et al. Single-Cell Phosphoproteomics Resolves Adaptive Signaling Dynamics and Informs Targeted Combination Therapy in Glioblastoma. *Cancer Cell* 2016; 29(4):563–573.
 73. Osuka S, Van Meir EG. Overcoming therapeutic resistance in glioblastoma: the way forward. *J. Clin. Invest.* 2017; 127(2):415–426.
 74. Ellis HP, Greenslade M, Powell B et al. Current Challenges in Glioblastoma: Intratumour Heterogeneity, Residual Disease, and Models to Predict Disease Recurrence. *Front Oncol* 2015; 5(26):251.
 75. Eskilsson E, Rosland GV, Talasila KM et al. EGFRvIII mutations can emerge as

- late and heterogenous events in glioblastoma development and promote angiogenesis through Src activation. *Neuro-Oncology* 2016; 18(12):1644–1655.
76. Schuster J, Lai RK, Recht LD et al. A phase II, multicenter trial of rindopepimut (CDX-110) in newly diagnosed glioblastoma: the ACT III study. *Neuro-Oncology* 2015; 17(6):854–861.
77. Dunn-Pirio AM, Vlahovic G. Immunotherapy approaches in the treatment of malignant brain tumors. *Cancer* 2016. doi:10.1002/cncr.30371.
78. Stupp R, Taillibert S, Kanner AA et al. Maintenance Therapy With Tumor-Treating Fields Plus Temozolomide vs Temozolomide Alone for Glioblastoma: A Randomized Clinical Trial. *JAMA* 2015; 314(23):2535–2543.

CHAPTER 4 FIGURES AND TABLES

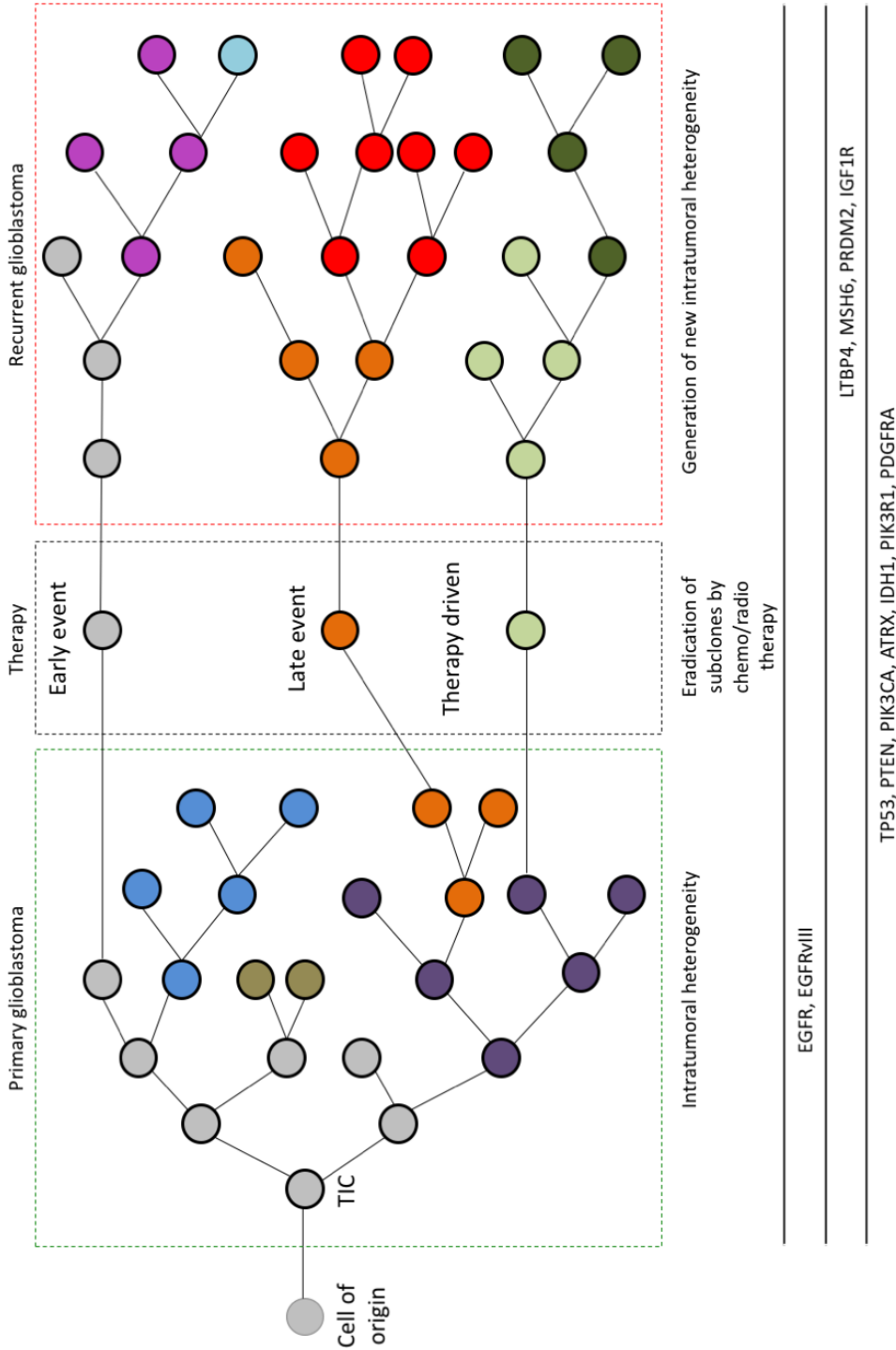


Figure 1: Subclonal populations in primary glioblastoma escape therapy and give rise to treatment-refractory, heterogeneous recurrent glioblastoma.

After a normal cell acquires mutations (black outlined circles), it expands into multiple subclonal populations of glioblastoma with selectable traits against any stress (represented by different coloured circles), including therapy. The administration of therapy for primary glioblastoma, leads to the selection of subclonal cell populations (early event subclone or late event subclone) or gives rise to a therapy-driven resistant subclone. These treatment-refractory subclonal populations then seed tumor relapse and lead to the formation of a heterogeneous recurrent glioblastoma that has a distinct clonal composition from primary glioblastoma. Mutations in multiple genes have been identified to be specific to either the primary GBM or the recurrent GBM as well as those common to both.

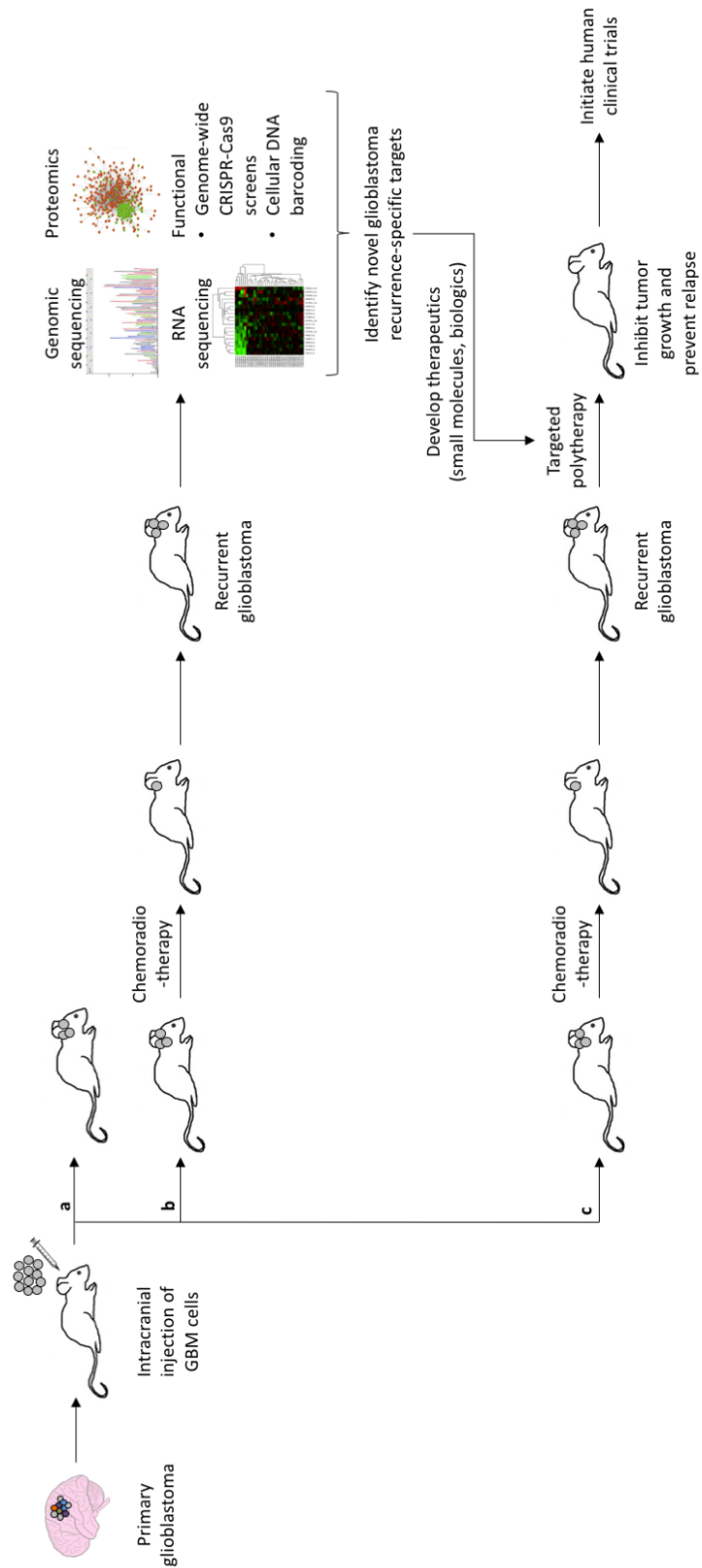


Figure 2: Development of recurrent glioblastoma models for the identification of novel targets to prevent disease relapse.

Primary glioblastoma cells can be intracranially injected in mice to develop patient-derived xenograft models to study tumor biology. (a) The primary tumor engraftment is used to study the treatment-naïve glioblastoma. (b) Treatment of primary tumor with model-adapted chemoradiotherapy (radiation and temozolomide) similar to therapy administered to patients will lead to the development of recurrent glioblastoma, which can then be studied using multiple biological parameters (genomic, transcriptomic, proteomic, functional) for the identification of novel recurrence-specific targets. Therapies (small molecules and/or biologics) can then be developed for the recurrence-specific targets and can be tested in the xenograft model in a polytherapy approach (c) to characterize therapeutic potential and advance successful candidates to human clinical trials.

Table 1: Characterization of intra-tumoral heterogeneity in GBM in the past decade.				
Primary author	Publication Year	Methodology	Samples	Key Findings
Stommel	2007	<ul style="list-style-type: none"> - RTK antibody array - Single cell immunofluorescence 	Glioma cell lines and primary GBM	<ul style="list-style-type: none"> - Co-activation of multiple RTKs including EGFR, PDGFRA and MET - Single GBM cells co-express activated RTKs - Co-targeting of multiple RTKs abrogates PI3K signaling
Snuderl	2011	<ul style="list-style-type: none"> - FISH analysis 	Archived GBM specimens	<ul style="list-style-type: none"> - Heterogeneous amplification of EGFR, PDGFRA and MET - Different regions of tumor represent differential RTK amplifications
Szerlip	2012	<ul style="list-style-type: none"> - FISH analysis 	Frozen GBM	<ul style="list-style-type: none"> - Coamplification of EGFR, PDGFRA and/or MET is not mutually exclusive in single cells
Sottoriva	2013	<ul style="list-style-type: none"> - Copy number arrays - Gene expression arrays 	Multiple sampling from each GBM	<ul style="list-style-type: none"> - Different regions of a brain tumor harbours different aberrations and alterations in gene copy numbers - Different fragments present distinct transcriptional profile and are classified into different GBM subgroups

Patel	2014	<ul style="list-style-type: none"> - Single cells RNA sequencing 	Primary GBM	<ul style="list-style-type: none"> - Single cells from the same tumor present distinct transcriptional profile and can be categorized in different subgroups - Tumors present with a gradient expression of stemness-related genes at a single cell level
Francis	2014	<ul style="list-style-type: none"> - Single cell whole genome sequencing 	Primary GBM	<ul style="list-style-type: none"> - Multiple mutations within the same gene coexist in GBM - Gene mutation variants can exist in mutually exclusive cell populations
Kim	2015	<ul style="list-style-type: none"> - Whole genome sequencing - Multi-sector exome sequencing 	Primary and recurrent GBM	<ul style="list-style-type: none"> - Recurrence follows two modes of evolution: 1. Linear, where recurrence shares extensive genetic profile with the primary; 2. Divergent, where recurrence branches off from an earlier ancestor of the tumor and shares fewer genomic similarity with the primary tumor
Meyer	2015	<ul style="list-style-type: none"> - Single-cell derived clonal population 	Primary and recurrent GBM	<ul style="list-style-type: none"> - Functionally heterogeneous cells exist in single GBM

				<ul style="list-style-type: none">- Single-cell derived clonal populations exhibit different MGMT promoter methylation status leading to differential response to TMZ- TMZ resistant cells pre-exist in primary GBM specimens
--	--	--	--	------------------------------------------------------------------------------------------------------------------------------------------------------------------------------------------------------------------------------------------------------

CHAPTER 5: A pre-clinical *in vivo* model of glioblastoma recurrence

Preamble

This chapter presents unpublished work on the development of a patient-derived xenograft model of GBM recurrence that is currently under preparation.

Qazi MA, Savage N, Winegarden N, Subapanditha MK, Desmond K, Ibeh N, Brown K, Nixon A, Venugopal C, Vora P, Mak A, Yelle N, Chokshi C, Bock N, Pugh T, Moffat J, Singh SK. A pre-clinical model of glioblastoma recurrence to identify personalized therapeutic targets.

MAQ conceived, designed and conducted the study, collected, analyzed and interpreted the data. SN assisted with animal studies and flow sorts. NW assisted with single cell RNA sequencing experiment and NI analyzed the data under the supervision of TP. MKS performed and analyzed flow cytometry experiments. KD performed MRI imaging on mice under the supervision of NB. KB and AN designed the cellular DNA barcoding library under the supervision of JM, who also supervised the study. VC and VP designed the study. AM, NY, and CC assisted with animal studies. SKS conceived and designed the study, interpreted the data, and supervised the study.

In this work, we show the development of a patient-derived xenograft model of GBM recurrence where we have developed a mouse-adapted standard of care chemoradiotherapy. We demonstrate the identification of MRI-guided minimal residual disease (MRD) time-

point in animal models and show that the model is amenable to any investigational therapy for use as a personalized pre-clinical model. Next, we show the use of single cell RNA-sequencing to characterize the cellular populations at MRD. We also demonstrate the use of cellular DNA barcoding technology to investigate the clonal composition of GBM through therapy in order to identify modes of therapy resistance. All data presented in this chapter is preliminary and needs further analysis.

Development of a therapy-adapted patient-derived xenograft model of GBM

recurrence

We hypothesize that subclonal populations of GBM cells may drive relapse of GBMs as they are refractory to therapy. Elucidating the pathways in these treatment-resistant subclones may provide potential therapeutic targets for patients with significantly diminished relapse-free and overall survival. We aimed to develop an *in vivo* model of GBM recurrence. We have adapted the existing treatment protocol for adults with newly diagnosed GBM, for treatment of mice engrafted with human GBM BTIC xenografts. Currently, during their concomitant phase, adult GBM patients receive 60 Gy of total cranial radiation with 75mg/m² TMZ as a radiosensitizer for 6 weeks. This is followed by oral chemotherapy with 150-200mg/m² of TMZ every 28 days for 6 cycles¹. We have developed a GBM treatment protocol tailored for the physiology and metabolism of NOD-SCID and NSG mice (Figure 1).

We intracranially engrafted GSC enriched primary, treatment-naïve GBM samples in NOD-SCID or NSG mice. Using MRI, tumor growth was monitored and once tumor was visible on MRI, *in vivo* chemoradiotherapy was initiated. We identified that 2-weeks post the completion of chemoradiotherapy, the tumour reached a minimal disease stage (Figure 2), where the symptoms of mice also started to improve (weight gain and improved fur condition). We termed this stage the minimal residual disease (MRD) state and postulated that the GBM cells at this time-point represent the roots of the imminent recurrence and profiling this stage would represent a window into understanding therapy-resistance at its

least heterogeneous stage. Using MRI, we are also able to ascertain whether the recurrence occurs locally or distally. In the MRI case presented, longitudinal MRI imaging of a mouse from the cohort showed tumor regression following chemoradiotherapy. However, 24 weeks after the end of chemoradiotherapy, we saw tumor regrowth in the left olfactory lobe. This was an exciting observation as a distal recurrence in human GBM patients denotes a divergent clonal evolution at the genomic level². We predict that this distal recurrence pattern in our animal model could also be reflective of a divergent pattern of clonal evolution in GBM through therapy. To date, we have modelled six different primary GBM samples through our *in vivo* model and we have performed bulk RNA-sequencing on the samples from the engraftment, MRD and recurrence time-points to profile the temporal evolution of pGBM through therapy. The data generated is currently under analysis and is therefore not presented in this thesis. On average, chemoradiotherapy treated mice experienced over 15 weeks of survival advantage as compared to control treated mice, at which point they succumbed to tumor burden.

Single cell RNA-sequencing to profile minimal residual disease

We wanted to investigate if we could incorporate other treatment modalities in our model to account for any additional treatment patients with GBM may receive. MBT06 sample was derived from the primary GBM of a 50-year old female who had an EGFR amplified tumor. The patient was enrolled in a double-blinded clinical trial for an EGFR-targeting antibody-drug conjugate therapy (ABT-414) by Abbvie. In order to recapitulate the patient's tumor progression in our model, we implemented a 3-arm study: control, chemoradiotherapy (T_R), chemoradiotherapy combined with ABT414 (T_R_A) (Figure

3).

At MRD, we flow sorted human cells from mouse brains and, as expected, we found a significant reduction in the number of human GBM cells present in the mouse brain post chemoradiotherapy (Figure 4A). We also saw significantly increased survival in mice that received treatment; however, we were surprised to find that all mice treated with additional ABT-414 succumbed to disease recurrence before mice that received just SoC chemoradiotherapy (Figure 4B). We then assessed the *in vitro* self-renewal capacity of the cells from each cohort using sphere formation assay, and found that each additional treatment slightly increased the sphere formation capacity of the GBM cells, with GBM cells from mice that received additional ABT-414 treatment having the highest sphere formation capacity, suggesting that treatment maybe enriching for a GSC population (Figure 4C).

We next performed single cell RNA sequencing using 10x Genomics platform on the cells from MRD time point. We found that control cells cluster separately from the treated cells (Figure 5A) and despite the additional ABT-414 treatment, the two treatment cohorts have overlapping clusters. We see same trend in gene expression heat map, whereby the treated GBM cells overexpress the same genes as compared to the control (Figure 5B). This suggests that even though long-term survival may differ between SoC chemoradiotherapy and additional ABT-414 treatment in mice, the GBM cell population at MRD have similar gene expression and therefore identifying therapeutic targets from this state could benefit

the patient regardless of whether they received ABT-414 treatment or not. We next performed unsupervised graph-based clustering of our cells and identified 8 gene expression clusters (Figure 6A and B). Control cells predominantly belonged to clusters 2, 4 and 5, while treated cells belonged to clusters 1, 3, 6 and 7. Interestingly, cluster 8 represented cells from both control and treated cell populations, suggesting that this cluster could represent the pre-existing population that also survives chemoradiotherapy.

Although comprehensive data analysis is still underway, one of the genes of interest identified so far from the scRNAseq is indolamine 2,3-dioxygenase (IDO1), a tryptophan catabolic enzyme, which is upregulated post-treatment at MRD and most highly expressed by cells in cluster 3. IDO1 is an important regulator of immune-suppressive environment in GBM^{3,4}. In addition, a recent study showed that IDO1 mediates resistance to PD-1 blockade in GBM, and therefore IDO1 inhibition in combination with PD-1 could overcome this resistance⁵. With renewed interest in checkpoint blockade and other immunotherapeutic opportunities for the treatment of GBM, we believe IDO1 could present a potential personalized therapeutic target for this patient. We are continuing to investigate and further validate IDO1 as a target and whether clinical trial options exist for the patient to enroll in.

Cellular DNA barcoding in GBM to identify clonal evolution through therapy

Cellular barcoding has been used to study patterns of clonal growth dynamics in cancer cells. In individually barcoded HCT-116 cells, Nolan-Stevaux *et al.* showed that upon *in vivo* tumor engraftment, majority of the barcoded cells retrieved from the tumor were

derived from a small population of initially tagged and injected clones⁶. They postulate that *in vivo* tumor growth is driven by clonal dominance of few clones even when starting with a presumably clonal cancer cell line. However, other studies have shown that tumor xenografts follow diverse *in vivo* clonal growth patterns. Studies by Connie Eaves group in breast cancer has shown that over the course of serial xenografts, multiple barcoded clonal populations can be detected and a constant flux in clonal composition of the tumor can be observed⁷. Subsequent studies from her research group to identify tumorigenic events early in disease progression showed that DNA barcoded normal mammary cells that were transduced with a single oncogene produced polyclonal carcinomas in mouse models. These studies have highlighted that polyclonality of the tumor population might be an intrinsic property that enables the cancer to proliferate under different conditions and more importantly, possibly enable the cancer to respond to multiple environmental factors, including therapy.

As studies in other cancer have shown, clonal dynamics informs us on how the tumor evolves through disease progression and how it responds to cancer therapy. Applying these concepts and technological advances to the study of GBM recurrence will be a significant step forward in the identification of mechanisms of therapy resistance. Although research has identified the genomic heterogeneity in GBM and the presence of genetic subclones in primary and recurrent tumors, no studies have identified how clonal subpopulations present within the GBM tumor play a role in therapy resistance. A study from Lan *et al.* used cellular DNA barcoding to attempt to identify treatment-resistance mechanisms following

chemotherapy of mice engrafted with barcoded human GBM cells⁸. They show that chemotherapy leads to a selection of a pre-existing clonal population that also survives retransplantation. However, the study was largely limited to a single GBM sample analysis and given intertumoral heterogeneity in GBM, multiple GBM samples must be studied to fully understand modes of therapy resistance. In addition, chemotherapy alone may select for a different clonal population that might be pre-existing. However, a combined chemoradiotherapy approach as is in clinical practice for the treatment of GBM may in fact lead to the selection of a different clonal population or may even lead to the generation of a therapy-driven clonal population.

We decided to use our GBM recurrence model to investigate the clonal composition of primary GBM and how it evolves over the course of chemoradiotherapy. Using a lentiviral 16-nucleotide based barcode library (BCLA) that also encodes for GFP, we determined the viral titer for each individual primary GBM sample (Figure 7A and B). This allowed us to transduce each GBM sample with barcoded lentiviral library at low MOI ($MOI \leq 0.3$) such that each GBM cell is uniquely barcoded. I optimized BCLA barcode library in eight different primary human GBM cell lines (GBM4, BT428, BT459, BT778, BT799, BT935, BT954 and MBT06). 72 hours post-transduction, I performed flow cytometry to isolate GFP+ barcoded cells (Figure 7C), which allowed me to also discard highly GFP+ cells that could represent more than one integration of the lentiviral vector.

To date, I have modelled 5 different barcoded primary GBM through our *in vivo*

chemoradiotherapy model. Considering that the GBM tumor population in a mouse brain is expected to be significantly smaller, especially at the MRD time-point, I optimized genomic DNA extraction protocols for snap-frozen mouse brain samples. I next optimized the PCR to amplify the barcode region for sequencing. I used mouse brains engrafted with barcoded cells ranging from 1×10^4 to 1×10^3 to identify the lower bound of our barcode library detection. I tested if a nested-PCR approach would enable us to amplify small amount of barcode from the genomic DNA. Hence, I first amplified a 800bp region of the lentiviral BCLA (PCR1) and then amplified the 137bp region (PCR2) for genomic sequencing (Figure 7D). Through the nested PCR, we were able to amplify 137 bp product from gDNA extracted from the mouse brains. I have processed gDNA samples from all mouse brains and are currently in the process of library preps for sequencing.

Materials and Methods

Intracranial human-mouse xenografts

1.0×10^6 GBM cells were intracranially injected for tumor formation in immunocompromised NOD-SCID or NSG mice as previously described⁹. Briefly, mice were anaesthetized using gas anaesthesia (Isoflurane: 2.5%). Using a 15-blade scalpel a 1.5 cm vertical midline incision was made on top of the skull. A small burr hole was then made (2-3 mm anterior to the coronal suture, 3 mm lateral to midline) using a drill held perpendicular to the skull. A Hamilton syringe was used to inject 10 μ l of cell suspension of GBM cells into the frontal lobe. The syringe was inserted through the burr hole at a 30° angle to a 5-mm depth. The incision was closed using interrupted stitches and sutures were sealed with a tissue adhesive. Mice were identified using ear notches and placed in recovery

cages. Mice were monitored weekly for signs of illness.

Chemoradiotherapy of mice

Once tumor formation was confirmed using MRI, mice were randomly assigned to control or treatment group and chemoradiotherapy treatment was started as described in Fig. 1. TMZ was administered orally through oral gavage 1 hour before irradiation was administered to mice. The mouse shield is designed such that only the head of the mice is irradiated. For additional ABT-414 treatment, mice received intraperitoneal injection of ABT-414 on a schedule as described in Fig. 3.

Flow cytometry

Mouse brains were dissociated with Liberase to single cell suspension and cultured in Neurocult complete media for 1 week. The percentage expression of Tra-1-85 was determined by flow cytometry (MoFlo XDP, Beckman Coulter) using APC-labeled anti-Tra-185 antibody (Miltenyi Biotec).

Self-renewal neurosphere formation assay

Tra-1-85⁺ cells from control and treated mouse brains were sorted at 200 cells/well density in a 96 well microwell plate in 0.2 mL volume of Neurocult complete media. The spheres were counted 7 days later.

Single cell RNA sequencing Analysis

The quality control metrics for the scRNA-seq data were obtained using the tool RNA-SeQC (v1.1.7). The raw FASTQ files were aligned to the appropriate genomes (mm10 and hg19) using the STAR aligner (STAR v2.5.2b). The CELLRANGER (v2.1.1) pipeline was used to obtain two types of gene-barcode matrices. The first matrix is an unfiltered gene-

barcode matrix. This matrix contains every barcode from the fixed list of known barcode sequences, including background and non-cellular barcodes. The next matrix type is the filtered gene-barcode matrix. The filtered matrix contains only the detected cellular barcodes. In the final filtered matrix, each row corresponds to a gene, and each column corresponds to a cell barcode sequence. The CELLRANGER pipeline also outputs a series of key metrics in text format. These metrics summarize critical information pertaining to the barcoding and sequencing process. The output of this pipeline and the matrices used for the following steps can be provided upon request. Using the aforementioned gene-barcode matrix, secondary analysis was conducted on the samples presented here (“Control1”, “T_R”, “T_R_A”, and Aggr (Control1+T_R+T_R_A)). The matrices were loaded into R (v3.5.1) for the final graphical output of results and statistical analysis. The data set was normalized using a variant on CPM (counts per million) specifically formulated for single-cell data (Lun et al. 2016). The choice of normalization strategy was validated using SCONE (v1.6.1), a data-driven framework for assessing the efficacy of various normalization workflows. We provide the results for unsupervised graph-based clustering using a KNN (K-nearest neighbor) algorithm.

Generation of cellular DNA barcode library (BCLA)

16 nucleotide-based oligonucleotides were generated with defined degenerate region (barcode and library code) and common flanking regions, which were amplified through nested PCR and ligated into pLJM1 ZsGreen lentiviral vector. Barcode library construct was packaged in lentiviruses as follows: BCLA plasmid (6 μ g), psPAX2 (6.0 μ g) and pMD2.G (4.0 μ g) plasmid was transfected into HEK293FT cells using lipofectamine 2000.

The viral suspension obtained after 48 hours was precipitated using PEG-it (System Biosciences) and the pellet was suspended in NSC media, aliquoted and frozen at -80°C. Different human GBM cell lines are transduced with barcoded lentiviral library at low MOI (MOI≤0.3) to uniquely barcode individual GBM cells.

Genomic DNA extraction and PCR amplification

We used Genra Puregene Tissue kit to extract all genomic DNA from our samples. We used NEB UltraQ II polymerase to amplify the 800bp region and the 137bp, which was then visualized on a 3% agarose gel. The primer sequences are in Table 1.

References

1. Stupp, R., Mason, W. P. & Van Den Bent, M. J. Radiotherapy plus concomitant and adjuvant temozolomide for glioblastoma. *N Engl J Med* **352**, 987–996 (2005).
2. Kim, H. *et al.* Whole-genome and multisector exome sequencing of primary and post-treatment glioblastoma reveals patterns of tumor evolution. *Genome Res.* gr.180612.114 (2015). doi:10.1101/gr.180612.114
3. Wainwright, D. A. *et al.* IDO expression in brain tumors increases the recruitment of regulatory T cells and negatively impacts survival. *Clin. Cancer Res.* **18**, 6110–6121 (2012).
4. Zhai, L. *et al.* Infiltrating T Cells Increase IDO1 Expression in Glioblastoma and Contribute to Decreased Patient Survival. *Clin. Cancer Res.* **23**, 6650–6660 (2017).
5. Ladomersky, E. *et al.* IDO1 Inhibition Synergizes with Radiation and PD-1 Blockade to Durably Increase Survival Against Advanced Glioblastoma. *Clin. Cancer Res.* **24**, 2559–2573 (2018).
6. Nolan-Stevaux, O. *et al.* Measurement of Cancer Cell Growth Heterogeneity through Lentiviral Barcoding Identifies Clonal Dominance as a Characteristic of In Vivo Tumor Engraftment. *PLoS ONE* **8**, e67316 (2013).
7. Nguyen, L. V. *et al.* DNA barcoding reveals diverse growth kinetics of human breast tumour subclones in serially passaged xenografts. *Nat Commun* **5**, 5871 (2014).
8. Lan, X. *et al.* Fate mapping of human glioblastoma reveals an invariant stem cell hierarchy. *Nature* **549**, 227–232 (2017).
9. Qazi *et al.* Generation of murine xenograft models of brain tumors from primary human tissue for in vivo analysis of the brain tumor-initiating cell. *Methods Mol. Biol.* **1210**, 37–49 (2014).

CHAPTER 5 FIGURES AND TABLES

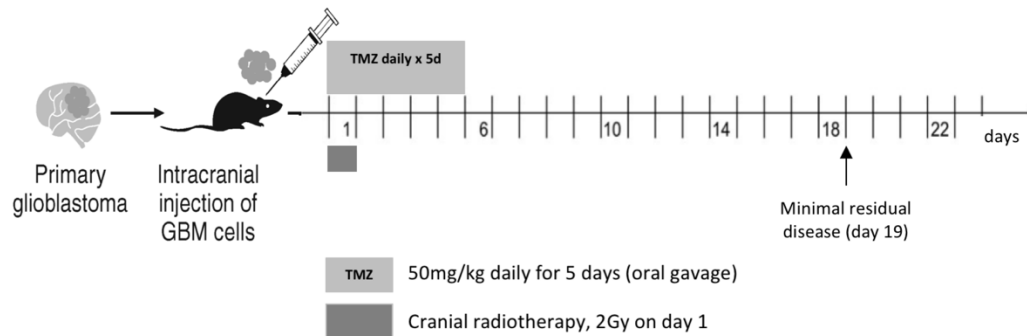


Figure 1: Mouse-adapted chemoradiotherapy protocol for human glioblastoma.

Immunodeficient mice are intracranially engrafted with human GBM cells in the right frontal lobe. Once tumor engrafts and is visible through MRI, chemoradiotherapy is started with 1 dose of 2Gy cranial radiation and 5 days of oral 50mg/kg of temozolomide (chemotherapy). 14 days after the end of chemoradiotherapy, mice are sacrificed or the minimal residual disease time-point.

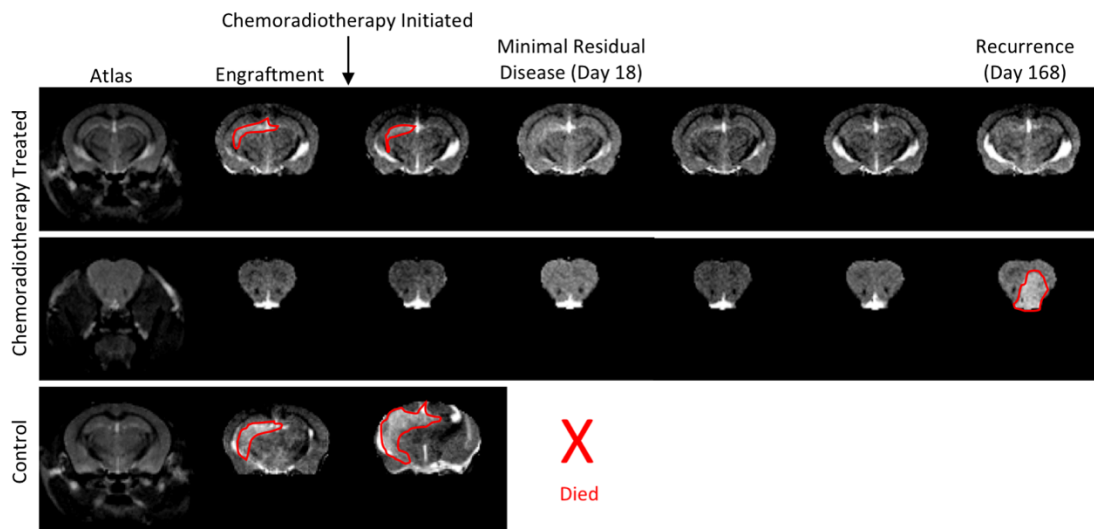


Figure 2: Chemoradiotherapy leads to tumor regression, which eventually relapses locally or distally.

(A) Longitudinal MRI images of a mouse engrafted with barcoded BT428 shows the complete regression of tumor following chemoradiotherapy treatment (row 1). However, eventually the tumor recurs at a distal local to the engraftment site (row 2). Areas in red lines represent the tumor. Row 3 represents a control mouse that succumbed to disease burden before Day 18. Column 1 represents corresponding normal mouse brain atlas images.

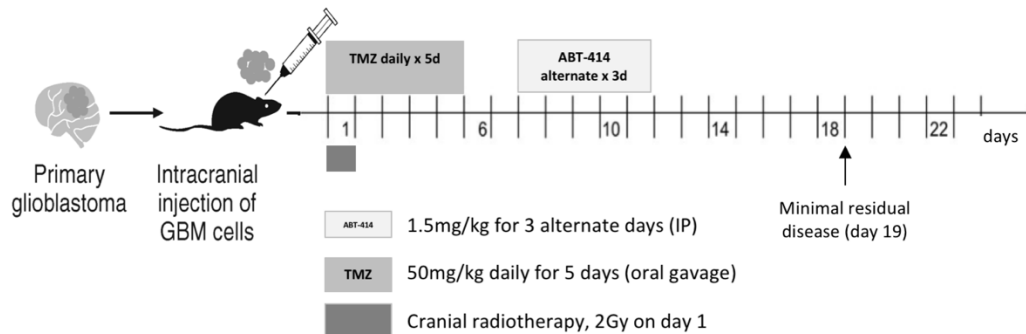


Figure 3: Modified chemoradiotherapy protocol for modelling MBT06 GBM recurrence.

Since the patient was enrolled in a double-blind clinical trial for ABT-414, we incorporated the treatment in our animal model, whereby a cohort of mice received ABT-414 treated in addition to the standard-of-care chemoradiotherapy.

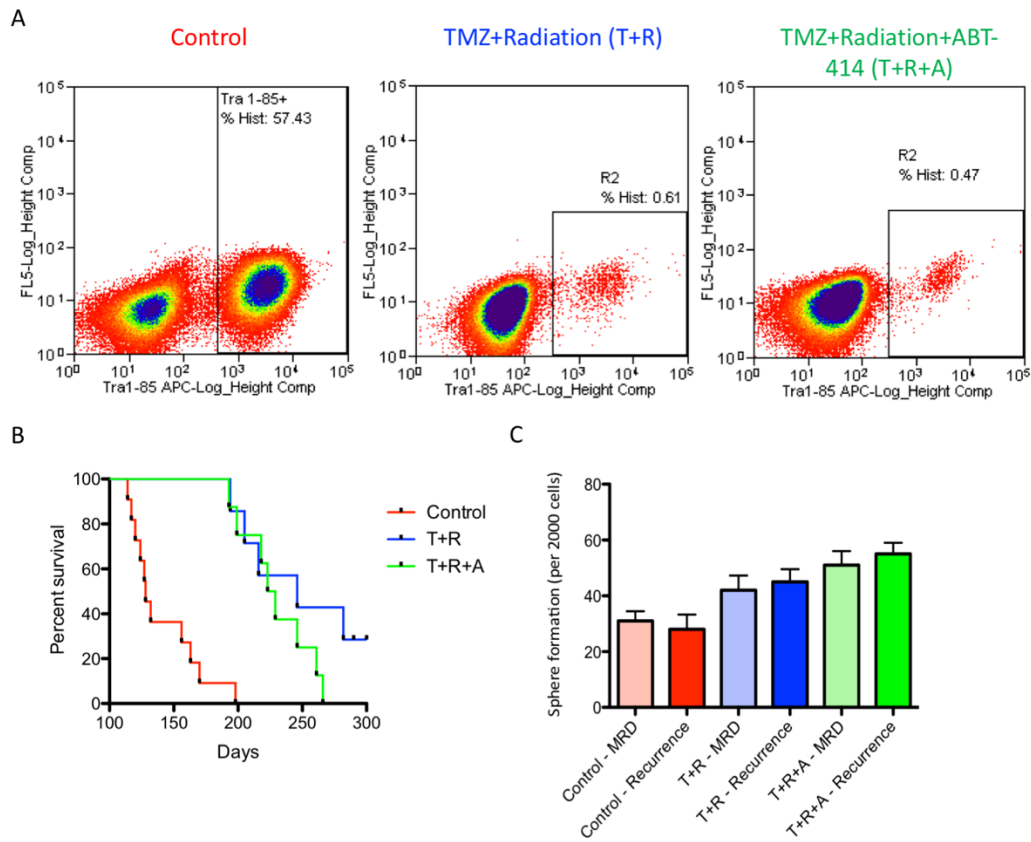


Figure 4: Treatment increases survival but also enriches for glioblastoma stem cell population in MBT06.

(A) Flow cytometry plots showing Tra-1-85+ GBM cell population in brains from control, Soc chemoradiotherapy treated (T_R), or chemoradiotherapy+ABT-414 treated (T_R_A) mice at minimal residual disease. (B) Kaplan Meier curve showing survival of control, T_R and T_R_A treated mice. (C) Sphere formation assay shows increasing self-renewal capacity with treatment at both minimal residual disease (MRD) time point as well as recurrence time point.

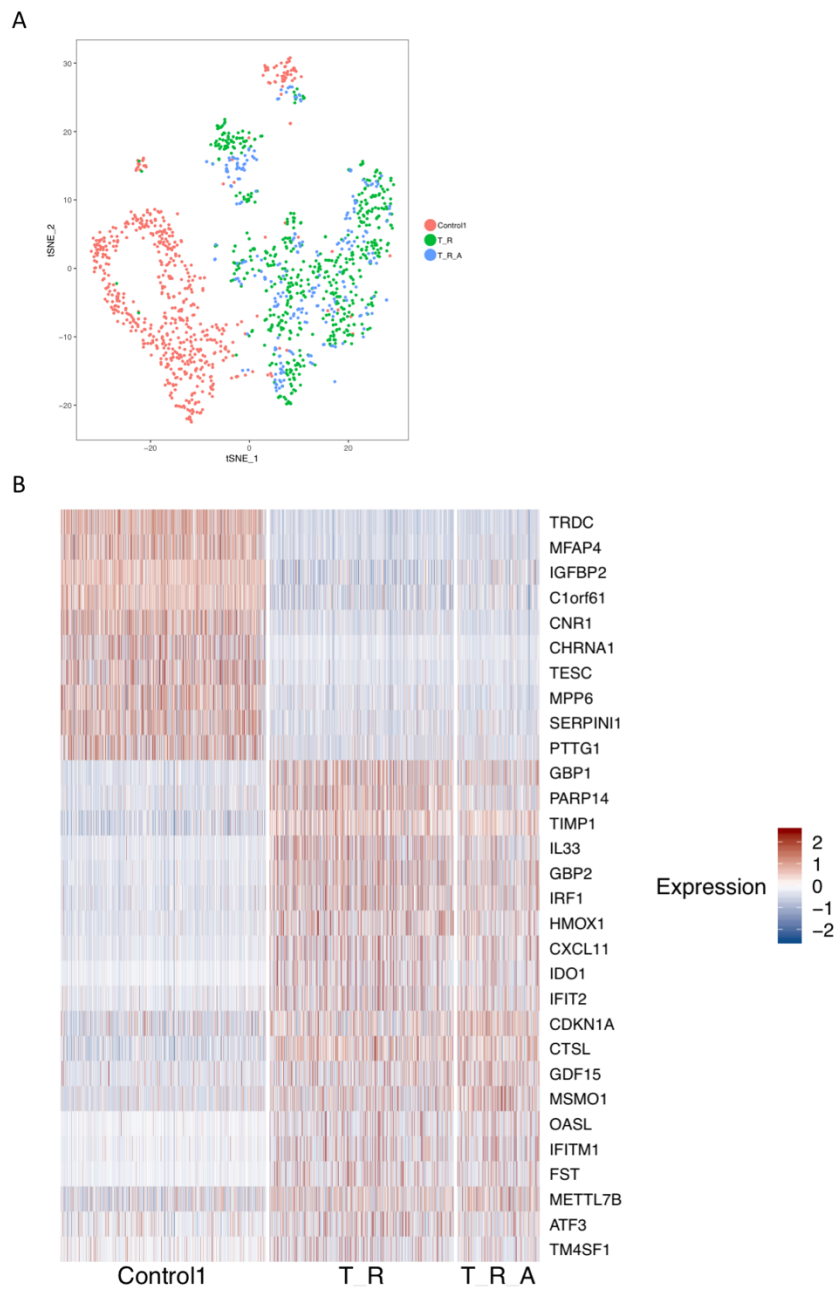


Figure 5: single cell RNA sequencing of MBT06 at MRD shows treatment-dependent changes in gene expression.

(A) tSNE plot showing clustering of single MBT06 GBM cells from control (in red), T_R (chemoradiotherapy; in green) and T_R_A (chemoradiotherapy+ABT-414; in blue) GBM cells isolated at MRD time point. (B) Heat map shows differential expression of top genes between control and treated cells.

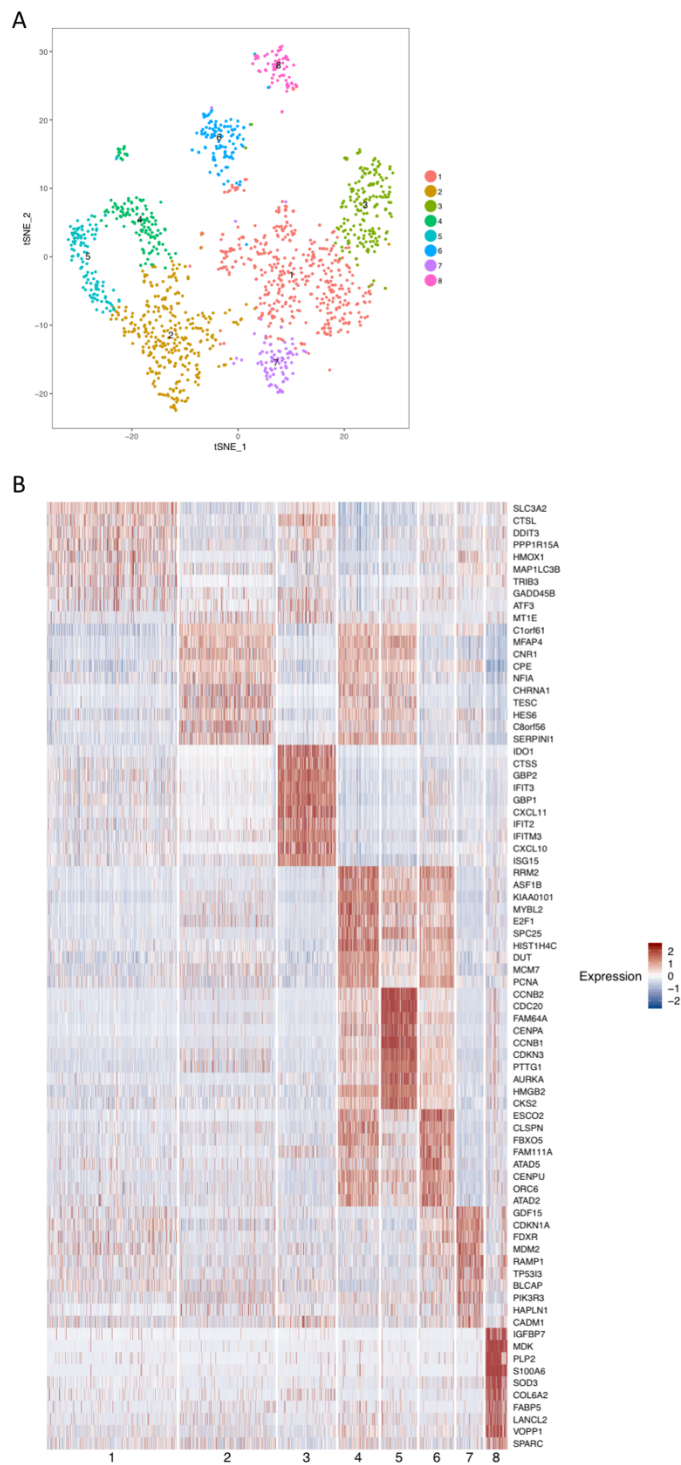


Figure 6: scRNAseq shows control and treated samples can be divided in 8 clusters with differential gene expression profile.

(A) Control and treated MBT06 GBM cells from MRD time point can be clustered in 8 different clusters, shown by different colors. Control cells are majorly represented in clusters 2,4 and 5 while treated cells are represented in clusters 1,3,6 and 7. Cluster 8 represents cells from both control and treated cohorts. (B) Heat map shows the expression of genes that are differentially expressed in each cluster.

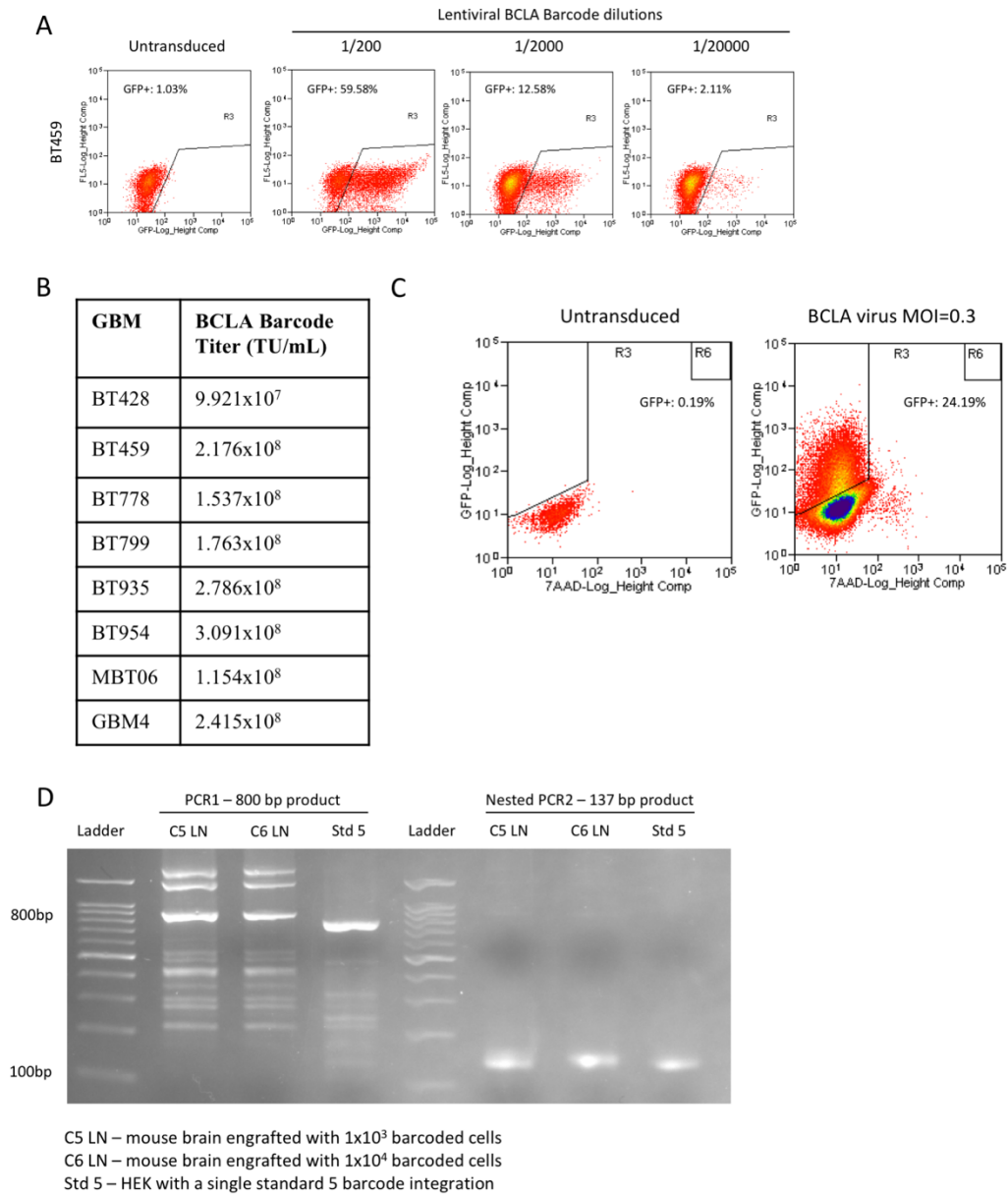


Figure 7: Optimization of cellular DNA barcoding and barcode amplification in primary human GBM cells.

(A) BCLA barcode viral titer was determined in eight different primary GBM cells (BT459 presented here). BCLA barcode viruses were added at dilutions ranging from 200 fold to 20,000 fold and GFP levels assessed using FACS 48 hours post-transduction. (B) BCLA barcode titer for each primary GBM sample. (C) GBM4 single cells were transduced with BCLA barcode viruses at MOI of 0.3. GFP+ cells were sorted 48 hours post transduction using FACS. GFP+ levels were determined to be 24% and cells were replated in neurcult complete media for expansion and subsequent *in vivo* chemoradiotherapy studies. (D) Nested PCR leads to amplification of a 137bp product from genomic DNA extracted from mouse brains engrafted with 1×10^4 or 1×10^5 cells using NEB UltraQ II polymerase. 1000ng of genomic DNA was used in each reaction.

Table 1: Primer sequences for BCLA barcode amplification

Name	Sequence 5'->3'
PCR1 Forward Primer	TCACAGTCTGGGGCATCAAG
PCR1 Reverse Primer	CTGCCAAAACCGCATCACC
PCR2 Forward Primer (with Illumina adapter)	CAAGCAGAAGACGGCATAACGAGAT CGTGATCGA TTAGTGAACGGATCTCGACGGT
PCR2 Reverse Primer	AATGATACGGCGACCACCGAGATCT

CHAPTER 6: Discussion and future directions

6.1 Modelling GBM recurrence

Although advances have been made in the understanding of recurrent GBM biology, the re-sampling of tumour recurrence may encounter problems: risk of infection, risk of neurological deficits and psychological deficits like depression (Barami & Fernandes, 2012; Chang et al., 2003). Therefore, matched recurrent GBM is a rare specimen, as patients do not always undergo additional surgical resections for their relapsed tumor. Therefore, the study GBM recurrence needs the development of models that take patient-derived treatment-naïve primary GBM and create recurrent GBM that have been generated using similar treatment paradigms as applied in the patient. In this work, I have developed an *in vitro* and *in vivo* model of GBM recurrence that employs cancer stem cell paradigms as well as clinically relevant chemoradiotherapy treatment to characterize resistance and disease relapse.

6.1.1 In vitro model of GBM recurrence

Previous studies had explored resistance to radiation (Bao et al., 2006) and chemotherapy (Beier et al., 2012) in GSCs; however, no study had assessed the effect of combined chemoradiotherapy on GBM given that most patient with GBM receive radiotherapy and TMZ treatment. Knowing that GBM presents with ITH and constitutes of multiple subclonal population, it would be safe to assume that different subclonal populations may respond to radiation, chemotherapy and to combined chemoradiotherapy, making it necessary that combinatorial treatments given to patients be studied in concurrence within our model systems as well. I developed our model based on

physiologically and clinically relevant doses of radiation and TMZ (25 μ M in concomitant phase and 50 μ M in adjuvant phase) and treated GSCs derived from primary GBM to assess post-treatment changes to stem cell phenotype (Chapter 2, Figure 2A and B). I found that combined chemoradiotherapy increases expression of known NSC transcription factors Bmi1 and Sox2 and also selects for a CD133-/CD15+ GSC population (Chapter 2, Figure 2C and D, Figure 3A and B). The loss of CD133 and enrichment of CD15 cell surface expression was a surprising yet interesting result as this suggests a difference in the GSC markers in primary vs recurrent GBM. Additionally, we can postulate that although CD133 is an important and well characterized marker of primary GBM, recurrent GBM owing to its evolution through therapy and accumulation of additional mutations may have a shift in GSC hierarchy and CD15 may represent a recurrence initiating GSC populations. In the context of marker loss, we find similar results with loss of EGFR and EGFRvIII in recurrent GBM despite the fact that EGFR represents an important signalling network in primary GBM (Jiguang Wang et al., 2016). Further experimentation to delineate GSC hierarchies in primary and recurrent GBM will allow for more clearer understanding of the role different GSC population play in the progression of the disease. Overall, I have presented our *in vitro* chemoradiotherapy protocol as an easy to employ benchtop model of GBM recurrence which can be used to study mechanisms of therapy resistance and can be combined with *in vitro* testing of novel therapies to ensure relevance to the recurrent GBM biology.

6.1.2 *In vivo* model of GBM recurrence

While *in vitro* models remain valuable for affordable and fast testing of disease mechanisms, solid tumour such as GBM interact extensively with their microenvironment,

which play important role in the tumorigenic profile of the GBM cells. As such, *in vivo* models of GBM are essential to characterize GBM biology in its native microenvironment through xenotransplantation in mouse brains (S. K. Singh et al., 2004). Moreover, a study by Miller et al. has shown that certain mechanisms are only needed for *in vivo* cell survival and may not become apparent in *in vitro* settings. Using an RNA interference platform, they identified GBM dependency on transcriptional elongation regulators which was only required for cell survival in *in vivo* xenografts and not in *in vitro* GSC cultures (Miller et al., 2017). In addition, GBM tumours present regional transcriptomic variations that influence their cellular phenotype and localization of GSCs (Puchalski et al., 2018). These variations can only be investigated in a xenograft model as even with neurosphere-based cell cultures the three-dimensional cell-cell and cell-microenvironment interactions cannot be studied. Moreover, since GBM recurrence can occur locally or distally with distinct evolutionary patterns associated with them, developing a model that is also able to account for and describe spatial recurrence patterns in combination with cellular expression profiling (J. Kim et al., 2015b). Using patient-derived primary GBM cells, I developed an *in vivo* model of GBM recurrence (Chapter 5, Figure 1). In this model, I engrafted GSC enriched primary, treatment naïve GBM cells in mouse brains. Using MRI, I was able to monitor tumour growth and once tumour was visible, I initiated a combined chemoradiotherapy adapted to mouse physiology with 2Gy of cranial irradiation and 50mg/kg of oral TMZ daily for 5 days. Although the treatment would lead to weight loss in mice much like as seen in patient population, the tumour became undetectable on MRI 2 weeks after the end of treatment. At this point the mice also started physically recovering

by gaining weight and had reduction in neurological symptoms as well. We termed this the minimal residual disease state, as it represents when the tumour has been significantly debulked but a very small fraction of treatment-refractory cell population still remains. Eventually, every single mouse that received chemoradiotherapy recurred and using MRI I was also able to determine the spatial pattern of recurrence that were associated with each GBM sample. The robustness of our model also made it amenable to the addition of any treatment modalities as required by the patient such that the exact mechanism of disease recurrence could be modelled in a personalized manner. Therefore, I developed a pre-clinical model of GBM recurrence that combines chemoradiotherapy and can be used to test treatment regimens and identify druggable targets in a patient-specific and personalized manner.

6.2 Targeting the minimal residual disease: a novel therapeutic window to prevent GBM recurrence

An important aspect of our *in vivo* model of GBM recurrence is the ability to profile and characterize the minimal residual disease, a stage that remains elusive to our current diagnostic technologies but nonetheless represents possibly the least heterogeneous stage of the disease progression. Given our ability to monitor tumour growth and regression following chemoradiotherapy using MRI, I was able to identify the MRD timepoint and isolate those cells for further analysis. As expected, at MRD, the number of treatment-refractory cells were very low, ranging between 100-1,000 cells depending on the GBM sample. I next characterized these cells using single cell RNA-sequencing to elucidate the transcriptomic heterogeneity present even at such low cell numbers. Although the data is

still under analysis, we find that MRD samples have a differential gene expression profile as compared to untreated control cells; however, the number of individual subpopulations do not differ between the two groups, suggesting that even at MRD, GBM is able to maintain transcriptomically heterogeneous populations. Nonetheless, MRD gives us a window into finding targets that maybe present clonally and could act as potential targets for therapy development. This would result in a significant shift in how patients with GBM recurrence are currently treated. Given that all patients with GBM experience disease relapse, the treatment of the disease at recurrence would prove as challenging as it has been for primary GBM due to reestablishment of extensive ITH in the recurrent GBM. Through this model, we can identify the transcriptomic composition of the MRD timepoint and predict possible genes/pathways that drive the recurrence and hence target the disease at its root before it has the time to relapse. The concept of a residual disease driving GBM recurrence was recently explored in a study by Spiteri et al. By comparing the genomic profile of the tumour mass to the infiltrating margin cells, the authors found that the cells in the infiltrative margins of the tumour represent the residual disease that then gives rise to the tumour and represents an earlier ancestor during the evolutionary course of the disease progression (Spiteri et al., 2018). Hence, identification and characterization of this unique cellular population through a multi-omics approach will enable researchers to identify targets that could potentially prevent disease relapse or at the least extend time to disease progression and increase overall survival.

Although further analysis of the present data is required, future studies should focus on studying the transcriptomic profile at recurrence as well and identify subclonal populations from the MRD that eventually leads to relapse. These results would also be supported by the use of cellular DNA barcoding that will allow for the interrogation of the subclonal composition at MRD and relate it to the composition at recurrence to identify recurrence-driving clones from the MRD timepoint. Together this data could tease out whether single agent targeting would allow for disease control or whether a multi-targeting approach is required to curb all recurrence-driving subclonal populations in MRD.

6.3 Improving EphA2/EphA3 targeting – developing immunotherapeutic modalities

As EphR represent important markers of GSCs and have therapeutic potential, we wanted to comprehensively profile all EphR in the context of both primary and recurrent GBM (Chapter 3). EphR represent the largest family of tyrosine kinases in human with 14 receptors and multiple ligands (Pasquale, 2008). Using an EphR profiler and CyTOF (CyTOF for EphR profiling is described in this methods article, which I co-authored (Hu et al., 2019)), I identified that EphA2 and EphA3 expression was higher in recurrent GBM as compared to primary GBM and normal NSC and that EphA2 and EphA3 together mark a GSC population in recurrent GBM (Chapter 3, Figure 1). Given the redundancy in the function of the different EphRs and knowing that EphA2 and EphA3 have individually been identified as GSC markers, the discovery that EphA2 and EphA3 together enriched for an even more potent GSC population emphasizes the importance of multi-targeting of GSCs. Through knockdown experiments, I show single knockdowns of EphA2 and EphA3 though reduce tumour burden but the combined knockdown of both EphA2 and EphA3

reduces tumour initiation frequency and significantly prolongs survival (Chapter 3 Figure 4). In fact, in the TCGA glioma database, patients with high expression of both EphA2 and EphA3 had much poorer survival than glioma patients with low expression of both EphA2 and EphA3, further underscoring the important of co-targeting these receptors (Chapter 3, Figure 2).

Having validated EphA2 and EphA3 as potential targets specifically in recurrent GBM, for which there is a lack of therapeutic options, we wanted to design a single agent that could target both receptors simultaneously. Together with our protein engineering team, we designed a bispecific antibody (BsAb) that could co-target EphA2 and EphA3. I discovered that treatment with BsAb leads to loss of cell surface EphA2 and EphA3 expression. The mechanism of action of BsAb seemed to be mediated by phosphorylation and internalization of EphA2 while EphA3 internalization seemed to be mediated by non-phosphorylation mechanisms and takes longer for cell-surface receptor expression. The reduction of tumorigenicity due to BsAb treatment was facilitated by a decrease in the levels of activated Akt and Erk, followed by increased cellular differentiation of GSCs.

While in its current format the BsAb was only able to reduce tumour burden by ~30%, further development of the antibody could result in increased efficacy. In particular, there has been a great interest in the use of chimeric antigen receptor T cells (CAR-T) to target GBM specific antigens and are currently in clinical trials for recurrent GBM (Brown et al., 2016; Johnson et al., 2015). CAR-T cells are engineered T cells that have the ability to bind

to a specific surface exposed tumour antigen against which the CAR is transduced. Upon binding to its antigen, CAR-T cells are activated leading to cytokine release, degranulation of the cytolytic molecules from the cell and T-cell proliferation. This leads to lysis of the antigen expressing tumour cell. The first success of CAR-T for the treatment of cancer was observed for CD19 targeting CAR-T cells in acute lymphoblastic leukemia (ALL) and is the FDA approved treatment for CD19+ B-cell precursor treatment-refractory or relapsed ALL for patients under the age of 25 (Bagley, Desai, Linette, June, & O'Rourke, 2018). This success of the CAR-T led to exploration of the CAR-T modality for the treatment of recurrent GBM and in particular, the targeting of EGFRvIII (Johnson et al., 2015) and IL-13R α 2 (Brown et al., 2016; 2015) using CAR-T has been tested in pre-clinical models of GBM and are now being tested as part of clinical trials for treatment of recurrent GBM. Another important concept that emerged from the use of CAR-T for brain tumour was to test direct intra-tumoural or intracranial delivery of therapeutics given the hurdle of BBB penetration of therapeutics in brain tumour treatment. Study by Brown et al. showed that intracavitary and intraventricular infusions of CAR-T using a catheter could be safely administered to GBM patients. In fact, for multifocal GBM tumours, intraventricular delivery was able to reduce tumour burden in all tumour nodes and could represent an effective mode to treat distally recurring and/or multifocal GBM tumours. Although CAR-T therapy still has challenges such as the presence of the immunosuppressive environment in GBM that may limit CAR-T activity, tumour heterogeneity, and antigen loss, development of a CAR-T that targets both EphA2 and EphA3 using our BsAb as a model could be a big step forward in improving the efficacy of our therapy. Instead of modulating

the downstream tumorigenic mechanisms governed by EphA2 and EphA3, our data shows that EphA2 and EphA3 mark a very tumorigenic GSC population and direct cytotoxicity against EphA2 and EphA3 expressing GSCs using a CAR-T could prove more effective. Recent work by Bielałowicz et al. demonstrated the development of a trivalent CAR-T that could target HER2, IL-13R α 2, and EphA2 simultaneously (Bielałowicz et al., 2018) and a similar approach could also be employed for the development of an EphA2/EphA3 dual targeting CAR-T for recurrent GBM. Interestingly, our data also shows that patients with high EphA2 and EphA3 expression also have high expression of IL-13R α 2 (Chapter 3, Figure 2G), suggesting that these three markers together could represent potent tumorigenic targets in recurrent GBM that when co-targeted could lead to decreased tumour burden and improved patient survival. Altogether our results show that EphA2 and EphA3 should be further explored as important targets of recurrent GBM and the development of more efficacious therapeutic modality, such as a CAR-T, is a possible future direction for this work.

6.4 Immune microenvironment of recurrent GBM

An important aspect of GBM biology that is currently under intense investigation is the immune microenvironment of GBM and how it contributes to tumour malignancy. GBM creates an immunosuppressive environment through the recruitment of tumour-associated macrophages and microglia (TAM), regulatory T cells (Treg) and myeloid derived suppressor cells (MDSC) (Razavi et al., 2016). In turn, these cells allow for immune evasion and promote tumour invasion and growth.

TAM maintain immunosuppression through the release of multiple cytokines such as IL-6, IL-10, prostaglandin E2 (PGE2), and TGF- β to suppress immune effector cells (CTL, NK and DC cells) and promote Treg activity. TGF- β signaling blocks T cell activation and proliferation, and suppresses NK cell activity as well. This is an interesting avenue as study of the recurrent GBM has shown activating mutations in LTBP4, which is a part of the TGF- β , suggesting that the recurrent tumour might be promoting an immune evasive phenotype (Jiguang Wang et al., 2016). At the same time, TAMs also release additional molecules in the tumour microenvironment to promote tumorigenesis such as IL-1 and bFGF. TAM also produce factors such as EGF and VEGF to promote tumour invasion, migration and vascular growth. The role of IL6 in suppressing immune effector cell function and promoting invasion correlates with our observation that high EphA2 and EphA3 expression in glioma patients also corresponds with high IL-6 expression as well (Chapter 3, Figure 2G). This promotes an interesting idea that EphA2 and EphA3 co-expressing cells are not only driving tumorigenesis through self-renewal signaling but might also be producing factors that promote an immunosuppressive environment for the tumour to continue to thrive and proliferate in.

TAM also cause self-polarization towards an M2 phenotype through the expression of CSF-1, TGF- β 1, and IL-10, whereby M2 TAMs can then drive the anti-inflammatory and tumour-promoting microenvironment. CSF-1 signaling serves as an important therapeutic target as researchers have shown that targeting of CSF-1 receptor in GBM led to decrease in M2 phenotype of TAMs, causing an impairment of the tumour-promoting effect and

therefore also led to a reduction in tumour growth(Pyonteck et al., 2013). Additionally, TAMs can produce factors such as pleiotrophin (PTN) that can activate tumorigenic PTPRZ1 signaling in the GSCs and further promoting tumour growth(Shi et al., 2017). At the same time, GBM cells can also influence M2 polarization of TAMs. GSCs have been shown to recruit M2 macrophages through the secretion of periostin (POSTN), an $\alpha V/\beta 3$ or $\alpha V/\beta 5$ integrin ligand, that results in tumour growth (Zhou et al., 2015). Similarly, osteopontin (OPN), another ligand for the $\alpha V/\beta 5$ integrin, also promotes M2 macrophage infiltration into tumour and promote tumour growth(Wei et al., 2019). Interestingly, as with IL-6 expression, POSTN expression was also correlated with EphA2 and EphA3 expression, further supporting the idea that EphA2 and EphA3 expression GSCs may also be modulating the tumour microenvironment towards an immunosuppressive phenotype. Together, this data suggests that the study of immune microenvironment could offer potential therapeutic targets and can be linked with the GBM models we have developed herein.

6.5 Concluding Remarks

In this thesis, I have presented an *in vitro* and *in vivo* model of GBM recurrence that can be used for personalized modeling of therapy resistance and disease relapse. Through these models we can identify new targets for therapeutic development against recurrent GBM and validate new therapies in these models as well. Moreover, the characterization of the MRD stage in disease progression could present novel paradigms for how we currently treat GBM and move to a more potentially preventative approach to disease recurrence. In addition, through the use of novel EphR profiler and GSC model, I also identified EphA2

and EphA3 as therapeutic targets in recurrent GBM. Further studies on the immunotherapeutic modalities and the role of immune microenvironment in conjunction with GSC biology could inform new therapeutic avenues for the treatment of recurrent GBM.

References

- Abdoh, M., Facchino, S., Chatoo, W., Balasingam, V., Ferreira, J., & Bernier, G. (2009). BMI1 sustains human glioblastoma multiforme stem cell renewal. *The Journal of Neuroscience : the Official Journal of the Society for Neuroscience*, 29(28), 8884–8896. <http://doi.org/10.1523/JNEUROSCI.0968-09.2009>
- Aldape, K., Zadeh, G., Mansouri, S., Reifenberger, G., & Deimling, von, A. (2015). Glioblastoma: pathology, molecular mechanisms and markers. *Acta Neuropathologica*, 129(6), 829–848. <http://doi.org/10.1007/s00401-015-1432-1>
- Ameratunga, M., Pavlakis, N., Wheeler, H., Grant, R., Simes, J., & Khasraw, M. (2018). Anti-angiogenic therapy for high-grade glioma. *The Cochrane Database of Systematic Reviews*, 11(26), CD008218. <http://doi.org/10.1002/14651858.CD008218.pub4>
- Bagley, S. J., Desai, A. S., Linette, G. P., June, C. H., & O'Rourke, D. M. (2018). CAR T-cell therapy for glioblastoma: recent clinical advances and future challenges. *Neuro-Oncology*, 20(11), 1429–1438. <http://doi.org/10.1093/neuonc/noy032>
- Bao, S., Wu, Q., Li, Z., Sathornsumetee, S., Wang, H., McLendon, R. E., et al. (2008). Targeting cancer stem cells through L1CAM suppresses glioma growth. *Cancer Research*, 68(15), 6043–6048. <http://doi.org/10.1158/0008-5472.CAN-08-1079>
- Bao, S., Wu, Q., McLendon, R. E., Hao, Y., Shi, Q., Hjelmeland, A. B., et al. (2006). Glioma stem cells promote radioresistance by preferential activation of the DNA damage response. *Nature*, 444(7120), 756–760. <http://doi.org/10.1038/nature05236>
- Barami, K., & Fernandes, R. (2012). Incidence, risk factors and management of delayed

wound dehiscence after craniotomy for tumor resection. *Journal of Clinical Neuroscience : Official Journal of the Neurosurgical Society of Australasia*, 19(6), 854–857. <http://doi.org/10.1016/j.jocn.2011.09.025>

Barnes, J. M., Kaushik, S., Bainer, R. O., Sa, J. K., Woods, E. C., Kai, F., et al. (2018). A tension-mediated glycocalyx-integrin feedback loop promotes mesenchymal-like glioblastoma. *Nature Cell Biology*, 20(10), 1203–1214. <http://doi.org/10.1038/s41556-018-0183-3>

Beier, D., Schriefer, B., Brawanski, K., Hau, P., Weis, J., & Schulz, J. B. (2012). Efficacy of clinically relevant temozolomide dosing schemes in glioblastoma cancer stem cell lines. *Journal of Neuro-Oncology*, 109(1), 45–52. <http://doi.org/10.1007/s11060-012-0878-4>

Beroukhi, R., Getz, G., Nghiemphu, L., Barretina, J., Hsueh, T., Linhart, D., et al. (2007). Assessing the significance of chromosomal aberrations in cancer: methodology and application to glioma. *Proceedings of the National Academy of Sciences of the United States of America*, 104(50), 20007–20012. <http://doi.org/10.1073/pnas.0710052104>

Bielamowicz, K., Fousek, K., Byrd, T. T., Samaha, H., Mukherjee, M., Aware, N., et al. (2018). Trivalent CAR T cells overcome interpatient antigenic variability in glioblastoma. *Neuro-Oncology*, 20(4), 506–518. <http://doi.org/10.1093/neuonc/nox182>

Binda, E., Visioli, A., Giani, F., Lamorte, G., Copetti, M., Pitter, K. L., et al. (2012). The EphA2 Receptor Drives Self-Renewal and Tumorigenicity in Stem-like Tumor-

Propagating Cells from Human Glioblastomas. *Cancer Cell*, 22(6), 765–780.

<http://doi.org/10.1016/j.ccr.2012.11.005>

Bonnet, D., & Dick, J. E. (1997). Human acute myeloid leukemia is organized as a hierarchy that originates from a primitive hematopoietic cell. *Nature Medicine*, 3(7), 730–737.

Bredel, M., Bredel, C., Juric, D., Harsh, G. R., Vogel, H., Recht, L. D., & Sikic, B. I. (2005). High-resolution genome-wide mapping of genetic alterations in human glial brain tumors. *Cancer Research*, 65(10), 4088–4096. <http://doi.org/10.1158/0008-5472.CAN-04-4229>

Brennan, C. W., Verhaak, R. G. W., McKenna, A., Campos, B., Nounshmehr, H., Salama, S. R., et al. (2013). The somatic genomic landscape of glioblastoma. *Cell*, 155(2), 462–477. <http://doi.org/10.1016/j.cell.2013.09.034>

Brown, C. E., Alizadeh, D., Starr, R., Weng, L., Wagner, J. R., Naranjo, A., et al. (2016). Regression of Glioblastoma after Chimeric Antigen Receptor T-Cell Therapy. *New England Journal of Medicine*, 375(26), 2561–2569. <http://doi.org/10.1056/NEJMoa1610497>

Brown, C. E., Badie, B., Barish, M. E., Weng, L., Ostberg, J. R., Chang, W.-C., et al. (2015). Bioactivity and Safety of IL13R α 2-Redirected Chimeric Antigen Receptor CD8⁺ T Cells in Patients with Recurrent Glioblastoma. *Clinical Cancer Research : an Official Journal of the American Association for Cancer Research*, 21(18), 4062–4072. <http://doi.org/10.1158/1078-0432.CCR-15-0428>

Bruggeman, S. W. M., Hulsman, D., Tanger, E., Buckle, T., Blom, M., Zevenhoven, J., et

al. (2007). Bmi1 controls tumor development in an ink4a/Arf-independent manner in a mouse model for glioma. *Cancer Cell*, 12(4), 328–341.

<http://doi.org/10.1016/j.ccr.2007.08.032>

Campos, L. S., Leone, D. P., Relvas, J. B., Brakebusch, C., Fässler, R., Suter, U., & ffrench-Constant, C. (2004). Beta1 integrins activate a MAPK signalling pathway in neural stem cells that contributes to their maintenance. *Development (Cambridge, England)*, 131(14), 3433–3444. <http://doi.org/10.1242/dev.01199>

Carruthers, R. D., Ahmed, S. U., Ramachandran, S., Strathdee, K., Kurian, K. M., Hedley, A., et al. (2018). Replication Stress Drives Constitutive Activation of the DNA Damage Response and Radioresistance in Glioblastoma Stem-like Cells. *Cancer Research*, 78(17), 5060–5071. <http://doi.org/10.1158/0008-5472.CAN-18-0569>

Chakravarti, A., Wang, M., Robins, H. I., Lautenschlaeger, T., Curran, W. J., Brachman, D. G., et al. (2013). RTOG 0211: A Phase 1/2 Study of Radiation Therapy With Concurrent Gefitinib for Newly Diagnosed Glioblastoma Patients. *Radiation Oncology Biology*, 85(5), 1206–1211. <http://doi.org/10.1016/j.ijrobp.2012.10.008>

Chang, S. M., Parney, I. F., McDermott, M., Barker, F. G., Schmidt, M. H., Huang, W., et al. (2003). Perioperative complications and neurological outcomes of first and second craniotomies among patients enrolled in the Glioma Outcome Project. *Journal of Neurosurgery*, 98(6), 1175–1181. <http://doi.org/10.3171/jns.2003.98.6.1175>

Chen, H.-M., Yu, K., Tang, X.-Y., Bao, Z.-S., Jing, T., Fan, X.-L., et al. (2015). Enhanced expression and phosphorylation of the MET oncoprotein by glioma-

specific PTPRZ1–MET fusions. *FEBS Letters*, 589(13), 1437–1443.

<http://doi.org/10.1016/j.febslet.2015.04.032>

Chen, R., Nishimura, M. C., Bumbaca, S. M., Kharbanda, S., Forrest, W. F., Kasman, I. M., et al. (2010). A Hierarchy of Self-Renewing Tumor-Initiating Cell Types in Glioblastoma. *Cancer Cell*, 17(4), 362–375. <http://doi.org/10.1016/j.ccr.2009.12.049>

Chroscinski, D., Sampey, D., Maherali, N., Reproducibility Project: Cancer Biology. (2015). Registered report: tumour vascularization via endothelial differentiation of glioblastoma stem-like cells. *eLife*, 4, 139. <http://doi.org/10.7554/eLife.04363>

Clarke, M. F., & Fuller, M. (2006). Stem Cells and Cancer: Two Faces of Eve. *Cell*, 124(6), 1111–1115. <http://doi.org/10.1016/j.cell.2006.03.011>

Dalerba, P., Cho, R. W., & Clarke, M. F. (2007). Cancer Stem Cells: Models and Concepts. *Annual Review of Medicine*, 58(1), 267–284.

<http://doi.org/10.1146/annurev.med.58.062105.204854>

Day, B. W., Stringer, B. W., & Boyd, A. W. (2014). Eph receptors as therapeutic targets in glioblastoma. *British Journal of Cancer*, 111(7), 1255–1261.

<http://doi.org/10.1038/bjc.2014.73>

Day, B. W., Stringer, B. W., Al-Ejeh, F., Ting, M. J., Wilson, J., Ensbey, K. S., et al. (2013). EphA3 Maintains Tumorigenicity and Is a Therapeutic Target in Glioblastoma Multiforme. *Cancer Cell*, 23(2), 238–248. <http://doi.org/10.1016/j.ccr.2013.01.007>

De Vleeschouwer, S., Fernandes, C., Costa, A., Osório, L., Lago, R. C., Linhares, P., et al. (2017). Current Standards of Care in Glioblastoma Therapy. *Glioblastoma [Internet]*, 197–241. <http://doi.org/10.15586/codon.glioblastoma.2017.ch11>

- Dunn, G. P., Rinne, M. L., Wykosky, J., Genovese, G., Quayle, S. N., Dunn, I. F., et al. (2012). Emerging insights into the molecular and cellular basis of glioblastoma. *Genes & Development*, 26(8), 756–784. <http://doi.org/10.1101/gad.187922.112>
- Favero, F., McGranahan, N., Salm, M., Birkbak, N. J., Sanborn, J. Z., Benz, S. C., et al. (2015). Glioblastoma adaptation traced through decline of an IDH1 clonal driver and macroevolution of a double minute chromosome. *Annals of Oncology : Official Journal of the European Society for Medical Oncology / ESMO*, mdv127. <http://doi.org/10.1093/annonc/mdv127>
- Francis, J. M., Zhang, C.-Z., Maire, C. L., Jung, J., Manzo, V. E., Adalsteinsson, V. A., et al. (2014). EGFR variant heterogeneity in glioblastoma resolved through single-nucleus sequencing. *Cancer Discovery*, 4(8), 956–971. <http://doi.org/10.1158/2159-8290.CD-13-0879>
- Frattini, V., Pagnotta, S. M., Tala, Fan, J. J., Russo, M. V., Lee, S. B., et al. (2018). A metabolic function of FGFR3-TACC3 gene fusions in cancer. *Nature*, 553(7687), 222–227. <http://doi.org/10.1038/nature25171>
- Frattini, V., Trifonov, V., Chan, J. M., Castano, A., Lia, M., Abate, F., et al. (2013). The integrated landscape of driver genomic alterations in glioblastoma. *Nature Genetics*, 45(10), 1141–1149. <http://doi.org/10.1038/ng.2734>
- Freije, W. A., Castro-Vargas, F. E., Fang, Z., Horvath, S., Cloughesy, T., Liau, L. M., et al. (2004). Gene Expression Profiling of Gliomas Strongly Predicts Survival. *Cancer Research*, 64(18), 6503–6510. <http://doi.org/10.1158/0008-5472.CAN-04-0452>
- Galli, R., Binda, E., Orfanelli, U., Cipelletti, B., Gritti, A., De Vitis, S., et al. (2004).

Isolation and characterization of tumorigenic, stem-like neural precursors from human glioblastoma. *Cancer Research*, 64(19), 7011–7021.

<http://doi.org/10.1158/0008-5472.CAN-04-1364>

Hau, P., Proescholdt, M., Lohmeier, A., Wischhusen, J., Oefner, P. J., Aigner, L., et al.

(2007). CD133+ and CD133- Glioblastoma-Derived Cancer Stem Cells Show Differential Growth Characteristics and Molecular Profiles. *Cancer Research*, 67(9), 4010–4015. <http://doi.org/10.1158/0008-5472.CAN-06-4180>

Hegi, M. E., Diserens, A.-C., Gorlia, T., Hamou, M.-F., de Tribolet, N., Weller, M., et al.

(2005). MGMT gene silencing and benefit from temozolomide in glioblastoma. *New England Journal of Medicine*, 352(10), 997–1003.

<http://doi.org/10.1056/NEJMoa043331>

Hemmati, H. D., Nakano, I., Lazareff, J. A., Masterman-Smith, M., Geschwind, D. H.,

Bronner-Fraser, M., & Kornblum, H. I. (2003). Cancerous stem cells can arise from pediatric brain tumors. *Proceedings of the National Academy of Sciences of the United States of America*, 100(25), 15178–15183.

<http://doi.org/10.1073/pnas.2036535100>

Hu, A. X., Adams, J. J., Vora, P., Qazi, Singh, S. K., Moffat, J., & Sidhu, S. S. (2019).

EPH Profiling of BTIC Populations in Glioblastoma Multiforme Using CyTOF. *Methods in Molecular Biology (Clifton, N.J.)*, 1869(6859), 155–168.

http://doi.org/10.1007/978-1-4939-8805-1_14

Hunter, C., Smith, R., Cahill, D. P., Stephens, P., Stevens, C., Teague, J., et al. (2006). A

hypermethylation phenotype and somatic MSH6 mutations in recurrent human

- malignant gliomas after alkylator chemotherapy. *Cancer Research*, 66(8), 3987–3991. <http://doi.org/10.1158/0008-5472.CAN-06-0127>
- Jin, X., Kim, L. J. Y., Wu, Q., Wallace, L. C., Prager, B. C., Sanvoranart, T., et al. (2017). Targeting glioma stem cells through combined BMI1 and EZH2 inhibition. *Nature Medicine*, 23(11), 1352–1361. <http://doi.org/10.1038/nm.4415>
- Johnson, L. A., Scholler, J., Ohkuri, T., Kosaka, A., Patel, P. R., McGettigan, S. E., et al. (2015). Rational development and characterization of humanized anti-EGFR variant III chimeric antigen receptor T cells for glioblastoma. *Science Translational Medicine*, 7(275), 275ra22–275ra22. <http://doi.org/10.1126/scitranslmed.aaa4963>
- Kim, H., Zheng, S., Amini, S. S., Virk, S. M., Mikkelsen, T., Brat, D. J., et al. (2015a). Whole-genome and multisector exome sequencing of primary and post-treatment glioblastoma reveals patterns of tumor evolution. *Genome Research*, gr.180612.114. <http://doi.org/10.1101/gr.180612.114>
- Kim, J., Lee, I.-H., Cho, H. J., Park, C.-K., Jung, Y.-S., Kim, Y., et al. (2015b). Spatiotemporal Evolution of the Primary Glioblastoma Genome. *Cancer Cell*, 28(3), 318–328. <http://doi.org/10.1016/j.ccell.2015.07.013>
- Kim, S.-H., Joshi, K., Ezhilarasan, R., Myers, T. R., Siu, J., Gu, C., et al. (2015c). EZH2 Protects Glioma Stem Cells from Radiation-Induced Cell Death in a MELK/FOXM1-Dependent Manner. *Stem Cell Reports*. <http://doi.org/10.1016/j.stemcr.2014.12.006>
- Klein, R., & Kania, A. (2014). Ephrin signalling in the developing nervous system. *Current Opinion in Neurobiology*, 27C, 16–24. <http://doi.org/10.1016/j.conb.2014.02.006>

- Klughammer, J., Kiesel, B., Roetzer, T., Fortelny, N., Nemc, A., Nenning, K.-H., et al. (2018). The DNA methylation landscape of glioblastoma disease progression shows extensive heterogeneity in time and space. *Nature Medicine*, 24(10), 1611–1624. <http://doi.org/10.1038/s41591-018-0156-x>
- Kotliarov, Y., Steed, M. E., Christopher, N., Walling, J., Su, Q., Center, A., et al. (2006). High-resolution global genomic survey of 178 gliomas reveals novel regions of copy number alteration and allelic imbalances. *Cancer Research*, 66(19), 9428–9436. <http://doi.org/10.1158/0008-5472.CAN-06-1691>
- Lathia, J. D., Gallagher, J., Heddleston, J. M., Wang, J., Eyler, C. E., Macswords, J., et al. (2010). Integrin alpha 6 regulates glioblastoma stem cells. *Cell Stem Cell*, 6(5), 421–432. <http://doi.org/10.1016/j.stem.2010.02.018>
- Lathia, J. D., Patton, B., Eckley, D. M., Magnus, T., Mughal, M. R., Sasaki, T., et al. (2007). Patterns of laminins and integrins in the embryonic ventricular zone of the CNS. *The Journal of Comparative Neurology*, 505(6), 630–643. <http://doi.org/10.1002/cne.21520>
- Lee, J. H., Lee, J. E., Kahng, J. Y., Kim, S. H., Park, J. S., Yoon, S. J., et al. (2018). Human glioblastoma arises from subventricular zone cells with low-level driver mutations. *Nature*, 560(7717), 243–247. <http://doi.org/10.1038/s41586-018-0389-3>
- Lee, J.-K., Wang, J., Sa, J. K., Ladewig, E., Lee, H.-O., Lee, I.-H., et al. (2017). Spatiotemporal genomic architecture informs precision oncology in glioblastoma. *Nature Genetics*, 54, 3988. <http://doi.org/10.1038/ng.3806>
- Leone, D. P., Relvas, J. B., Campos, L. S., Hemmi, S., Brakebusch, C., Fässler, R., et al.

- (2005). Regulation of neural progenitor proliferation and survival by beta1 integrins. *Journal of Cell Science*, 118(Pt 12), 2589–2599. <http://doi.org/10.1242/jcs.02396>
- Li, Z., Bao, S., Wu, Q., Wang, H., Eyler, C., Sathornsumetee, S., et al. (2009). Hypoxia-inducible factors regulate tumorigenic capacity of glioma stem cells. *Cancer Cell*, 15(6), 501–513. <http://doi.org/10.1016/j.ccr.2009.03.018>
- Liu, G., Yuan, X., Zeng, Z., Tunici, P., Ng, H., Abdulkadir, I. R., et al. (2006). **Analysis of gene expression and chemoresistance of CD133+ cancer stem cells in glioblastoma**. *Molecular Cancer*, 5(1), 67. <http://doi.org/10.1186/1476-4598-5-67>
- Louis, D. N., Perry, A., Reifenberger, G., Deimling, von, A., Figarella-Branger, D., Cavenee, W. K., et al. (2016). The 2016 World Health Organization Classification of Tumors of the Central Nervous System: a summary. *Acta Neuropathologica*, 131(6), 803–820. <http://doi.org/10.1007/s00401-016-1545-1>
- Mak, A. B., Nixon, A. M. L., Kittanakom, S., Stewart, J. M., Chen, G. I., Curak, J., et al. (2012). Regulation of CD133 by HDAC6 Promotes β -Catenin Signaling to Suppress Cancer Cell Differentiation. *Cell Reports*, 2(4), 951–963. <http://doi.org/10.1016/j.celrep.2012.09.016>
- Man, J., Yu, X., Huang, H., Zhou, W., Xiang, C., Huang, H., et al. (2018). Hypoxic Induction of Vasorin Regulates Notch1 Turnover to Maintain Glioma Stem-like Cells. *Cell Stem Cell*, 22(1), 104–118.e6. <http://doi.org/10.1016/j.stem.2017.10.005>
- Manoranjan, B., Wang, X., Hallett, R. M., Venugopal, C., Mack, S. C., McFarlane, N., et al. (2013). FoxG1 Interacts with Bmi1 to Regulate Self-Renewal and Tumorigenicity

of Medulloblastoma Stem Cells. *Stem Cells*, 31(7), 1266–1277.

<http://doi.org/10.1002/stem.1401>

McLendon, R., Friedman, A., Bigner, D., Van Meir, E. G., Brat, D. J., M Mastrogiannis, G., et al. (2008). Comprehensive genomic characterization defines human glioblastoma genes and core pathways. *Nature*, 455(7216), 1061–1068.

<http://doi.org/10.1038/nature07385>

Merlos-Suárez, A., & Batlle, E. (2008). Eph–ephrin signalling in adult tissues and cancer. *Current Opinion in Cell Biology*, 20(2), 194–200.

<http://doi.org/10.1016/j.ceb.2008.01.011>

Meyer, M., Reimand, J., Lan, X., Head, R., Zhu, X., Kushida, M., et al. (2015). Single cell-derived clonal analysis of human glioblastoma links functional and genomic heterogeneity. *Proceedings of the National Academy of Sciences of the United States of America*, 201320611. <http://doi.org/10.1073/pnas.1320611111>

Miao, H., Gale, N. W., Guo, H., Qian, J., Petty, A., Kaspar, J., et al. (2014). EphA2 promotes infiltrative invasion of glioma stem cells in vivo through cross-talk with Akt and regulates stem cell properties. *Oncogene*.

<http://doi.org/10.1038/onc.2013.590>

Miao, H., Li, D.-Q., Mukherjee, A., Guo, H., Petty, A., Cutter, J., et al. (2009). EphA2 Mediates Ligand-Dependent Inhibition and Ligand-Independent Promotion of Cell Migration and Invasion via a Reciprocal Regulatory Loop with Akt. *Cancer Cell*, 16(1), 9–20. <http://doi.org/10.1016/j.ccr.2009.04.009>

Miller, T. E., Liao, B. B., Wallace, L. C., Morton, A. R., Xie, Q., Dixit, D., et al. (2017).

- Transcription elongation factors represent in vivo cancer dependencies in glioblastoma. *Nature*, 547(7663), 355–359. <http://doi.org/10.1038/nature23000>
- Mischel, P. S., Shai, R., Shi, T., Horvath, S., Lu, K. V., Choe, G., et al. (2003). Identification of molecular subtypes of glioblastoma by gene expression profiling. *Oncogene*, 22(15), 2361–2373. <http://doi.org/10.1038/sj.onc.1206344>
- Molofsky, A. V., He, S., Bydon, M., Morrison, S. J., & Pardal, R. (2005). Bmi-1 promotes neural stem cell self-renewal and neural development but not mouse growth and survival by repressing the p16Ink4a and p19Arf senescence pathways. *Genes & Development*, 19(12), 1432–1437. <http://doi.org/10.1101/gad.1299505>
- Muscat, A. M., Wong, N. C., Drummond, K. J., Algar, E. M., Khasraw, M., Verhaak, R., et al. (2018). The evolutionary pattern of mutations in glioblastoma reveals therapy-mediated selection. *Oncotarget*, 9(8), 7844–7858. <http://doi.org/10.18632/oncotarget.23541>
- Nutt, C. L., Mani, D. R., Betensky, R. A., Tamayo, P., Cairncross, J. G., Ladd, C., et al. (2003). Gene Expression-based Classification of Malignant Gliomas Correlates Better with Survival than Histological Classification. *Cancer Research*, 63(7), 1602–1607. <http://doi.org/10.1002/ana.410230408>
- Ohgaki, H., & Kleihues, P. (2013). The definition of primary and secondary glioblastoma. *Clinical Cancer Research : an Official Journal of the American Association for Cancer Research*, 19(4), 764–772. <http://doi.org/10.1158/1078-0432.CCR-12-3002>
- Ostrom, Q. T., Gittleman, H., Xu, J., Kromer, C., Wolinsky, Y., Kruchko, C., & Barnholtz-Sloan, J. S. (2016). CBTRUS Statistical Report: Primary Brain and Other

Central Nervous System Tumors Diagnosed in the United States in 2009-2013.

Neuro-Oncology, 18(suppl_5), v1–v75. <http://doi.org/10.1093/neuonc/now207>

Pallini, R., Ricci-Vitiani, L., Banna, G. L., Signore, M., Lombardi, D., Todaro, M., et al.

(2008). Cancer stem cell analysis and clinical outcome in patients with glioblastoma

multiforme. *Clinical Cancer Research : an Official Journal of the American*

Association for Cancer Research, 14(24), 8205–8212. <http://doi.org/10.1158/1078->

0432.CCR-08-0644

Parker, J. J., Canoll, P., Niswander, L., Kleinschmidt-DeMasters, B. K., Foshay, K., &

Waziri, A. (2018). Intratumoral heterogeneity of endogenous tumor cell invasive

behavior in human glioblastoma. *Scientific Reports*, 8(1), 18002.

<http://doi.org/10.1038/s41598-018-36280-9>

Parker, N. R., Hudson, A. L., Khong, P., Parkinson, J. F., Dwight, T., Ikin, R. J., et al.

(2016). Intratumoral heterogeneity identified at the epigenetic, genetic and

transcriptional level in glioblastoma. *Scientific Reports*, 6(1), 22477.

<http://doi.org/10.1038/srep22477>

Parsons, D. W., Jones, S., Zhang, X., Lin, J. C. H., Leary, R. J., Angenendt, P., et al.

(2008). An Integrated Genomic Analysis of Human Glioblastoma Multiforme.

Science, 321(5897), 1807–1812. <http://doi.org/10.1126/science.1164382>

Pasquale, E. B. (2008). Eph-Ephrin Bidirectional Signaling in Physiology and Disease.

Cell, 133(1), 38–52. <http://doi.org/10.1016/j.cell.2008.03.011>

Patel, A. P., Tirosh, I., Trombetta, J. J., Shalek, A. K., Gillespie, S. M., Wakimoto, H., et

al. (2014). Single-cell RNA-seq highlights intratumoral heterogeneity in primary

glioblastoma. *Science*, 344(6190), 1396–1401.

<http://doi.org/10.1126/science.1254257>

Peereboom, D. M., Shepard, D. R., Ahluwalia, M. S., Brewer, C. J., Agarwal, N., Stevens, G. H. J., et al. (2010). Phase II trial of erlotinib with temozolomide and radiation in patients with newly diagnosed glioblastoma multiforme. *Journal of Neuro-Oncology*, 98(1), 93–99. <http://doi.org/10.1007/s11060-009-0067-2>

Phillips, A. C., Boghaert, E. R., Vaidya, K. S., Mitten, M. J., Norvell, S., Falls, H. D., et al. (2016). ABT-414, an Antibody-Drug Conjugate Targeting a Tumor-Selective EGFR Epitope. *Molecular Cancer Therapeutics*, 15(4), 661–669.

<http://doi.org/10.1158/1535-7163.MCT-15-0901>

Phillips, H. S., Kharbanda, S., Chen, R., Forrest, W. F., Soriano, R. H., Wu, T. D., et al. (2006). Molecular subclasses of high-grade glioma predict prognosis, delineate a pattern of disease progression, and resemble stages in neurogenesis. *Cancer Cell*, 9(3), 157–173. <http://doi.org/10.1016/j.ccr.2006.02.019>

Puchalski, R. B., Shah, N., Miller, J., Dalley, R., Nomura, S. R., Yoon, J.-G., et al. (2018). An anatomic transcriptional atlas of human glioblastoma. *Science*, 360(6389), 660–663. <http://doi.org/10.1126/science.aaf2666>

Pyonteck, S. M., Akkari, L., Schuhmacher, A. J., Bowman, R. L., Sevenich, L., Quail, D. F., et al. (2013). CSF-1R inhibition alters macrophage polarization and blocks glioma progression. *Nature Medicine*, 19(10), 1264–1272. <http://doi.org/10.1038/nm.3337>

Quail, D. F., Bowman, R. L., Akkari, L., Quick, M. L., Schuhmacher, A. J., Huse, J. T., et al. (2016). The tumor microenvironment underlies acquired resistance to CSF-1R

inhibition in gliomas. *Science*, 352(6288), aad3018–aad3018.

<http://doi.org/10.1126/science.aad3018>

Raizer, J. J., Abrey, L. E., Lassman, A. B., Chang, S. M., Lamborn, K. R., Kuhn, J. G., et al. (2010). A phase I trial of erlotinib in patients with nonprogressive glioblastoma multiforme postradiation therapy, and recurrent malignant gliomas and meningiomas. *Neuro-Oncology*, 12(1), 87–94. <http://doi.org/10.1093/neuonc/nop017>

Razavi, S.-M., Lee, K. E., Jin, B. E., Aujla, P. S., Gholamin, S., & Li, G. (2016). Immune Evasion Strategies of Glioblastoma. *Frontiers in Surgery*, 3(32), 11.

<http://doi.org/10.3389/fsurg.2016.00011>

Reardon, D. A., Lassman, A. B., van den Bent, M., Kumthekar, P., Merrell, R., Scott, A. M., et al. (2017). Efficacy and safety results of ABT-414 in combination with radiation and temozolomide in newly diagnosed glioblastoma. *Neuro-Oncology*, 19(7), 965–975. <http://doi.org/10.1093/neuonc/now257>

Reinartz, R., Wang, S., Kebir, S., Silver, D. J., Wieland, A., Zheng, T., et al. (2016). Functional Subclone Profiling for Prediction of Treatment-Induced Intratumor Population Shifts and Discovery of Rational Drug Combinations in Human Glioblastoma. *Clinical Cancer Research : an Official Journal of the American Association for Cancer Research*. <http://doi.org/10.1158/1078-0432.CCR-15-2089>

Reynolds, B. A., & Weiss, S. (1992). Generation of Neurons and Astrocytes from Isolated Cells of the Adult Mammalian Central Nervous System. *Science*, 255(5052), 1707–1710. <http://doi.org/10.2307/2876641?ref=no-x-route:f716eeb137643a6f720ba7b526c7a09c>

Ricci-Vitiani, L., Pallini, R., Biffoni, M., Todaro, M., Invernici, G., Cenci, T., et al.

(2010). Tumour vascularization via endothelial differentiation of glioblastoma stem-like cells. *Nature*, *468*(7325), 824–828. <http://doi.org/10.1038/nature09557>

Sanai, N., Polley, M.-Y., McDermott, M. W., Parsa, A. T., & Berger, M. S. (2011). An extent of resection threshold for newly diagnosed glioblastomas. *Journal of Neurosurgery*, *115*(1), 3–8. <http://doi.org/10.3171/2011.7.JNS10238>

Shah, N., Lankerovich, M., Lee, H., Yoon, J.-G., Schroeder, B., & Foltz, G. (2013).

Exploration of the gene fusion landscape of glioblastoma using transcriptome sequencing and copy number data. *BMC Genomics*, *14*(1), 818.

<http://doi.org/10.1186/1471-2164-14-818>

Shi, Y., Ping, Y.-F., Zhou, W., He, Z.-C., Chen, C., Bian, B.-S.-J., et al. (2017). Tumour-

associated macrophages secrete pleiotrophin to promote PTPRZ1 signalling in glioblastoma stem cells for tumour growth. *Nature Communications*, *8*, 15080.

<http://doi.org/10.1038/ncomms15080>

Singh, D., Chan, J. M., Pietro Zoppoli, Niola, F., Sullivan, R., Castano, A., et al. (2012).

Transforming Fusions of FGFR and TACC Genes in Human Glioblastoma. *Science*, *337*(6099), 1231–1235. <http://doi.org/10.1126/science.1220834>

Singh, S. K. (2003). Identification of a Cancer Stem Cell in Human Brain Tumors.

Cancer Research, 1–9.

Singh, S. K., Clarke, I. D., Terasaki, M., Bonn, V. E., Hawkins, C., Squire, J., & Dirks, P.

B. (2003). Identification of a cancer stem cell in human brain tumors. *Cancer Research*, *63*(18), 5821–5828.

- Singh, S. K., Hawkins, C., Clarke, I. D., Squire, J. A., Bayani, J., Hide, T., et al. (2004). Identification of human brain tumour initiating cells. *Nature*, *432*(7015), 396–401. <http://doi.org/10.1038/nature03128>
- Snuderl, M., Fasllollahi, L., Le, L. P., Nitta, M., Zhelyazkova, B. H., Davidson, C. J., et al. (2011). Mosaic Amplification of Multiple Receptor Tyrosine Kinase Genes in Glioblastoma. *Cancer Cell*, *20*(6), 810–817. <http://doi.org/10.1016/j.ccr.2011.11.005>
- Soda, Y., Marumoto, T., Friedmann-Morvinski, D., Soda, M., Liu, F., Michiue, H., et al. (2011). Transdifferentiation of glioblastoma cells into vascular endothelial cells. *Proceedings of the National Academy of Sciences of the United States of America*, *108*(11), 4274–4280. <http://doi.org/10.1073/pnas.1016030108>
- Son, M. J., Woolard, K., Nam, D.-H., Lee, J., & Fine, H. A. (2009). SSEA-1 is an enrichment marker for tumor-initiating cells in human glioblastoma. *Cell Stem Cell*, *4*(5), 440–452. <http://doi.org/10.1016/j.stem.2009.03.003>
- Song, W.-S., Yang, Y.-P., Huang, C.-S., Lu, K.-H., Liu, W.-H., Wu, W.-W., et al. (2016). Sox2, a stemness gene, regulates tumor-initiating and drug-resistant properties in CD133-positive glioblastoma stem cells. *Journal of the Chinese Medical Association : JCMA*, *79*(10), 538–545. <http://doi.org/10.1016/j.jcma.2016.03.010>
- Sottoriva, A., Spiteri, I., Piccirillo, S. G. M., Touloumis, A., Collins, V. P., Marioni, J. C., et al. (2013). Intratumor heterogeneity in human glioblastoma reflects cancer evolutionary dynamics. *Proceedings of the National Academy of Sciences of the United States of America*, *110*(10), 4009–4014. <http://doi.org/10.1073/pnas.1219747110>

Spiteri, I., Caravagna, G., Cresswell, G. D., Vatsiou, A., Nichol, D., Acar, A., et al.

(2018). Evolutionary dynamics of residual disease in human glioblastoma. *Annals of Oncology : Official Journal of the European Society for Medical Oncology / ESMO*.

<http://doi.org/10.1093/annonc/mdy506>

Stommel, J. M., Kimmelman, A. C., Ying, H., Nabioullin, R., Ponugoti, A. H.,

Wiedemeyer, R., et al. (2007). Coactivation of receptor tyrosine kinases affects the response of tumor cells to targeted therapies. *Science*, 318(5848), 287–290.

<http://doi.org/10.1126/science.1142946>

Stummer, W., Pichlmeier, U., Meinel, T., Wiestler, O. D., Zanella, F., Reulen, H.-J.,

ALA-Glioma Study Group. (2006). Fluorescence-guided surgery with 5-aminolevulinic acid for resection of malignant glioma: a randomised controlled multicentre phase III trial. *Lancet Oncology*, 7(5), 392–401.

[http://doi.org/10.1016/S1470-2045\(06\)70665-9](http://doi.org/10.1016/S1470-2045(06)70665-9)

Stupp, R., Mason, W. P., & Van Den Bent, M. J. (2005). Radiotherapy plus concomitant

and adjuvant temozolomide for glioblastoma. *New England Journal of Medicine*, 352(10), 987–996. <http://doi.org/10.1056/NEJMoa043330>

Suva, M. L., Rheinbay, E., Gillespie, S. M., Patel, A. P., Wakimoto, H., Rabkin, S. D., et

al. (2014). Reconstructing and reprogramming the tumor-propagating potential of glioblastoma stem-like cells. *Cell*, 157(3), 580–594.

<http://doi.org/10.1016/j.cell.2014.02.030>

Szerlip, N. J., Pedraza, A., & Chakravarty, D. (2012). Intratumoral heterogeneity of

receptor tyrosine kinases EGFR and PDGFRA amplification in glioblastoma defines

subpopulations with distinct growth factor response. Presented at the Proceedings of the

Uchida, N., Buck, D. W., He, D., Reitsma, M. J., Masek, M., Phan, T. V., et al. (2000).

Direct isolation of human central nervous system stem cells. *Proceedings of the National Academy of Sciences of the United States of America*, 97(26), 14720–14725.

<http://doi.org/10.1073/pnas.97.26.14720>

Uhm, J. H., Ballman, K. V., Wu, W., Giannini, C., Krauss, J. C., Buckner, J. C., et al.

(2011). Phase II evaluation of gefitinib in patients with newly diagnosed Grade 4 astrocytoma: Mayo/North Central Cancer Treatment Group Study N0074.

International Journal of Radiation Oncology, Biology, Physics, 80(2), 347–353.

<http://doi.org/10.1016/j.ijrobp.2010.01.070>

van den Bent, M., Gan, H. K., Lassman, A. B., Kumthekar, P., Merrell, R., Butowski, N.,

et al. (2017). Efficacy of depatuxizumab mafodotin (ABT-414) monotherapy in patients with EGFR-amplified, recurrent glioblastoma: results from a multi-center, international study. *Cancer Chemotherapy and Pharmacology*, 80(6), 1209–1217.

<http://doi.org/10.1007/s00280-017-3451-1>

van Thuijl, H. F., Mazor, T., Johnson, B. E., Fouse, S. D., Aihara, K., Hong, C., et al.

(2015). Evolution of DNA repair defects during malignant progression of low-grade gliomas after temozolomide treatment. *Acta Neuropathologica*.

<http://doi.org/10.1007/s00401-015-1403-6>

Venugopal, C., Hallett, R., Vora, P., Manoranjan, B., Mahendram, S., Qazi, et al. (2015).

Pyrvinium targets CD133 in human glioblastoma brain tumor-initiating cells. *Clinical*

- Cancer Research : an Official Journal of the American Association for Cancer Research*, clincanres.3147.2014. <http://doi.org/10.1158/1078-0432.CCR-14-3147>
- Verhaak, R. G. W., Hoadley, K. A., Purdom, E., Wang, V., Qi, Y., Wilkerson, M. D., et al. (2010). Integrated genomic analysis identifies clinically relevant subtypes of glioblastoma characterized by abnormalities in PDGFRA, IDH1, EGFR, and NF1. *Cancer Cell*, 17(1), 98–110. <http://doi.org/10.1016/j.ccr.2009.12.020>
- Walker, E. V., Davis, F. G., CBTR founding affiliates. (2019). Malignant primary brain and other central nervous system tumors diagnosed in Canada from 2009 to 2013. *Neuro-Oncology*. <http://doi.org/10.1093/neuonc/noy195>
- Wang, Jialiang, Wakeman, T. P., Lathia, J. D., Hjelmeland, A. B., Wang, X.-F., White, R. R., et al. (2010a). Notch promotes radioresistance of glioma stem cells. *Stem Cells*, 28(1), 17–28. <http://doi.org/10.1002/stem.261>
- Wang, Jiguang, Cazzato, E., Ladewig, E., Frattini, V., Rosenbloom, D. I. S., Zairis, S., et al. (2016). Clonal evolution of glioblastoma under therapy. *Nature Genetics*, 48(7), 768–776. <http://doi.org/10.1038/ng.3590>
- Wang, Qianghu, Hu, B., Hu, X., Kim, H., Squatrito, M., Scarpace, L., et al. (2017). Tumor Evolution of Glioma-Intrinsic Gene Expression Subtypes Associates with Immunological Changes in the Microenvironment. *Cancer Cell*, 32(1), 42–56.e6. <http://doi.org/10.1016/j.ccell.2017.06.003>
- Wang, Rong, Chadalavada, K., Wilshire, J., Kowalik, U., Hovinga, K. E., Geber, A., et al. (2010b). Glioblastoma stem-like cells give rise to tumour endothelium. *Nature*, 468(7325), 829–833. <http://doi.org/10.1038/nature09624>

- Wang, X, Venugopal, C., Manoranjan, B., McFarlane, N., O'Farrell, E., Nolte, S., et al. (2012). Sonic hedgehog regulates Bmi1 in human medulloblastoma brain tumor-initiating cells. *Oncogene*, 31(2), 187–199. <http://doi.org/10.1038/onc.2011.232>
- Wei, J., Marisetty, A., Schrand, B., Gabrusiewicz, K., Hashimoto, Y., Ott, M., et al. (2019). Osteopontin mediates glioblastoma-associated macrophage infiltration and is a potential therapeutic target. *The Journal of Clinical Investigation*, 129(1), 137–149. <http://doi.org/10.1172/JCI121266>
- Wick, W., Weller, M., van den Bent, M., Sanson, M., Weiler, M., Deimling, von, A., et al. (2014). MGMT testing--the challenges for biomarker-based glioma treatment. *Nature Reviews. Neurology*, 10(7), 372–385. <http://doi.org/10.1038/nrneurol.2014.100>
- Wykosky, J. (2005). EphA2 as a Novel Molecular Marker and Target in Glioblastoma Multiforme. *Molecular Cancer Research*, 3(10), 541–551. <http://doi.org/10.1158/1541-7786.MCR-05-0056>
- Zhang, J., Stevens, M. F. G., & Bradshaw, T. D. (2012). Temozolomide: mechanisms of action, repair and resistance. *Current Molecular Pharmacology*, 5(1), 102–114.
- Zhang, S., Zhao, B. S., Zhou, A., Lin, K., Zheng, S., Lu, Z., et al. (2017). m6A Demethylase ALKBH5 Maintains Tumorigenicity of Glioblastoma Stem-like Cells by Sustaining FOXM1 Expression and Cell Proliferation Program. *Cancer Cell*, 31(4), 591–606.e6. <http://doi.org/10.1016/j.ccell.2017.02.013>
- Zhou, W., Ke, S. Q., Huang, Z., Flavahan, W., Fang, X., Paul, J., et al. (2015). Periostin secreted by glioblastoma stem cells recruits M2 tumour-associated macrophages and

promotes malignant growth. *Nature Cell Biology*, 17(2), 170–182.

<http://doi.org/10.1038/ncb3090>

Appendix - Article Re-use Permissions

From: **JOURNALS PERMISSIONS** Journals.Permissions@oup.com 
Subject: RE: Re-use permission for article
Date: February 11, 2019 at 4:35 AM
To: Maleeha Qazi qazi.maleeha@gmail.com

JP

Dear Maleeha,

RE. M. A. Qazi et al. Intratumoral heterogeneity: pathways to treatment resistance and relapse in human glioblastoma. *Annals of Oncology* (2017) 28 (7): 1448-1456

I'm afraid that the License Agreement you received is incorrect, and that Rightslink does not cover author reuse in their thesis. I am going to request that your License Agreement #4523700948214 is cancelled. However, please find details on how you may reuse your article in your thesis below:

As part of your copyright agreement with Oxford University Press you have retained the right, after publication, to use all or part of the article and abstract, in the preparation of derivative works, extension of the article into a booklength work, in a thesis/dissertation, or in another works collection, provided that a full acknowledgement is made to the original publication in the journal. As a result, you should not require direct permission from Oxford University Press to reuse your article.

However, in line with the journal self-archiving policy, you may only include your **Accepted Manuscript (AM)** in your thesis/dissertation and public availability must be delayed until **12 months** after first online publication in the journal. You should include the following acknowledgment as well as a link to the version of record.

This is a pre-copyedited, author-produced version of an article accepted for publication in [insert journal title] following peer review. The version of record [insert complete citation information here] is available online at: xxxxxx [insert URL and DOI of the article on the OUP website].

Please Note: Inclusion under a Creative Commons license or any other open-access license allowing onward reuse is prohibited.

For full details of our publication and rights policy please see the attached link to our website: <http://www.oxfordjournals.org/en/access-purchase/rights-and-permissions/self-archiving-policyb.html>

If you have any other queries, please feel free to contact us.

Kind regards,
Katie

Katie Randall | Permissions Assistant | Rights Department
Academic and Journals Divisions | Global Business Development
Oxford University Press | Great Clarendon Street | Oxford | OX2 6DP



2/7/2019

RightsLink Printable License

JOHN WILEY AND SONS ORDER DETAILS

Feb 07, 2019

Order Number	501462211
Order date	Feb 07, 2019
Licensed Content Publisher	John Wiley and Sons
Licensed Content Publication	Wiley Books
Licensed Content Title	Isolation and Identification of Neural Cancer Stem/Progenitor Cells
Licensed Content Author	David Bakhshinyan, Maleeha A. Qazi, Neha Garg, et al
Licensed Content Date	Mar 6, 2015
Licensed Content Pages	23
Type of use	Dissertation/Thesis
Requestor type	University/Academic
Format	Electronic
Portion	Text extract
Number of Pages	10
Will you be translating?	No
Title of your thesis / dissertation	A pre-clinical model of glioblastoma recurrence to identify personalized therapeutic targets
Expected completion date	Mar 2019
Expected size (number of pages)	1
Requestor Location	Maleeha A Qazi 1280 Main Street West MDCL 5061 Hamilton, ON L8S4K1 Canada Attn: Maleeha A Qazi
Publisher Tax ID	EU826007151
Total	Not Available

<https://s100.copyright.com/AppDispatchServlet>

2/24/2019

RightsLink Printable License

**SPRINGER NATURE LICENSE
TERMS AND CONDITIONS**

Feb 24, 2019

This Agreement between Maleeha A Qazi ("You") and Springer Nature ("Springer Nature") consists of your license details and the terms and conditions provided by Springer Nature and Copyright Clearance Center.

License Number	4535460065074
License date	Feb 24, 2019
Licensed Content Publisher	Springer Nature
Licensed Content Publication	Journal of Neuro-Oncology
Licensed Content Title	A novel stem cell culture model of recurrent glioblastoma
Licensed Content Author	Maleeha A. Qazi, Parvez Vora, Chitra Venugopal et al
Licensed Content Date	Jan 1, 2015
Licensed Content Volume	126
Licensed Content Issue	1
Type of Use	Thesis/Dissertation
Requestor type	academic/university or research institute
Format	electronic
Portion	full article/chapter
Will you be translating?	no
Circulation/distribution	>50,000
Author of this Springer Nature content	yes
Title	A pre-clinical model of glioblastoma recurrence to identify personalized therapeutic targets
Institution name	McMaster University
Expected presentation date	Mar 2019
Requestor Location	Maleeha A Qazi 1280 Main Street West MDCL 5061

<https://s100.copyright.com/AppDispatchServlet>

1/4

2/24/2019

RightsLink Printable License

Hamilton, ON L8S4K1
Canada
Attn: Maleeha A Qazi

Billing Type Invoice

Billing Address Maleeha A Qazi
1280 Main Street West
MDCL 5061

Hamilton, ON L8S4K1
Canada
Attn: Maleeha A Qazi

Total 0.00 CAD

Terms and Conditions

Springer Nature Terms and Conditions for RightsLink Permissions
Springer Nature Customer Service Centre GmbH (the Licensor) hereby grants you a non-exclusive, world-wide licence to reproduce the material and for the purpose and requirements specified in the attached copy of your order form, and for no other use, subject to the conditions below:

1. The Licensor warrants that it has, to the best of its knowledge, the rights to license reuse of this material. However, you should ensure that the material you are requesting is original to the Licensor and does not carry the copyright of another entity (as credited in the published version).

If the credit line on any part of the material you have requested indicates that it was reprinted or adapted with permission from another source, then you should also seek permission from that source to reuse the material.
2. Where **print only** permission has been granted for a fee, separate permission must be obtained for any additional electronic re-use.
3. Permission granted **free of charge** for material in print is also usually granted for any electronic version of that work, provided that the material is incidental to your work as a whole and that the electronic version is essentially equivalent to, or substitutes for, the print version.
4. A licence for 'post on a website' is valid for 12 months from the licence date. This licence does not cover use of full text articles on websites.
5. Where **'reuse in a dissertation/thesis'** has been selected the following terms apply:
Print rights of the final author's accepted manuscript (for clarity, NOT the published version) for up to 100 copies, electronic rights for use only on a personal website or institutional repository as defined by the Sherpa guideline (www.sherpa.ac.uk/romeo/).

<https://s100.copyright.com/AppDispatchServlet>

2/4

2/24/2019

RightsLink Printable License

6. Permission granted for books and journals is granted for the lifetime of the first edition and does not apply to second and subsequent editions (except where the first edition permission was granted free of charge or for signatories to the STM Permissions Guidelines <http://www.stm-assoc.org/copyright-legal-affairs/permissions/permissions-guidelines/>), and does not apply for editions in other languages unless additional translation rights have been granted separately in the licence.
7. Rights for additional components such as custom editions and derivatives require additional permission and may be subject to an additional fee. Please apply to Journalpermissions@springernature.com/bookpermissions@springernature.com for these rights.
8. The Licensor's permission must be acknowledged next to the licensed material in print. In electronic form, this acknowledgement must be visible at the same time as the figures/tables/illustrations or abstract, and must be hyperlinked to the journal/book's homepage. Our required acknowledgement format is in the Appendix below.
9. Use of the material for incidental promotional use, minor editing privileges (this does not include cropping, adapting, omitting material or any other changes that affect the meaning, intention or moral rights of the author) and copies for the disabled are permitted under this licence.
10. Minor adaptations of single figures (changes of format, colour and style) do not require the Licensor's approval. However, the adaptation should be credited as shown in Appendix below.

Appendix — Acknowledgements:

For Journal Content:

Reprinted by permission from [the Licensor]: [Journal Publisher (e.g. Nature/Springer/Palgrave)] [JOURNAL NAME] [REFERENCE CITATION (Article name, Author(s) Name), [COPYRIGHT] (year of publication)]

For Advance Online Publication papers:

Reprinted by permission from [the Licensor]: [Journal Publisher (e.g. Nature/Springer/Palgrave)] [JOURNAL NAME] [REFERENCE CITATION (Article name, Author(s) Name), [COPYRIGHT] (year of publication), advance online publication, day month year (doi: 10.1038/sj.[JOURNAL ACRONYM].)]

For Adaptations/Translations:

Adapted/Translated by permission from [the Licensor]: [Journal Publisher (e.g. Nature/Springer/Palgrave)] [JOURNAL NAME] [REFERENCE CITATION (Article name, Author(s) Name), [COPYRIGHT] (year of publication)]

<https://s100.copyright.com/AppDispatchServlet>

3/4

2/24/2019

RightsLink Printable License

Note: For any republication from the British Journal of Cancer, the following credit line style applies:

Reprinted/adapted/translated by permission from [the Licensor]: on behalf of Cancer Research UK: : [Journal Publisher (e.g. Nature/Springer/Palgrave)] [JOURNAL NAME] [REFERENCE CITATION (Article name, Author(s) Name), [COPYRIGHT] (year of publication)

For Advance Online Publication papers:

Reprinted by permission from The [the Licensor]: on behalf of Cancer Research UK: [Journal Publisher (e.g. Nature/Springer/Palgrave)] [JOURNAL NAME] [REFERENCE CITATION (Article name, Author(s) Name), [COPYRIGHT] (year of publication), advance online publication, day month year (doi: 10.1038/sj. [JOURNAL ACRONYM])

For Book content:

Reprinted/adapted by permission from [the Licensor]: [Book Publisher (e.g. Palgrave Macmillan, Springer etc) [Book Title] by [Book author(s)] [COPYRIGHT] (year of publication)

Other Conditions:

Version 1.1

Questions? customercare@copyright.com or +1-855-239-3415 (toll free in the US) or +1-978-646-2777.

Ph.D. Thesis – M. A. Qazi; McMaster University – Biochemistry and Biomedical Sciences

From: **Rac, Karola** karola.rac@aacr.org
Subject: RE: Re-use permission for article / Qazi
Date: February 25, 2019 at 3:34 PM
To: Maleeha Qazi qazi.maleeha@gmail.com



Dear Maleeha –

Provided point 3 of the guidelines is adhered to, all should be well.

1. Reproduce parts of their article, including figures and tables, in books, reviews, or subsequent research articles they write;
2. Use parts of their article in presentations, including figures downloaded into PowerPoint, which can be done directly from the journal's website;
3. **Post the accepted version of their article (after revisions resulting from peer review, but before editing and formatting) on their institutional website, if this is required by their institution. The version on the institutional repository must contain a link to the final, published version of the article on the AACR journal website. The posted version may be released publicly (made open to anyone) 12 months after its publication in the journal;**
4. Submit a copy of the article to a doctoral candidate's university in support of a doctoral thesis or dissertation.

Best regards,
~Karola

Karola Rac

ASSISTANT DIRECTOR, INSTITUTIONAL SALES AND OUTREACH
Publishing Division



American Association for Cancer Research
615 Chestnut Street, 17th Floor | Philadelphia, PA 19106-4404
215-446-7231 Direct | 267-765-1006 Fax
karola.rac@aacr.org | www.AACR.org



Please note that this e-mail and any files transmitted with it may be privileged, confidential, and protected from disclosure under applicable law. This information is intended only for the person or entity to which it is addressed and may contain confidential or privileged material. Any review, retransmission, dissemination, or other use of, or taking of any action in reliance upon, this information by persons or entities other than the intended recipient is prohibited. If you received this in error, please contact the sender and delete the material from any computer.